AD-A147 663 ELECTRONIC STRUCTURE OF SEMICONDUCTOR INTERFACES(U) IBM 1/1
RESEARCH DIV SAN JOSE CALIF F HERMAN 01 NOV 84
N00014-79-C-0814

UNCLASSIFIED F/G 20/12 NL

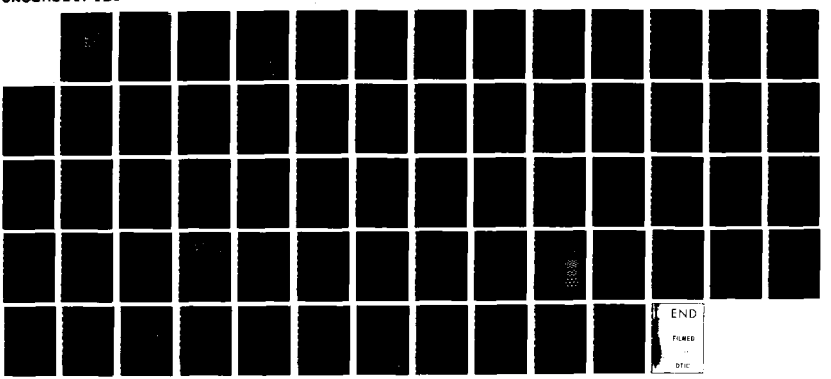

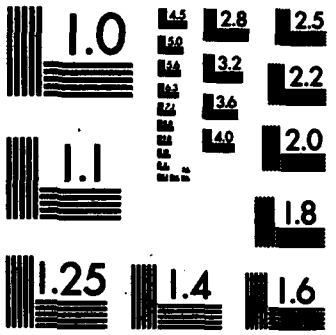
1.0
1.1
1.25
1.4
1.6
1.8
2.0
2.2
2.5
2.8
3.2
3.6
4.0
4.5
5.0
5.6
6.3
7.1
8.0
9.0
10
11
12
14
16
18
20
22
25
28
32
36
40
45
50
56
63
71
80
90
100
110
125
140
160
180
200
220
250
280
320
360
400
450
500
560
630
710
800
900
1000
1100
1250
1400
1600
1800
2000
2200
2500
2800
3200
3600
4000
4500
5000
5600
6300
7100
8000
9000
10000
11000
12500
14000
16000
18000
20000
22000
25000
28000
32000
36000
40000
45000
50000
56000
63000
71000
80000
90000
100000
110000
125000
140000
160000
180000
200000
220000
250000
280000
320000
360000
400000
450000
500000
560000
630000
710000
800000
900000
1000000
1100000
1250000
1400000
1600000
1800000
2000000
2200000
2500000
2800000
3200000
3600000
4000000
4500000
5000000
5600000
6300000
7100000
8000000
9000000
10000000
11000000
12500000
14000000
16000000
18000000
20000000
22000000
25000000
28000000
32000000
36000000
40000000
45000000
50000000
56000000
63000000
71000000
80000000
90000000
100000000
110000000
125000000
140000000
160000000
180000000
200000000
220000000
250000000
280000000
320000000
360000000
400000000
450000000
500000000
560000000
630000000
710000000
800000000
900000000
1000000000
1100000000
1250000000
1400000000
1600000000
1800000000
2000000000
2200000000
2500000000
2800000000
3200000000
3600000000
4000000000
4500000000
5000000000
5600000000
6300000000
7100000000
8000000000
9000000000
10000000000
11000000000
12500000000
14000000000
16000000000
18000000000
20000000000
22000000000
25000000000
28000000000
32000000000
36000000000
40000000000
45000000000
50000000000
56000000000
63000000000
71000000000
80000000000
90000000000
100000000000
110000000000
125000000000
140000000000
160000000000
180000000000
200000000000
220000000000
250000000000
280000000000
320000000000
360000000000
400000000000
450000000000
500000000000
560000000000
630000000000
710000000000
800000000000
900000000000
1000000000000
1100000000000
1250000000000
1400000000000
1600000000000
1800000000000
2000000000000
2200000000000
2500000000000
2800000000000
3200000000000
3600000000000
4000000000000
4500000000000
5000000000000
5600000000000
6300000000000
7100000000000
8000000000000
9000000000000
10000000000000
11000000000000
12500000000000
14000000000000
16000000000000
18000000000000
20000000000000
22000000000000
25000000000000
28000000000000
32000000000000
36000000000000
40000000000000
45000000000000
50000000000000
56000000000000
63000000000000
71000000000000
80000000000000
90000000000000
100000000000000
110000000000000
125000000000000
140000000000000
160000000000000
180000000000000
200000000000000
220000000000000
250000000000000
280000000000000
320000000000000
360000000000000
400000000000000
450000000000000
500000000000000
560000000000000
630000000000000
710000000000000
800000000000000
900000000000000
1000000000000000
1100000000000000
1250000000000000
1400000000000000
1600000000000000
1800000000000000
2000000000000000
2200000000000000
2500000000000000
2800000000000000
3200000000000000
3600000000000000
4000000000000000
4500000000000000
5000000000000000
5600000000000000
6300000000000000
7100000000000000
8000000000000000
9000000000000000
10000000000000000
11000000000000000
12500000000000000
14000000000000000
16000000000000000
18000000000000000
20000000000000000
22000000000000000
25000000000000000
28000000000000000
32000000000000000
36000000000000000
40000000000000000
45000000000000000
50000000000000000
56000000000000000
63000000000000000
71000000000000000
80000000000000000
90000000000000000
100000000000000000
110000000000000000
125000000000000000
140000000000000000
160000000000000000
180000000000000000
200000000000000000
220000000000000000
250000000000000000
280000000000000000
320000000000000000
360000000000000000
400000000000000000
450000000000000000
500000000000000000
560000000000000000
630000000000000000
710000000000000000
800000000000000000
900000000000000000
1000000000000000000
1100000000000000000
1250000000000000000
1400000000000000000
1600000000000000000
1800000000000000000
2000000000000000000
2200000000000000000
2500000000000000000
2800000000000000000
3200000000000000000
3600000000000000000
4000000000000000000
4500000000000000000
5000000000000000000
5600000000000000000
6300000000000000000
7100000000000000000
8000000000000000000
9000000000000000000
10000000000000000000
11000000000000000000
12500000000000000000
14000000000000000000
16000000000000000000
18000000000000000000
20000000000000000000
22000000000000000000
25000000000000000000
28000000000000000000
32000000000000000000
36000000000000000000
40000000000000000000
45000000000000000000
50000000000000000000
56000000000000000000
63000000000000000000
71000000000000000000
80000000000000000000
90000000000000000000
100000000000000000000
110000000000000000000
125000000000000000000
140000000000000000000
160000000000000000000
180000000000000000000
200000000000000000000
220000000000000000000
250000000000000000000
280000000000000000000
320000000000000000000
360000000000000000000
400000000000000000000
450000000000000000000
500000000000000000000
560000000000000000000
630000000000000000000
710000000000000000000
800000000000000000000
900000000000000000000
1000000000000000000000
1100000000000000000000
1250000000000000000000
1400000000000000000000
1600000000000000000000
1800000000000000000000
2000000000000000000000
2200000000000000000000
2500000000000000000000
2800000000000000000000
3200000000000000000000
3600000000000000000000
4000000000000000000000
4500000000000000000000
5000000000000000000000
5600000000000000000000
6300000000000000000000
7100000000000000000000
8000000000000000000000
9000000000000000000000
10000000000000000000000
11000000000000000000000
12500000000000000000000
14000000000000000000000
16000000000000000000000
18000000000000000000000
20000000000000000000000
22000000000000000000000
25000000000000000000000
28000000000000000000000
32000000000000000000000
36000000000000000000000
40000000000000000000000
45000000000000000000000
50000000000000000000000
56000000000000000000000
63000000000000000000000
71000000000000000000000
80000000000000000000000
90000000000000000000000
100000000000000000000000
110000000000000000000000
125000000000000000000000
140000000000000000000000
160000000000000000000000
180000000000000000000000
200000000000000000000000
220000000000000000000000
250000000000000000000000
280000000000000000000000
320000000000000000000000
360000000000000000000000
400000000000000000000000
450000000000000000000000
500000000000000000000000
560000000000000000000000
630000000000000000000000
710000000000000000000000
800000000000000000000000
900000000000000000000000
1000000000000000000000000
1100000000000000000000000
1250000000000000000000000
1400000000000000000000000
1600000000000000000000000
1800000000000000000000000
2000000000000000000000000
2200000000000000000000000
2500000000000000000000000
2800000000000000000000000
3200000000000000000000000
3600000000000000000000000
4000000000000000000000000
4500000000000000000000000
5000000000000000000000000
5600000000000000000000000
6300000000000000000000000
7100000000000000000000000
8000000000000000000000000
9000000000000000000000000
10000000000000000000000000
11000000000000000000000000
12500000000000000000000000
14000000000000000000000000
16000000000000000000000000
18000000000000000000000000
20000000000000000000000000
22000000000000000000000000
25000000000000000000000000
28000000000000000000000000
32000000000000000000000000
36000000000000000000000000
40000000000000000000000000
45000000000000000000000000
50000000000000000000000000
56000000000000000000000000
63000000000000000000000000
71000000000000000000000000
80000000000000000000000000
90000000000000000000000000
100000000000000000000000000
110000000000000000000000000
125000000000000000000000000
140000000000000000000000000
160000000000000000000000000
180000000000000000000000000
200000000000000000000000000
220000000000000000000000000
250000000000000000000000000
280000000000000000000000000
320000000000000000000000000
360000000000000000000000000
400000000000000000000000000
450000000000000000000000000
500000000000000000000000000
560000000000000000000000000
630000000000000000000000000
710000000000000000000000000
800000000000000000000000000
900000000000000000000000000
1000000000000000000000000000
1100000000000000000000000000
1250000000000000000000000000
1400000000000000000000000000
1600000000000000000000000000
1800000000000000000000000000
2000000000000000000000000000
2200000000000000000000000000
2500000000000000000000000000
2800000000000000000000000000
3200000000000000000000000000
3600000000000000000000000000
4000000000000000000000000000
4500000000000000000000000000
5000000000000000000000000000
5600000000000000000000000000
6300000000000000000000000000
7100000000000000000000000000
8000000000000000000000000000
9000000000000000000000000000
10000000000000000000000000000
11000000000000000000000000000
12500000000000000000000000000
14000000000000000000000000000
16000000000000000000000000000
18000000000000000000000000000
20000000000000000000000000000
22000000000000000000000000000
25000000000000000000000000000
28000000000000000000000000000
32000000000000000000000000000
36000000000000000000000000000
40000000000000000000000000000
45000000000000000000000000000
50000000000000000000000000000
56000000000000000000000000000
63000000000000000000000000000
71000000000000000000000000000
80000000000000000000000000000
90000000000000000000000000000
100000000000000000000000000000
110000000000000000000000000000
125000000000000000000000000000
140000000000000000000000000000
160000000000000000000000000000
180000000000000000000000000000
200000000000000000000000000000
220000000000000000000000000000
250000000000000000000000000000
280000000000000000000000000000
320000000000000000000000000000
360000000000000000000000000000
400000000000000000000000000000
450000000000000000000000000000
500000000000000000000000000000
560000000000000000000000000000
630000000000000000000000000000
710000000000000000000000000000
800000000000000000000000000000
900000000000000000000000000000
1000000000000000000000000000000
1100000000000000000000000000000
1250000000000000000000000000000
1400000000000000000000000000000
1600000000000000000000000000000
1800000000000000000000000000000
2000000000000000000000000000000
2200000000000000000000000000000
2500000000000000000000000000000
2800000000000000000000000000000
3200000000000000000000000000000
3600000000000000000000000000000
4000000000000000000000000000000
4500000000000000000000000000000
5000000000000000000000000000000
5600000000000000000000000000000
6300000000000000000000000000000
7100000000000000000000000000000
8000000000000000000000000000000
9000000000000000000000000000000
10000000000000000000000000000000
11000000000000000000000000000000
12500000000000000000000000000000
14000000000000000000000000000000
16000000000000000000000000000000
18000000000000000000000000000000
20000000000000000000000000000000
22000000000000000000000000000000
25000000000000000000000000000000
28000000000000000000000000000000
32000000000000000000000000000000
36000000000000000000000000000000
40000000000000000000000000000000
45000000000000000000000000000000
50000000000000000000000000000000
56000000000000000000000000000000
63000000000000000000000000000000
71000000000000000000000000000000
80000000000000000000000000000000
90000000000000000000000000000000
100000000000000000000000000000000
110000000000000000000000000000000
125000000000000000000000000000000
140000000000000000000000000000000
160000000000000000000000000000000
180000000000000000000000000000000
200000000000000000000000000000000
220000000000000000000000000000000
250000000000000000000000000000000
280000000000000000000000000000000
320000000000000000000000000000000
360000000000000000000000000000000
400000000000000000000000000000000
450000000000000000000000000000000
500000000000000000000000000000000
560000000000000000000000000000000
630000000000000000000000000000000
710000000000000000000000000000000
800000000000000000000000000000000
900000000000000000000000000000000
1000000000000000000000000000000000
1100000000000000000000000000000000
1250000000000000000000000000000000
1400000000000000000000000000000000
1600000000000000000000000000000000
1800000000000000000000000000000000
2000000000000000000000000000000000
2200000000000000000000000000000000
2500000000000000000000000000000000
2800000000000000000000000000000000
3200000000000000000000000000000000
3600000000000000000000000000000000
4000000000000000000000000000000000
4500000000000000000000000000000000
5000000000000000000000000000000000
5600000000000000000000000000000000
6300000000000000000000000000000000
7100000000000000000000000000000000
8000000000000000000000000000000000
9000000000000000000000000000000000
10000000000000000000000000000000000
11000000000000000000000000000000000
12500000000000000000000000000000000
14000000000000000000000000000000000
16000000000000000000000000000000000
18000000000000000000000000000000000
20000000000000000000000000000000000
22000000000000000000000000000000000
25000000000000000000000000000000000
28000000000000000000000000000000000
32000000000000000000000000000000000
36000000000000000000000000000000000
40000000000000000000000000000000000
45000000000000000000000000000000000
50000000000000000000000000000000000
56000000000000000000000000000000000
63000000000000000000000000000000000
71000000000000000000000000000000000
80000000000000000000000000000000000
90000000000000000000000000000000000
100000000000000000000000000000000000
110000000000000000000000000000000000
125000000000000000000000000000000000
140000000000000000000000000000000000
160000000000000000000000000000000000
180000000000000000000000000000000000
200000000000000000000000000000000000
220000000000000000000000000000000000
250000000000000000000000000000000000
280000000000000000000000000000000000
320000000000000000000000000000000000
360000000000000000000000000000000000
400000000000000000000000000000000000
450000000000000000000000000000000000
500000000000000000000000000000000000
560000000000000000000000000000000000
630000000000000000000000000000000000
710000000000000000000000000000000000
800000000000000000000000000000000000
900000000000000000000000000000000000
1000000000000000000000000000000000000
1100000000000000000000000000000000000
1250000000000000000000000000000000000
1400000000000000000000000000000000000
1600000000000000000000000000000000000
1800000000000000000000000000000000000
2000000000000000000000000000000000000
2200000000000000000000000000000000000
2500000000000000000000000000000000000
2800000000000000000000000000000000000
3200000000000000000000000000000000000
3600000000000000000000000000000000000
4000000000000000000000000000000000000
4500000000000000000000000000000000000
5000000000000000000000000000000000000
5600000000000000000000000000000000000
6300000000000000000000000000000000000
7100000000000000000000000000000000000
8000000000000000000000000000000000000
9000000000000000000000000000000000000
10000000000000000000000000000000000000
11000000000000000000000000000000000000
12500000000000000000000000000000000000
14000000000000000000000000000000000000
16000000000000000000000000000000000000
18000000000000000000000000000000000000
20000000000000000000000000000000000000
22000000000000000000000000000000000000
25000000000000000000000000000000000000
28000000000000000000000000000000000000
32000000000000000000000000000000000000
36000000000000000000000000000000000000
40000000000000000000000000000000000000
45000000000000000000000000000000000000
50000000000000000000000000000000000000
56000000000000000000000000000000000000
63000000000000000000000000000000000000
71000000000000000000000000000000000000
80000000000000000000000000000000000000
90000000000000000000000000000000000000
100000000000000000000000000000000000000
110000000000000000000000000000000000000
125000000000000000000000000000000000000
140000000000000000000000000000000000000
160000000000000000000000000000000000000
180000000000000000000000000000000000000
200000000000000000000000000000000000000
220000000000000000000000000000000000000
250000000000000000000000000000000000000
280000000000000000000000000000000000000
320000000000000000000000000000000000000
360000000000000000000000000000000000000
400000000000000000000000000000000000000
450000000000000000000000000000000000000
500000000000000000000000000000000000000
560000000000000000000000000000000000000
630000000000000000000000000000000000000
710000000000000000000000000000000000000
800000000000000000000000000000000000000
900000000000000000000000000000000000000
1000000000000000000000000000000000000000
1100000000000000000000000000000000000000
1250000000000000000000000000000000000000
1400000000000000000000000000000000000000
1600000000000000000000000000000000000000
1800000000000000000000000000000000000000
2000000000000000000000000000000000000000
2200000000000000000000000000000000000000
2500000000000000000000000000000000000000
2800000000000000000000000000000000000000
3200000000000000000000000000000000000000
3600000000000000000000000000000000000000
4000000000000000000000000000000000000000
4500000000000000000000000000000000000000
5000000000000000000000000000000000000000
5600000000000000000000000000000000000000
6300000000000000000000000000000000000000
7100000000000000000000000000000000000000
8000000000000000000000000000000000000000
9000000000000000000000000000000000000000
10000000000000000000000000000000000000000
11000000000000000000000000000000000000000
12500000000000000000000000000000000000000
14000000000000000000000000000000000000000
16000000000000000000000000000000000000000
18000000000000000000000000000000000000000
20000000000000000000000000000000000000000
22000000000000000000000000000000000000000
25000000000000000000000000000000000000000
28000000000000000000000000000000000000000
32000000000000000000000000000000000000000
36000000000000000000000000000000000000000
40000000000000000000000000000000000000000
45000000000000000000000000000000000000000
50000000000000000000000000000000000000000
56000000000000000000000000000000000000000
63000000000000000000000000000000000000000
71000000000000000000000000000000000000000
80000000000000000000000000000000000000000
90000000000000000000000000000000000000000
100000000000000000000000000000000000000000
110000000000000000000000000000000000000000
125000000000000000000000000000000000000000
140000000000000000000000000000000000000000
160000000000000000000000000000000000000000
180000000000000000000000000000000000000000
200000000000000000000000000000000000000000
220000000000000000000000000000000000000000
250000000000000000000000000000000000000000
280000000000000000000000000000000000000000
320000000000000000000000000000000000000000
360000000000000000000000000000000000000000
400000000000000000000000000000000000000000
450000000000000000000000000000000000000000
500000000000000000000000000000000000000000
560000000000000000000000000000000000000000
630000000000000000000000000000000000000000
710000000000000000000000000000000000000000
800000000000000000000000000000000000000000
900000000000000000000000000000000000000000
1000000000000000000000000000000000000000000
1100000000000000000000000000000000000000000
1250000000000000000000000000000000000000000
1400000000000000000000000000000000000000000
1600000000000000000000000000000000000000000
1800000000000000000000000000000000000000000
2000000000000000000000000000000000000000000
2200000000000000000000000000000000000000000
2500000000000000000000000000000000000000000
2800000000000000000000000000000000000000000
3200000000000000000000000000000000000000000
3600000000000000000000000000000000000000000
4000000000000000000000000000000000000000000
4500000000000000000000000000000000000000000
5000000000000000000000000000000000000000000
5600000000000000000000000000000000000000000
6300000000000000000000000000000000000000000
7100000000000000000000000000000000000000000
8000000000000000000000000000000000000000000
9000000000000000000000000000000000000000000
10000000000000000000000000000000000000000000
11000000000000000000000000000000000000000000
12500000000000000000000000000000000000000000
14000000000000000000000000000000000000000000
16000000000000000000000000000000000000000000
18000000000000000000000000000000000000000000
20000000000000000000000000000000000000000000
22000000000000000000000000000000000000000000
25000000000000000000000000000000000000000000
28000000000000000000000000000000000000000000
32000000000000000000000000000000000000000000
36000000000000000000000000000000000000000000
40000000000000000000000000000000000000000000
45000000000000000000000000000000000000000000
50000000000000000000000000000000000000000000
56000000000000000000000000000000000000000000
63000000000000000000000000000000000000000000
71000000000000000000000000000000000000000000
80000000000000000000000000000000000000000000
90000000000000000000000000000000000000000000
100000000000000000000000000000000000000000000
110000000000000000000000000000000000000000000
125000000000000000000000000000000000000000000
140000000000000000000000000000000000000000000
160000000000000000000000000000000000000000000
180000000000000000000000000000000000000000000
200000000000000000000000000000000000000000000
220000000000000000000000000000000000000000000
250000000000000000000000000000000000000000000
280000000000000000000000000000000000000000000
320000000000000000000000000000000000000000000
360000000000000000000000000000000000000000000
400000000000000000000000000000000000000000000
450000000000000000000000000000000000000000000
500000000000000000000000000000000000000000000
560000000000000000000000000000000000000000000
630000000000000000000000000000000000000000000
710000000000000000000000000000000000000000000
800000000000000000000000000000000000000000000
900000000000000000000000000000000000000000000
1000000000000000000000000000000000000000000000
1100000000000000000000000000000000000000000000
1250000000000000000000000000000000000000000000
1400000000000000000000000000000000000000000000
1600000000000000000000000000000000000000000000
1800000000000000000000000000000000000000000000
2000000000000000000000000000000000000000000000
2200000000000000000000000000000000000000000000
2500000000000000000000000000000000000000000000
2800000000000000000000000000000000000000000000
3200000000000000000000000000000000000000000000
3600000000000000000000000000000000000000000000
4000000000000000000000000000000000000000000000
4500000000000000000000000000000000000000000000
5000000000000000000000000000000000000000000000
5600000000000000000000000000000000000000000000
6300000000000000000000000000000000000000000000
7100000000000000000000000000000000000000000000
8000000000000000000000000000000000000000000000
9000000000000000000000000000000000000000000000
10000000000000000000000000000000000000000000000
11000000000000000000000000000000000000000000000
12500000000000000000000000000000000000000000000
14000000000000000000000000000000000000000000000
16000000000000000000000000000000000000000000000
18000000000000000000000000000000000000000000000
20000000000000000000000000000000000000000000000
22000000000000000000000000000000000000000000000
25000000000000000000000000000000000000000000000
28000000000000000000000000000000000000000000000
32000000000000000000000000000000000000000000000
36000000000000000000000000000000000000000000000
40000000000000000000000000000000000000000000000
45000000000000000000000000000000000000000000000
50000000000000000000000000000000000000000000000
56000000000000000000000000000000000000000000000
63000000000000000000000000000000000000000000000
71000000000000000000000000000000000000000000000
80000000000000000000000000000000000000000000000
90000000000000000000000000000000000000000000000
100000000000000000000000000000000000000000000000
110000000000000000000000000000000000000000000000
125000000000000000000000000000000000000000000000
140000000000000000000000000000000000000000000000
160000000000000000000000000000000000000000000000
180000000000000000000000000000000000000000000000
200000000000000000000000000000000000000000000000
220000000000000000000000000000000000000000000000
250000000000000000000000000000000000000000000000
280000000000000000000000000000000000000000000000
320000000000000000000000000000000000000000000000
360000000000000000000000000000000000000000000000
400000000000000000000000000000000000000000000000
450000000000000000000000000000000000000000000000
500000000000000000000000000000000000000000000000
560000000000000000000000000000000000000000000000
630000000000000000000000000000000000000000000000
710000000000000000000000000000000000000000000000
800000000000000000000000000000000000000000000000
900000000000000000000000000000000000000000000000
1000000000000000000000000000000000000000000000000
1100000000000000000000000000000000000000000000000
1250000000000000000000000000000000000000000000000
1400000000000000000000000000000000000000000000000
1600000000000000000000000000000000000000000000000
1800000000000000000000000000000000000000000000000
2000000000000000000000000000000000000000000000000
2200000000000000000000000000000000000000000000000
2500000000000000000000000000000000000000000000000
2800000000000000000000000000000000000000000000000
3200000000000000000000000000000000000000000000000
3600000000000000000000000000000000000000000000000
4000000000000000000000000000000000000000000000000
4500000000000000000000000000000000000000000000000
5000000000000000000000000000000000000000000000000
5600000000000000000000000000000000000000000000000
6300000000000000000000000000000000000000000000000
7100000000000000000000000000000000000000000000000
8000000000000000000000000000000000000000000000000
9000000000000000000000000000000000000000000000000
10000000000000000000000000000000000000000000000000
11000000000000000000000000000000000000000000000000
12500000000000000000000000000000000000000000000000
14000000000000000000000000000000000000000000000000
16000000000000000000000000000000000000000000000000
18000000000000000000000000000000000000000000000000
20000000000000000000000000000000000000000000000000
22000000000000000000000000000000000000000000000000
25000000000000000000000000000000000000000000000000
28000000000000000000000000000000000000000000000000
32000000000000000000000000000000000000000000000000
36000000000000000000000000000000000000000000000000
40000000000000000000000000000000000000000000000000
45000000000000000000000000000000000000000000000000
50000000000000000000000000000000000000000000000000
56000000000000000000000000000000000000000000000000
63000000000000000000000000000000000000000000000000
71000000000000000000000000000000000000000000000000
80000000000000000000000000000000000000000000000000
90000000000000000000000000000000000000000000000000
100000000000000000000000000000000000000000000000000
110000000000000000000000000000000000000000000000000
125000000000000000000000000000000000000000000000000
140000000000000000000000000000000000000000000000000
160000000000000000000000000000000000000000000000000
180000000000000000000000000000000000000000000000000
200000000000000000000000000000000000000000000000000
220000000000000000000000000000000000000000000000000
250000000000000000000000000000000000000000000000000
280000000000000000000000000000000000000000000000000
320000000000000000000000000000000000000000000000000
360000000000000000000000000000000000000000000000000
400000000000000000000000000000000000000000000000000
450000000000000000000000000000000000000000000000000
500000000000000000000000000000000000000000000000000
560000000000000000000000000000000000000000000000000
630000000000000000000000000000000000000000000000000
710000000000000000000000000000000000000000000000000
800000000000000000000000000000000000000000000000000
900000000000000000000000000000000000000000000000000
1000000000000000000000000000000000000000000000000000
1100000000000000000000000000000000000000000000000000
1250000000000000000000000000000000000000000000000000
1400000000000000000000000000000000000000000000000000
1600000000000000000000000000000000000000000000000000
1800000000000000000000000000000000000000000000000000
2000000000000000000000000000000000000000000000000000
2200000000000000000000000000000000000000000000000000
2500000000000000000000000000000000000000000000000000
2800000000000000000000000000000000000000000000000000
3200000000000000000000000000000000000000000000000000
3600000000000000000000000000000000000000000000000000
4000000000000000000000000000000000000000000000000000
4500000000000000000000000000000000000000000000000000
5000000000000000000000000000000000000000000000000000
5600000000000000000000000000000000000000000000000000
6300000000000000000000000000000000000000000000000000
7100000000000000000000000000000000000000000000000000
8000000000000000000000000000000000000000000000000000
9000000000000000000000000000000000000000000000000000
10000000000000000000000000000000000000000000000000000
11000000000000000000000000000000000000000000000000000
12500000000000000000000000000000000000000000000000000
14000000000000000000000000000000000000000000000000000
16000000000000000000000000000000000000000000000000000
18000000000000000000000000000000000000000000000000000
20000000000000000000000000000000000000000000000000000
22000000000000000000000000000000000000000000000000000
25000000000000000000000000000000000000000000000000000
28000000000000000000000000000000000000000000000000000
32000000000000000000000000000000000000000000000000000
36000000000000000000000000000000000000000000000000000
40000000000000000000000000000000000000000000000000000
45000000000000000000000000000000000000000000000000000
50000000000000000000000000000000000000000000000000000
56000000000000000000000000000000000000000000000000000
63000000000000000000000000000000000000000000000000000
71000000000000000000000000000000000000000000000000000
80000000000000000000000000000000000000000000000000000
90000000000000000000000000000000000000000000000000000
100000000000000000000000000000000000000000000000000000
110000000000000000000000000000000000000000000000000000
125000000000000000000000000000000000000000000000000000
140000000000000000000000000000000000000000000000000000
160000000000000000000000000000000000000000000000000000
180000000000000000000000000000000000000000000000000000
200000000000000000000000000000000000000000000000000000
220000000000000000000000000000000000000000000000000000
250000000000000000000000000000000000000000000000000000
280000000000000000000000000000000000000000000000000000
320000000000000000000000000000000000000000000000000000
360000000000000000000000000000000000000000000000000000
400000000000000000000000000000000000000000000000000000
450000000000000000000000000000000000000000000000000000
500000000000000000000000000000000000000000000000000000
560000000000000000000000000000000000000000000000000000
630000000000000000000000000000000000000000000000000000
710000000000000000000000000000000000000000000000000000
800000000000000000000000000000000000000000000000000000
900000000000000000000000000000000000000000000000000000
1000000000000000000000000000000000000000000000000000000
1100000000000000000000000000000000000000000000000000000
1250000000000000000000000000000000000000000000000000000
1400000000000000000000000000000000000000000000000000000
1600000000000000000000000000000000000000000000000000000
1800000000000000000000000000000000000000000000000000000
2000000000000000000000000000000000000000000000000000000
2200000000000000000000000000000000000000000000000000000
2500000000000000000000000000000000000000000000000000000
2800000000000000000000000000000000000000000000000000000
3200000000000000000000000000000000000000000000000000000
3600000000000000000000000000000000000000000000000000000
4000000000000000000000000000000000000000000000000000000
4500000000000000000000000000000000000000000000000000000
5000000000000000000000000000000000000000000000000000000
5600000000000000000000000000000000000000000000000000000
6300000000000000000000000000000000000000000000000000000
7100000000000000000000000000000000000000000000000000000
8000000000000000000000000000000000000000000000000000000
9000000000000000000000000000000000000000000000000000000
10000000000000000000000000000000000000000000000000000000
11000000000000000000000000000000000000000000000000000000
12500000000000000000000000000000000000000000000000000000
14000000000000000000000000000000000000000000000000000000
16000000000000000000000000000000000000000000000000000000
18000000000000000000000000000000000000000000000000000000
20000000000000000000000000000000000000000000000000000000
22000000000000000000000000000000000000000000000000000000
25000000000000000000000000000000000000000000000000000000
28000000000000000000000000000000000000000000000000000000
32000000000000000000000000000000000000000000000000000000
36000000000000000000000000000000000000000000000000000000
40000000000000000000000000000000000000000000000000000000
45000000000000000000000000000000000000000000000000000000
50000000000000000000000000000000000000000000000000000000
56000000000000000000000000000000000000000000000000000000
63000000000000000000000000000000000000000000000000000000
71000000000000000000000000000000000000000000000000000000
80000000000000000000000000000000000000000000000000000000
90000000000000000000000000000000000000000000000000000000
100000000000000000000000000000000000000000000000000000000
110000000000000000000000000000000000000000000000000000000
125000000000000000000000000000000000000000000000000000000
140000000000000000000000000000000000000000000000000000000
160000000000000000000000000000000000000000000000000000000
180000000000000000000000000000000000000000000000000000000
200000000000000000000000000000000000000000000000000000000
220000000000000000000000000000000000000000000000000000000
250000000000000000000000000000000000000000000000000000000
280000000000000000000000000000000000000000000000000000000
320000000000000000000000000000000000000000000000000000000
360000000000000000000000000000000000000000000000000000000
400000000000000000000000000000000000000000000000000000000
450000000000000000000000000000000000000000000000000000000
500000000000000000000000000000000000000000000000000000000
560000000000000000000000000000000000000000000000000000000
630000000000000000000000000000000000000000000000000000000
710000000000000000000000000000000000000000000000000000000
800000000000000000000000000000000000000000000000000000000
900000000000000000000000000000000000000000000000000000000
1000000000000000000000000000000000000000000000000000000000
1100000000000000000000000000000000000000000000000000000000
1250000000000000000000000000000000000000000000000000000000
1400000000000000000000000000000000000000000000000000000000
1600000000000000000000000000000000000000000000000000000000
1800000000000000000000000000000000000000000000000000000000
2000000000000000000000000000000000000000000000000000000000
2200000000000000000000000000000000000000000000000000000000
2500000000000000000000000000000000000000000000000000000000
2800000000000000000000000000000000000000000000000000000000
3200000000000000000000000000000000000000000000000000000000
3600000000000000000000000000000000000000000000000000000000
4000000000000000000000000000000000000000000000000000000000
4500000000000000000000000000000000000000000000000000000000
5000000000000000000000000000000000000000000000000000000000
5600000000000000000000000000000000000000000000000000000000
6300000000000000000000000000000000000000000000000000000000
7100000000000000000000000000000000000000000000000000000000
8000000000000000000000000000000000000000000000000000000000
9000000000000000000000000000000000000000000000000000000000
10000000000000000000000000000000000000000000000000000000000
11000000000000000000000000000000000000000000000000000000000
12500000000000000000000000000000000000000000000000000000000
14000000000000000000000000000000000000000000000000000000000
16000000000000000000000000000000000000000000000000000000000
18000000000000000000000000000000000000000000000000000000000
20000000000000000000000000000000000000000000000000000000000
22000000000000000000000000000000000000000000000000000000000
25000000000000000000000000000000000000000000000000000000000
28000000000000000000000000000000000000000000000000000000000
32000000000000000000000000000000000000000000000000000000000
36000000000000000000000000000000000000000000000000000000000
40000000000000000000000000000000000000000000000000000000000
45000000000000000000000000000000000000000000000000000000000
50000000000000000000000000000000000000000000000000000000000
56000000000000000000000000000000000000000000000000000000000
63000000000000000000000000000000000000000000000000000000000
71000000000000000000000000000000000000000000000000000000000
80000000000000000000000000000000000000000000000000000000000
90000000000000000000000000000000000000000000000000000000000
100000000000000000000000000000000000000000000000000000000000
110000000000000000000000000000000000000000000000000000000000
125000000000000000000000000000000000000000000000000000000000
140000000000000000000000000000000000000000000000000000000000
160000000000000000000000000000000000000000000000000000000000
180000000000000000000000000000000000000000000000000000000000
200000000000000000000000000000000000000000000000000000000000
220000000000000000000000000000000000000000000000000000000000
250000000000000000000000000000000000000000000000000000000000
280000000000000000000000000000000000000000000000000000000000
320000000000000000000000000000000000000000000000000000000000
360000000000000000000000000000000000000000000000000000000000
400000000000000000000000000000000000000000000000000000000000
450000000000000000000000000000000000000000000000000000000000
500000000000000000000000000000000000000000000000000000000000
560000000000000000000000000000000000000000000000000000000000
630000000000000000000000000000000000000000000000000000000000
710000000000000000000000000000000000000000000000000000000000
800000000000000000000000000000000000000000000000000000000000
900000000000000000000000000000000000000000000000000000000000
1000000000000000000000000000000000000000000000000000000000000
1100000000000000000000000000000000000000000000000000000000000
1250000000000000000000000000000000000000000000000000000000000
1400000000000000000000000000000000000000000000000000000000000
1600000000000000000000000000000000000000000000000000000000000
1800000000000000000000000000000000000000000000000000000000000
2000000000000000000000000000000000000000000000000000000000000
2200000000000000000000000000000000000000000000000000000000000
2500000000000000000000000000000000000000000000000000000000000
2800000000000000000000000000000000000000000000000000000000000
3200000000000000000000000000000000000000000000000000000000000
3600000000000000000000000000000000000000000000000000000000000
4000000000000000000000000000000000000000000000000000000000000
4500000000000000000000000000000000000000000000000000000000000
5000000000000000000000000000000000000000000000000000000000000
5600000000000000000000000000000000000000000000000000000000000
6300000000000000000000000000000000000000000000000000000000000
7100000000000000000000000000000000000000000000000000000000000
8000000000000000000000000000000000000000000000000000000000000
9000000000000000000000000000000000000000000000000000000000000
10000000000000000000000000000000000000000000000000000000000000
11000000000000000000000000000000000000000000000000000000000000
12500000000000000000000000000000000000000000000000000000000000
14000000000000000000000000000000000000000000000000000000000000
16000000000000000000000000000000000000000000000000000000000000
18000000000000000000000000000000000000000000000000000000000000
20000000000000000000000000000000000000000000000000000000000000
22000000000000000000000000000000000000000000000000000000000000
25000000000000000000000000000000000000000000000000000000000000
28000000000000000000000000000000000000000000000000000000000000
32000000000000000000000000000000000000000000000000000000000000
36000000000000000000000000000000000000000000000000000000000000
40000000000000000000000000000000000000000000000000000000000000
45000000000000000000000000000000000000000000000000000000000000
50000000000000000000000000000000000000000000000000000000000000
56000000000000000000000000000000000000000000000000000000000000
63000000000000000000000000000000000000000000000000000000000000
71000000000000000000000000000000000000000000000000000000000000
80000000000000000000000000000000000000000000000000000000000000
90000000000000000000000000000000000000000000000000000000000000
100000000000000000000000000000000000000000000000000000000000000
110000000000000000000000000000000000000000000000000000000000000
125000000000000000000000000000000000000000000000000000000000000
140000000000000000000000000000000000000000000000000000000000000
160000000000000000000000000000000000000000000000000000000000000
180000000000000000000000000000000000000000000000000000000000000
200000000000000000000000000000000000000000000000000000000000000
220000000000000000000000000000000000000000000000000000000000000
250000000000000000000000000000000000000000000000000000000000000
280000000000000000000000000000000000000000000000000000000000000
320000000000000000000000000000000000000000000000000000000000000
360000000000000000000000000000000000000000000000000000000000000
400000000000000000000000000000000000000000000000000000000000000
450000000000000000000000000000000000000000000000000000000000000
500000000000000000000000000000000000000000000000000000000000000
560000000000000000000000000000000000000000000000000000000000000
630000000000000000000000000000000000000000000000000000000000000
710000000000000000000000000000000000000000000000000000000000000
800000000000000000000000000000000000000000000000000000000000000
900000000000000000000000000000000000000000000000000000000000000
1000000000000000000000000000000000000000000000000000000000000000
1100000000000000000000000000000000000000000000000000000000000000
1250000000000000000000000000000000000000000000000000000000000000
1400000000000000000000000000000000000000000000000000000000000000
1600000000000000000000000000000000000000000000000000000000000000
1800000000000000000000000000000000000000000000000000000000000000
2000000000000000000000000000000000000000000000000000000000000000
2200000000000000000000000000000000000000000000000000000000000000
2500000000000000000000000000000000000000000000000000000000000000
2800000000000000000000000000000000000000000000000000000000000000
3200000000000000000000000000000000000000000000000000000000000000
3600000000000000000000000000000000000000000000000000000000000000
4000000000000000000000000000000000000000000000000000000000000000
4500000000000000000000000000000000000000000000000000000000000000
5000000000000000000000000000000000000000000000000000000000000000
5600000000000000000000000000000000000000000000000000000000000000
6300000000000000000000000000000000000000000000000000000000000000
7100000000000000000000000000000000000000000000000000000000000000
8000000000000000000000000000000000000000000000000000000000000000
9000000000000000000000000000000000000000000000000000000000000000
10000000000000000000000000000000000000000000000000000000000000000
11000000000000000000000000000000000000000000000000000000000000000
12500000000000000000000000000000000000000000000000000000000000000
14000000000000000000000000000000000000000000000000000000000000000
16000000000000000000000000000000000000000000000000000000000000000
18000000000000000000000000000000000000000000000000000000000000000
20000000000000000000000000000000000000000000000000000000000000000
22000000000000000000000000000000000000000000000000000000000000000
25000000000000000000000000000000000000000000000000000000000000000
28000000000000000000000000000000000000000000000000000000000000000
32000000000000000000000000000000000000000000000000000000000000000
36000000000000000000000000000000000000000000000000000000000000000
40000000000000000000000000000000000000000000000000000000000000000
45000000000000000000000000000000000000000000000000000000000000000
50000000

AD-A147 663

SECURITY CLASSIFICATION OF THIS PAGE (When Data Entered) UNCLASSIFIED

(12)

REPORT DOCUMENTATION PAGE

READ INSTRUCTIONS BEFORE COMPLETING FORM

1. REPORT NUMBER	2. GOVT ACCESSION NO.	3. RECIPIENT'S CATALOG NUMBER

4. TITLE (and Subtitle)
ELECTRONIC STRUCTURE OF SEMICONDUCTOR INTERFACES

5. TYPE OF REPORT & PERIOD COVERED
FINAL REPORT: 1 Sept. 1979 - 31 May 1984

6. PERFORMING ORG. REPORT NUMBER

7. AUTHOR(s)
Frank Herman

8. CONTRACT OR GRANT NUMBER(s)
N00014-79-C-0814

9. PERFORMING ORGANIZATION NAME AND ADDRESS
International Business Machines Corp.
IBM Research Laboratory/5600 Cottle Road
San Jose, California 95193

10. PROGRAM ELEMENT, PROJECT, TASK AREA & WORK UNIT NUMBERS

11. CONTROLLING OFFICE NAME AND ADDRESS
Office of Naval Research, Dept. of the Navy
800 N. Quincy St., Arlington, VA 22217

12. REPORT DATE
1 November 1984

13. NUMBER OF PAGES
62

14. MONITORING AGENCY NAME & ADDRESS(if different from Controlling Office)
Defense Contract Administration Services
Management Area, San Francisco
1250 Bayhill Drive
San Bruno, California 94066

15. SECURITY CLASS. (of this report)
UNCLASSIFIED

15a. DECLASSIFICATION/DOWNGRADING SCHEDULE

16. DISTRIBUTION STATEMENT (of this Report)

Approved for Public Release - Distribution Unlimited

17. DISTRIBUTION STATEMENT (of the abstract entered in Block 20, if different from Report)

Approved for Public Release - Distribution Unlimited.

18. SUPPLEMENTARY NOTES

DTIC ELECTE NOV 23 1984 S E

19. KEY WORDS. Electronic Structure; Semiconductor Heterostructures; Artifically Layered Metals; Semiconductor Interfaces; Semiconductor Superlattices; Ferromagnetic-Antiferromagnetic Interfaces; Crystalline-Amorphous Interfaces; Ge/GaAs Heterostructures; Si/SiO_2 Interfaces; Passivating Oxide Layers; Schottky Barriers; $Pd_2Si/Si(111)$ Interfaces; Linearized Muffin Tin Orbital Method; Energy Band Calculations.

20. ABSTRACT. During the period covered by this contract, we carried out theoretical studies of the electronic structure of various types of interfaces, including (a) interfaces between different semiconductors, such as Ge and GaAs; (b) interfaces between semiconductors and insulators, such as Si and SiO_2; (c) interfaces between metals and semiconductors, such as Pd_2Si and Si; (d) interfaces between crystalline and amorphous semiconductors; and (e) interfaces between ferromagnetic and antiferromagnetic metals, such as Permalloy/MnFe and Co/Cr. Our overall goal was to elucidate the inter-relationship

DD FORM 1 JAN 73 1473

UNCLASSIFIED
SECURITY CLASSIFICATION OF THIS PAGE (When Data Entered)

DTIC FILE COPY

84 11 19 056

20. ABSTRACT (concluded)

between the atomic-scale structure of interfaces and their electronic, optical, and magnetic characteristics. For some of these systems, the effects of structural and chemical imperfections on interfacial properties were taken into account explicitly. Theoretical results were related to relevant experimental information where possible. In this Final Report, we will briefly summarize our major research studies, stating the objectives, the general approach, the principal conclusions, and where the subject stands today. Additional information may be found in the six representative research papers and reviews that are reproduced in the Appendices.

Contract Number N00014-79C-0814

ELECTRONIC STRUCTURE OF SEMICONDUCTOR INTERFACES

Frank Herman
IBM Research Laboratory
San Jose, California 95193

FINAL REPORT

Contract Period: 1 September 1979 - 31 May 1984
Contract Monitor: Dr. George B. Wright
Report Date: 1 November 1984

Approved for Public Release - Distribution Unlimited

Prepared for

Office of Naval Research
Department of the Navy
Arlington, Virginia 22217

Accession For
NTIS GRA&I ☒
DTIC TAB ☐
Unannounced ☐
Justification
By
Distribution/
Availability Codes
Dist | Avail and/or Special
A-1

FINAL REPORT

Office of Naval Research Contract Number: N 00014-79-C-0814
Contract Period: 1 September 1979 to 31 May 1984
Contract Monitor: Dr. George B. Wright

ELECTRONIC STRUCTURE OF SEMICONDUCTOR INTERFACES

Frank Herman, Principal Investigator
IBM Research Laboratory, San Jose, California 95193

This report concerns

ABSTRACT. During the period covered by this contract, we carried out theoretical studies of the electronic structure of various types of interfaces, including (a) interfaces between different semiconductors, such as Ge and GaAs; (b) interfaces between semiconductors and insulators, such as Si and SiO_2; (c) interfaces between metals and semiconductors, such as Pd_2Si and Si; (d) interfaces between crystalline and amorphous semiconductors; and (e) interfaces between ferromagnetic and antiferromagnetic metals, such as Permalloy/MnFe and Co/Cr. The overall goal was to elucidate the inter-relationship between the atomic-scale structure of interfaces and their electronic, optical, and magnetic characteristics. For some of these systems, the effects of structural and chemical imperfections on interfacial properties were taken into account explicitly. Theoretical results were related to relevant experimental information where possible. In this Final Report, we will briefly summarize our major research studies, stating the objectives, the general approach, the principal conclusions, and where the subject stands today. Additional information may be found in the six representative research papers and reviews that are reproduced in the Appendices.

TABLE OF CONTENTS

1. Introduction 2
2. Electronic Structure of [110] Ge/GaAs Interfaces 3
3. Electronic Structure of Si/SiO_2 Interfaces 5
4. Improved Computational Methods for Complex Crystals 6
5. Schottky Barrier Heights at $Pd_2Si/Si(111)$ Interfaces 7
6. Interfaces Between Crystalline and Amorphous Semiconductors 8
7. Ferromagnetic-Antiferromagnetic Metallic Multilayers 10
8. Other Publications 11
9. Professional Activities 12
10. Presentations 12
11. Acknowledgments 14
Appendix A. Semiconductor Interfaces 15
Appendix B. Silicon-Silicon Dioxide Interfaces 29
Appendix C. Complex Crystals 43
Appendix D. Schottky Barriers at Silicide-Silicon Interfaces 47
Appendix E. Crystalline Si - Amorphous Si Interfaces 51
Appendix F. Cobalt-Chromium Multilayers 57

1. INTRODUCTION

During the past decade, the study of artificially layered structures has become an increasingly important subject in condensed matter physics and solid state electronics. Progress in the controlled growth of semiconductor heterostructures and compositionally modulated metals has resulted in the synthesis of many new types of physical structures. Experimental and theoretical studies of inversion layers at semiconductor interfaces have provided a better understanding of the physical properties of confined two-dimensional electron gases. These studies have also led to the discovery of new and interesting phenomena such as the fractional quantum Hall effect, and to the invention and practical utilization of novel electronic devices such as the high electron mobility GaAs transistor. Future progress in VLSI and submicron electronics will undoubtedly reflect the results of current research on semiconductor heterostructures, passivating oxide overlayers, metal-semiconductor interfaces, and metallic multilayers.

For the past several years we have been studying the electronic structure and related physical properties of interfaces that play a key role in microelectronics. We have been particularly interested in understanding the relationship between the atomic-scale structure of interfaces and the local electronic structure, such as the energy level spectrum and the spatial range of interface states. Since we are dealing with very complex systems, it is necessary to represent actual interfaces by highly simplified but instructive atomic-scale models. Using these models, we can carry out first-principles electronic structure calculations, obtaining detailed information about localized interface states and related optical and magnetic properties. In many cases our theoretical results can be used directly to understand and interpret specific experimental results, or indirectly, to predict general trends.

During the period covered by this contract, we studied interfaces between (a) different semiconductors, such as Ge and GaAs; (b) semiconductors and insulators, such as Si and SiO_2; (c) metals and semiconductors, such as Pd_2Si and Si; and (d) different metals, such as Co and Cr. We also examined interfaces between crystalline and amorphous tetrahedrally coordinated semiconductors. Our earlier studies were concerned primarily with electronic and optical properties, while more recent ones focused on electronic and magnetic properties.

In the next several sections we will briefly summarize our major research studies, including the objectives, the general approach, the principal conclusions, and where the subject stands today. References to our publications are given at the end of the first section in which they are mentioned.

Additional information may be found in the representative research papers and reviews that are reproduced in the Appendices. We have not included all the papers we have published during this period, but only those that we feel will be of interest to the readers of this Final Report. We have excluded highly theoretical papers as well as those already published in widely available scientific journals such as the Journal of Chemical Physics, Physical Review, or Journal of Vacuum Science and Technology. Some of the papers appearing in the Appendices have been published in conference proceedings and research journals that are not as widely available, while others are still in press.

2. ELECTRONIC STRUCTURE OF [110] Ge/GaAs INTERFACES

Our earliest study in this field[1] was devoted to the prototypic atomically abrupt heterojunction between lattice-matched semiconductors, namely, the non-polar [110] interface between Ge and GaAs. For simplicity, we considered [110] Ge/GaAs superlattices having repeat periods of 8 and 12 layers. There are two atoms per layer, so that the unit cells contain 16 and 24 atoms. Of these, 8 atoms lie at the surfaces of the Ge and GaAs slabs, while the remaining (8 and 16) atoms lie inside these slabs. The 8-layer model is the simplest that can be used to study [110] Ge/GaAs interfaces, while the 12-layer model is somewhat more accurate. Both models are pictured in Fig. 1 below.

If one calculates the electronic structure of these superlattices, one would expect to find localized interface states associated with the Ge-Ga and Ge-As bonds. Such interface states do indeed exist, but we find that none lies inside the range of the thermal gap, so that none of these states is electronically active, acting as a trap or as a recombination center. This is our most significant result. Moreover, we find that all atomic layers are electrically neutral (there is no interlayer charge transfer), and that the interface orbitals are quite compact, being confined almost entirely to the interfacial layers. For this reason adjacent interfaces in our superlattice models are effectively isolated from one another. In short, the discontinuities in chemical composition (Ge to GaAs) and crystal structure (diamond to sphalerite) are not sufficiently large to produce interface states in the thermal gap.

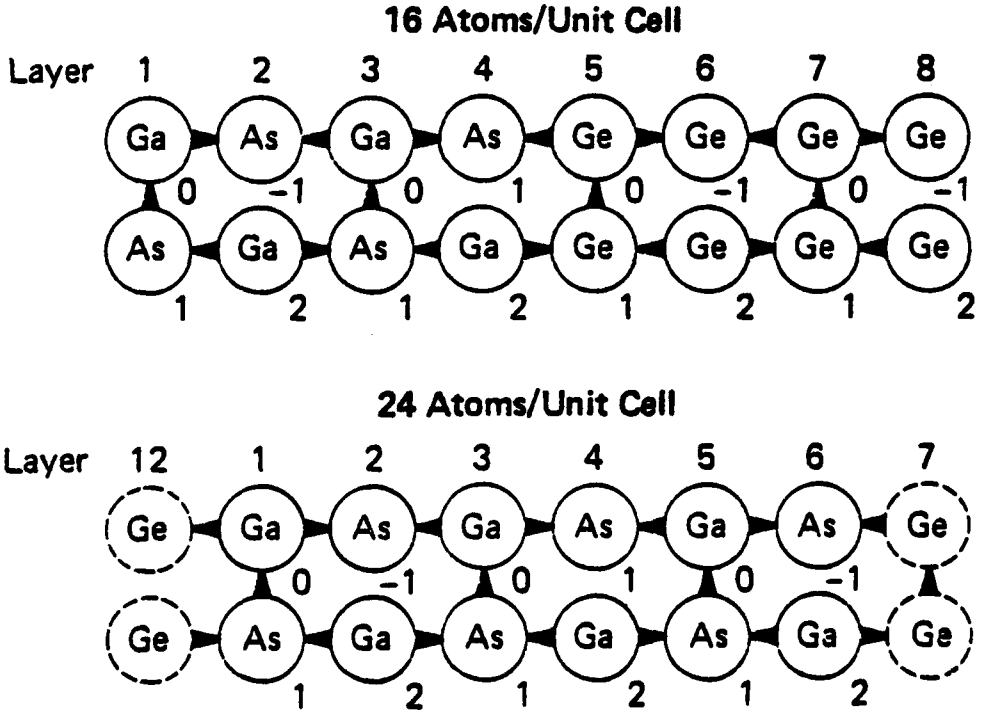

Fig. 1 Atomic arrangements of [110] Ge/GaAs superlattices with 16 and 24 atoms per unit cell. The numbers to the right and below the atoms indicate the coordinates in the direction perpendicular to the page. In the lower panel, the bulk Ge layers are not shown but their arrangement is readily inferred. After. Ref. 1.

Further studies suggest that interface states in the thermal gap can only be produced by substantially larger discontinuities, such as those associated with interfacial vacancies or misfit dislocations and characterized by dangling bonds.

Since the band gaps of Ge and GaAs differ by several tenths of an eV, it would be useful to know how much of this band offset takes place at the conduction band edge, and how much at the valence band edge. Numerical results for band offsets are very sensitive to the computational details of the calculation. Our calculations[1] were not sufficiently detailed to allow us to obtain accurate values for the band offsets, but qualitatively we found that the conduction band offset is considerably larger than the valence band offset. So far as we are aware, accurate numerical results for band offsets have not yet been obtained for any heterostructure by first-principles methods, nor have systematically accurate results been obtained for a large class of heterostructures by semi-empirical methods.

Although our own work and that of others has elucidated the nature of idealized [110] Ge/GaAs interfaces, the experimental situation has proved to be far more complicated than anybody imagined originally. Because of interatomic diffusion and interfacial chemical reactions, the atomic-scale structure of actual Ge/GaAs interfaces is still not understood. Band offsets have been measured for various crystallographic orientations, but the measured results are undoubtedly influenced by structural and chemical abnormalities at the interfaces that are ignored in the idealized models used by ourselves and others. It is difficult to make further theoretical progress on Ge/GaAs heterostructures because of the uncertain nature of the atomic-scale structure.

There have been many experimental attempts to grow atomically abrupt Ge/GaAs interfaces, but interfacial diffusion and interfacial chemical reactions have frustrated all of these efforts. The Ge/GaAs system continues to be of great scientific interest because of its inherent simplicity — at least in principle — but this system has not yet been exploited for practical purposes because of the difficulties encountered in growing atomically abrupt, structurally perfect interfaces. Most practical research focuses on the more complicated $GaAs/Ga_xAl_{1-x}As$ system, which is more easily grown in near-perfect form.

Further information as well as detailed references concerning Ge/GaAs heterostructures may be found in our original paper,[1] in our summary of PCSI-9[2], and in two recent review articles.[3-4] Note that Ref. 4 is included in this report as Appendix A.

REFERENCES

1. F. Herman and R.V. Kasowski, "Electronic Structure of [110] Ge-GaAs Superlattices and Heterojunctions," Phys. Rev. B17, 672 (1978).
2. F. Herman, "Recent Developments in the Physics and Chemistry of Semiconductor Interfaces," in *Proceedings PCSI-9* (American Vacuum Society, New York, 1982), p. xli.
3. F. Herman, "Physics and Chemistry of Semiconductor Interfaces: Some New Directions," J. Vac. Sci. Techn. 21, 643 (1982).
4. F. Herman, "Electronic Structure of Semiconductor Interfaces," J. Phys. (Paris) Colloque 45 C5-375 (1984) (cf. Appendix A).

3. ELECTRONIC STRUCTURE OF Si/SiO_2 INTERFACES

The interface between Si and its native oxide is undoubtedly the most important interface in modern solid state electronics. Passivating oxide layers protect integrated circuits from environmental contaminants and also serve to isolate individual circuits from neighboring ones. Even though there is a vast literature on the Si/SiO_2 interface, our understanding of this interface is still rudimentary. Although the density of localized interface states has been reduced empirically to an acceptable minimum for present-day applications, there is still considerable interest in understanding the structural and chemical features responsible for residual interface states. It is anticipated that such knowledge will be used eventually to control or totally eliminate residual interface states in future device applications, for which present levels would be intolerable.

In order to come to grips with this interface, we developed an idealized structural model which ignores structural disorder in the oxide and replaces the amorphous SiO_2 with a crystalline form of SiO_2 (cristobalite) that can be lattice-matched to crystalline Si.[5-8] In this way we establish a computationally tractable model for the interface between crystalline Si and crystalline SiO_2. According to this model, roughly half the interfacial Si atoms are bonded to the SiO_2 region, while the remaining half are not. Because of the open nature of SiO_2, it is postulated that H, O, and OH groups can move through the oxide, and, upon reaching the interface, saturate most of the dangling bonds arising from the partially bonded Si atoms at the interface. Clearly, the motion and concentration of these species will depend strongly on growth conditions.

On the basis of this simple model of the Si/SiO_2 interface, we investigated the nature of localized electronic states arising from various types of structural defects located at or near this interface.[6-8] The results are too detailed to summarize here, but some defects were shown to give rise to levels that lie within the Si thermal gap, while others produced levels that overlap the Si valence and conduction bands and hence are electrically inactive. The most important electronically active defects are unsaturated Si atoms at the interface. In order to make further progress, it would be necessary to deal not only with the Si substrate and the oxide overlayer, but also with the H, O, and OH species that take part in the formation of the interface.

Recent experimental work has shown that the Si/SiO_2 interface is almost atomically abrupt, spanning one or two atomic layers of strained Si substrate and one or two SiO_2 layers. In our idealized model, the interface is atomically abrupt, but there is considerable lattice strain at the interface which, if relieved, would extend the effective range of the interface to a few atomic layers on either side, in agreement with experimental indications.

In more recent work (cf. Section 6), we made a start toward constructing interfaces between crystalline and amorphous semiconductors. Judging by the results obtained thus far for the interface between crystalline and amorphous Si, we expect to be able to obtain an atomic-scale model for the interface between crystalline Si and amorphous SiO_2. This model would be more realistic than the idealized model described above, in that structural disorder at the interface is taken into account explicitly. However, we would still expect a significant number of dangling Si bonds to be present at or near the interface. We believe that these dangling bonds are the principal source of localized interface states in the thermal gap of Si. In practice, we would expect more of these states to be eliminated by the saturation of

dangling bonds by H, O, and OH groups than by structural rearrangements (lattice relaxation). We believe that further insight into the nature of the Si/SiO_2 interface will come only after the formation and growth of this interface is modeled theoretically, taking into account the role played by co-existing H, O, and OH species.

For further information and detailed references concerning the Si/SiO_2 interface, see Refs. 5 through 8. Note that Ref. 7 appears in this report as Appendix B.

REFERENCES

5. F. Herman, I.P. Batra, and R.V. Kasowski, "Electronic Structure of a Model Si-SiO_2 Interface," in *The Physics of SiO_2 and its Interfaces*, edited by S.T. Pantelides (Pergamon Press, New York, 1978), p. 333.
6. F. Herman, D.J. Henderson, and R.V. Kasowski, "Electronic Structure of Vacancies and Interstitials in SiO_2," in *The Physics of MOS Insulators*, edited by G. Lucovsky, S.T. Pantelides, and F.L. Galeener (Pergamon Press, New York, 1980), p. 107.
7. F. Herman, "Electronic Structure of the Si-SiO_2 Interface," in *Insulating Films on Semiconductors*, edited by M. Schulz and G. Pensl (Springer-Verlag, Berlin, 1981) p. 2 (cf. Appendix B).
8. F. Herman and R.V. Kasowski, "Electronic Structure of Defects at Si-SiO_2 Interfaces," J. Vac. Sci. Techn. 19, 395 (1981).

4. IMPROVED COMPUTATIONAL METHODS FOR COMPLEX CRYSTALS

In addition to preparing a review paper on computational methods for surfaces, overlayers, and interfaces,[9] we wrote two original theoretical papers suggesting improvements in the treatment of complex crystals by the extended muffin-tin orbital (EMTO) method.[10,11] By complex crystals we mean not only bulk crystals containing a large number of atoms per unit cell, but also superlattices, including atomic layers chemisorbed on crystalline substrates and represented by repeating slab geometries. At present, self-consistent EMTO programs are being refined (principally by Kasowski and his associates) so that these programs could be used to determine total energies and optimal atomic geometries. We expect the improvements proposed in Refs. 10 and 11 to be incorporated in next-generation EMTO computer programs.

The detailed formalism of our theoretical approach appears in Ref. 10. The essential ideas are summarized in Ref. 11, which is included in this report as Appendix C.

9. F. Herman, "Electronic Structure Calculations of Interfaces and Overlayers in the 1980's," J. Vac. Sci. Techn. 16, 1101 (1979).
10. F. Casula and F. Herman, "Generalized Muffin-Tin Orbitals for Electronic Structure Studies of Surfaces, Interfaces, and Organic Solids," J. Chem. Phys. 78, 858 (1983).
11. F. Herman and F. Casula, "Electronic Structure Calculations for Complex Crystals," Nuovo Cimento 2D, 1636 (1983) (cf. Appendix C).

5. ELECTRONIC STRUCTURE AND SCHOTTKY BARRIER HEIGHTS AT Pd_2Si/Si(111) INTERFACES

One of the most interesting problems in the physics of semiconductor interfaces is the nature of rectifying metal-semiconductor contacts. In particular, what are the mechanisms primarily responsible for rectifying (Schottky) barriers at such contacts? In order to come to grips with this subject, we decided to study a particularly simple but technologically important system, namely, epitaxially grown Pd overlayers on Si(111) substrates.[4,12]

On the basis of LMTO electronic structure calculations, we concluded that hybridized Pd-Si states at the interface could not by themselves account for measured Schottky barriers heights, and that another mechanism or structural feature had to be invoked. After examining various possibilities, we conjectured that Pd atoms moved into the Si substrate in advance of a growing interface, and that these Pd atoms could form triangular clusters, these being precursors to the arrangement of Pd atoms in Pd_2Si. According to our model, two adjacent Si atoms are replaced by a triangular Pd cluster lying in the plane bisecting the bond between the two Si atoms that have been removed. That is to say, Si divacancies are replaced by Pd_3 clusters.

We also noted that Pd_3 clusters are more easily accommodated in hexagonal Si than in cubic Si because of the different shapes of the interstitial cavities in these two structures. We reasoned that the presence of Pd_3 clusters in the region ahead of the growing interface would cause the Si layers to grow with the hexagonal rather than the cubic stacking sequence. The net effect would be a transition layer of hexagonal Si between the Pd_2Si overlayer and the cubic Si substrate. Since hexagonal Si has a smaller band gap than cubic Si, the effective band gap at the Pd_2/hexagonal-Si interface would be a few tenths of an eV less than at a Pd_2/cubic-Si interface, this reduction being sufficient to account for the measured Schottky barrier height for this system.

Some attempts have been made to observe triangular Pd clusters and hexagonal stacking experimentally, but so far there is no direct evidence in favor of this model. However, the idea of stacking disorder has been used recently to account for some features of the reconstructed Si(111) 7x7 surface. Interstitial Pd atoms have also been invoked in other models of the Pd_2Si/Si(111) interface.

The epitaxially grown Pd_2Si/Si(111) interface continues to be of interest because of the nearly perfect lattice match, and because only one silicide forms when Pd is reacted with Si. Many different models for the interfacial atomic structure have been proposed, but there is still no common agreement among different investigators. It is anticipated that much more work will have to be done before this system — which is one of the simplest — is understood. We believe that our own work is significant because it is the first to call attention to the possibility of stacking disorder in the neighborhood of internal surfaces as a possible factor determining Schottky barrier heights.

For further details, see our original paper,[12] which appears in this report as Appendix D. See also Ref. 4, which is reproduced in Appendix A.

12. F. Herman, F. Casula, and R.V. Kasowski, "Electronic States and Schottky Barriers at Pd_2Si/Si(111) Interfaces," Physica 117B-118B, 837 (1983) (cf. Appendix D).

6. INTERFACES BETWEEN CRYSTALLINE AND AMORPHOUS TETRAHEDRALLY COORDINATED SEMICONDUCTORS

Ball-and-stick models of disordered regions and of interfaces between ordered and disordered regions have been constructed by hand by various investigators. We do not regard these models as trustworthy because they represent the outcome of a long series of subjective and largely arbitrary human judgments. One can usually fashion a structure that satisfies one's own preconceived notions. For example, a model of amorphous Si containing no dangling bonds can be built in the form of a continuous random network, but is this what actually occurs in nature? We thought it would be useful to develop a fully automatic method for constructing interfaces between crystalline and amorphous semiconductors, thereby avoiding subjective influences. Our approach is based on a set of rules according to which such interfaces can be constructed by computer without human intervention. Of course, the rules embodied in the computer programs represent plausible physical and chemical constraints, such as tetrahedral coordination, most likely bond lengths and bond angles, etc.

For mathematical purposes we begin with a superlattice composed of alternating slabs of ordered and disordered close-packed hard spheres. The interaction between spheres is represented by a Lennard-Jones potential. The ordered slabs have the face-centered cubic structure, while the disordered slabs are characterized by random close-packing. These slabs may be regarded as co-existing frozen and melted regions of hard-sphere systems held together by Lennard-Jones forces.

Treating the centers of these spheres as the vertices of regular or irregular tetrahedra, we can select a subset of these centers which forms a network of tetrahedra and in contact only at their vertices. That is to say, adjacent tetrahedra touch at vertices but not along common edges. In the ordered regions this tetrahedral network (or simplicial graph) includes all the sphere centers, while in the disordered regions most but not all the sphere centers belong to the tetrahedral network. We now examine each of the tetrahedra in turn and discard those having highly irregular shapes. We then place Si atoms at the vertices of all the tetrahedra still belonging to the network. We also place atoms at the centroids of these tetrahedra. Finally, we join each centroid atom to its four vertex atoms, thus establishing tetrahedrally coordinated chemical bonds between centroid and neighboring vertex atoms.

In the ordered regions, this procedure generates a diamond lattice, with each centroid atom and each vertex atom lying at the center of a regular tetrahedron. In the disordered regions and at interfaces, this procedure generates a discontinuous random network which is for the most part tetrahedrally coordinated. Here all centroid atoms have four nearest neighbors lying at the vertices of their tetrahedra. However, not all vertex atoms are shared by four touching tetrahedra, so that many vertex atoms have fewer than four nearest neighbor atoms. At the completion of this first stage of the construction, the atomic positions have not yet been relaxed, still being determined by the frozen and melted hard sphere Lennard-Jones systems with which we started. We have already published a brief account of this first stage.[13]

At the end of Stage I, the interface extends over a few atomic layers. The average coordination number in the interior of disordered regions is 3, and this rapidly increases to 4 in the neighborhood of interfaces. Thus, the model is characterized by many dangling bonds in the disordered regions. The number of dangling bonds decreases rapidly as one passes

through the interfacial region into the ordered regions. We have also calculated the electronic density of states for this model using the recursion method, and we find a direct correlation between the number of dangling bonds in a given layer and the layer density of electronic states in the thermal gap.

The second stage of the construction is now in progress. During this stage the model is improved in two important respects. First, the lattice is relaxed in accordance with a semi-empirical potential energy function of the Keating type. Second, bonds are formed between nearby pairs of atoms which have dangling bonds at the end of Stage I. Most but not all of the Stage I dangling bonds are eliminated during Stage II, leading to a considerably more realistic atomic-scale model. In the third stage, now being designed, there will be a random interchange of adjacent vertex and centroid atoms in the disordered regions and at the interfaces, so that the original distinction between these two types of atoms will be eliminated. The interchange is being patterned after that used recently by Weaire and Wooten in their computer generated models of bulk amorphous Si.

The construction as it stands applies equally to interfaces between crystalline and amorphous C, Si, Ge, and grey Sn. The construction is readily generalized to deal with interfaces between crystalline Si and amorphous SiO_2. The model automatically includes dangling bonds at and near the interfaces. One can saturate some or all of these dangling bonds by diffusing H, O, and OH groups into the structure in accordance with prescribed statistical rules. This can be done during or after the second stage of construction, thereby simulating different oxide and interface growth conditions.

We believe that computer modeling of the growth of semiconductor interfaces will provide new insights into the nature of the structural defects that occur naturally during interface growth.[4] The present study,[13] which appears here as Appendix E, represents a step in this direction.

13. F. Herman and P. Lambin, "Electronic Structure of Interfaces between Crystalline and Amorphous Tetrahedrally Coordinated Semiconductors," *Proceedings of the 17th International Conference on the Physics of Semiconductors* (Springer-Verlag, Berlin, 1984) in press (cf. Appendix E).

7. FERROMAGNETIC-ANTIFERROMAGNETIC INTERFACES AND MULTILAYERS

During the past year we broadened our interests to include interfacial problems involving magnetic materials. As a means for getting into this new field and learning the experimental situation, we wrote a review paper dealing with exchange and magnetocrystalline anisotropy.[14] During a search for idealized models, our attention was drawn to jellium, which can be paramagnetic, ferromagnetic, or antiferromagnetic depending on the electron density. This led us to study phase transitions in jellium.[15] Our work yielded more precise estimates of the densities at which phase transitions occur, but also indicated that the stability range for the ferromagnetic phase could be very narrow or nonexistent altogether. We had originally intended to construct interfaces between ferromagnetic and antiferromagnetic jellium, but since our calculations indicated that the stability range of the ferromagnetic state of jellium was too uncertain for our purposes, we abandoned this idea.

We then decided to study simplified but realistic interfaces rather than highly idealized electron gas models. Since we wanted to study close-packed metals, we switched from the extended muffin-tin orbital method — which is particularly useful for open structures — to the LMTO/ASA method of O.K. Andersen — which is among the most powerful methods presently available for carrying out first-principles, spin-polarized, self-consistent electronic and magnetic structure calculations for complex metallic systems.

Our first set of LMTO/ASA calculations dealt with interfaces between ferromagnetic Ni_3Fe and antiferromagnetic MnFe.[16] To avoid problems associated with structural disorder, we represented alloys by suitably chosen ordered compounds, and on this basis studied the exchange coupling across bilayers composed of Permalloy (75 percent Ni and 25 percent Fe) and 50-50 MnFe alloy. In practice, we studied spin distributions in superlattices composed of the ordered compounds Ni_3Fe (Cu_3Au structure) and MnFe (rocksalt structure). The spin distributions that we obtained are consistent with experiment.

Our second set of LMTO/ASA calculations dealt with interfaces between ferromagnetic Co and antiferromagnetic Cr.[17,18] We were again interested in understanding exchange coupling and spin distributions near ferromagnetic/antiferromagnetic interfaces. The Cr regions were represented by a theoretically stabilized commensurate antiferromagnetic spin arrangement which simulates its experimental counterpart, the impurity-stabilized commensurate antiferromagnetic phase of Cr. In the case of single Co layers separated by Cr multilayers, the coupling across the interfaces was ferromagnetic, while for Co multilayers separated by Cr multilayers, the coupling could be ferromagnetic or antiferromagnetic. The spin arrangements in the Cr regions could be weakly or strongly antiferromagnetic depending on the crystallographic orientation of the interfaces, and on the degree to which the commensurate antiferromagnetic phase of Cr is stabilized by the addition of suitable transition metal impurities.

We believe that Co/Cr multilayers will eventually be synthesized in the laboratory, and our calculations are intended to provide some insight into the magnetic structure of such multilayers, as a guide to the design and interpretation of future experiments. For further information, see Refs. 17 and 18. Ref. 17, an abbreviated version of Ref 18, appears here as Appendix F. We are also in the process of writing two additional papers on magnetic problems associated with interfaces.[19,20]

14. N.H. March, P. Lambin, and F. Herman, "Exchange and Magnetocrystalline Anisotropy in 3d Cooperative Magnets in Single- and Two-Phase Metallic Systems," J. Magnetism and Magnetic Materials (in press)
15. F. Herman and N.H. March, "Cooperative Magnetism in Metallic Jellium and in the Insulating Wigner Electron Crystal," Solid State Comm. 50, 725 (1984).
16. P. Lambin and F. Herman, "Electronic and Magnetic Structure of Idealized Metallic Multilayers: Ni_3Fe/FeMn System," Phys. Rev. B (in press).
17. F. Herman, P. Lambin, and O. Jepsen, "Electronic Structure of Idealized Cobalt-Chromium Multilayers," J. Appl. Phys. (in press): *Proc. 30th Annual Conf. Magnetism and Magnetic Materials* (cf. Appendix F).
18. F. Herman, P. Lambin, and O. Jepsen, "Electronic Structure of Idealized Cobalt-Chromium Superlattices," submitted to Phys. Rev. B
19. F. Herman, P. Lambin, and N.H. March, "Response of Antiferromagnetic Metals to Changes in Exchange Field" (in preparation).
20. F. Herman, P. Lambin, and N.H. March, "Description of Magnetic Inhomogeneities in Ferromagnetic Metals" (in preparation).

8. OTHER PUBLICATIONS

Carburized tungsten is of considerable interest because of its catalytic properties. In order to get some insight into the nature of this material, experimental efforts were undertaken at Stanford to understand the electronic structure of crystalline tungsten carbide, which provides a convenient structural model for carburized tungsten. As part of an IBM-Stanford collaboration, we calculated the energy band structure of tungsten carbide and contributed to the analysis of angular resolved photoemission spectra of tungsten carbide single crystals. Many of the salient features of these spectra were successfully interpreted on the basis of our theoretical band structure.[21,22] We also contributed to a theoretical study of the electronic structure of idealized lattice-matched Ge/Al interfaces.[23] We published the outline of two survey lectures on semiconductor interfaces presented at the 1983 Brazilian Summer School on Semiconductor Physics,[24] as well as a historical account of our early days in semiconductors[25] based on an interview conducted by Dr. Kris Szymborski on behalf of the International Project on the History of Solid State Physics.

21. P.M. Stefan, M.L. Shek, I. Lindau, W.E. Spicer, F. Herman, L.I. Johansson, and G. Brogren, "Electronic Structure and Photoemission Studies of Tungsten Carbide," J. Vac. Sci. Techn. 20, 622 (1982).
22. P.M. Stefan, M.L. Shek, I. Lindau, W.E. Spicer, L.I. Johansson, F. Herman, R.V. Kasowski, and G. Brogren, "A Photoemission Study of Tungsten Carbide (0001)," Phys. Rev. B 24, 5423 (1984).
23. I.P. Batra and F. Herman, "Electronic States in Model Ge-Al Interfaces," J. Vac. Sci. Techn. A1, 1080 (1983).
24. F. Herman, "Electronic Structure of Semiconductor Interfaces," Brazilian J. Phys., Special Volume: Physics of Semiconductors, (1983), p. 335.
25. F. Herman, "Elephants and Mahouts -- Early Days in Semiconductor Physics," Physics Today 37, 56, (1984).

9. PROFESSIONAL ACTIVITIES

Member, Organizing Committee, Workshop on Effective One-Electron Potentials in Real Materials, Ossining, New York, Mar. 21-22, 1980

Member, Organizing Committee, Annual Conferences on the Physics and Chemistry of Semiconductor Interfaces (PCSI), 1980-1984

Conference Chairman, Ninth Annual Conference on the Physics and Chemistry of Semiconductor Interfaces (PCSI-9), Asilomar, California, Jan. 27-29, 1982

Lecturer, Summer School of Semiconductor Physics, University of Campinas, Brazil, Feb. 8-9, 1983

Member, Executive Committee, 17th International Conference on the Physics of Semiconductors, San Francisco, California, Aug. 6-10, 1984

10. PRESENTATIONS

Electronic Structure of [110] Ge-GaAs Superlattices and Interfaces

- 5th Annual Conference on the Physics of Compound Semiconductor Interfaces, UCLA, Los Angeles, California, Jan. 17, 1978
- American Physical Society, Washington, D.C., Mar. 29, 1978

Electronic Structure of Model Si-SiO_2 Interfaces

- International Topical Conference on the Physics of SiO_2 and its Interfaces, IBM Yorktown Heights, New York, Mar. 22, 1978 (with I.P. Batra and R.V. Kasowski)
- Navy Workshop on Surfaces and Interfaces, Rockwell Science Center, Thousand Oak, California, Nov. 15, 1979
- Workshop on Si-SiO_2 Interfaces, Stanford University, Dec. 13, 1979
- American Physical Society, New York, Mar. 26, 1980 (with D.J. Henderson and R.V. Kasowski)

Electronic Structure of Cuprous Chloride

- American Physical Society, Chicago, Mar. 23, 1979 (with R.V. Kasowski)

Critique of $X\alpha$ and $X\alpha\beta$ Methods

- Workshop on Effective One-Electron Potentials in Real Materials, Ossining, New York, Mar. 21-22, 1980 (Invited Paper)

Electronic Structure of Vacancies and Interstitials in SiO_2

- Topical Conference on the Physics of MOS Insulators, Raleigh, North Carolina, June 18-20, 1980 (with D.J. Henderson and R.V. Kasowski)
- 8th Annual Conference on the Physics of Compound Semiconductor Interfaces, Williamsburg, Virginia, Jan. 27-29, 1981.

Energy Band Theory - Elementary Solid State Physics Course

- IBM Research Laboratory, San Jose, California, June 29, 1980

Electronic Structure of Idealized Si-SiO_2 Superlattices and Interfaces

- Materials Research Society, Boston, Mass., Nov. 16-20, 1980 (with D.J. Henderson and R.V. Kasowski)

Interaction of CN Molecules with Smooth and Microscopically Rough Silver Surfaces

- American Physical Society, Phoenix, Arizona, Mar. 18, 1981

Improved Basis Sets for Linearized-Muffin-Tin-Orbital Calculations

- American Physical Society, Phoenix, Arizona, Mar. 18, 1981 (with F. Casula)

Electronic Structure of Poly p-Phenylene Sulphide

- American Physical Society, Phoenix, Arizona, Mar. 19, 1981

Interpretation of Angle-Integrated and Angle-Resolved Photoemission Measurements on Tungsten Carbide

- American Physical Society, Phoenix, Arizona, Mar. 19, 1981 (with P. Stefan and W.E. Spicer)

Electronic Structure of the Si-SiO_2 Interface

- Condensed Matter Group, Cambridge University, United Kingdom, Apr. 22, 1981
- Max-Planck-Institute for Solid State Research, Stuttgart, Germany, Apr. 24, 1981
- International Conference on Insulating Films on Semiconductors, Erlangen, Germany, Apr. 27, 1981 (Invited Paper)
- University of Dortmund, Germany, May 1, 1981
- Laboratory for the Physics of Solids, University of Paris VI, France, May 5, 1981
- Institute of Solid State Physics, Autonomous University, Cantoblanco, Madrid, Spain, May 8, 1981
- IBM Yorktown Heights, May 13, 1981

Angle-Resolved Photoemission Results from Tungsten Carbide [0001],

- American Vacuum Society, Anaheim, California, Nov. 1, 1981 (with P. Stefan and W.E. Spicer)

Electronic Band Structure of Tungsten Carbide

- American Physical Society, Dallas, Texas, Mar. 8, 1982 (with R.V. Kasowski, P. Stefan, and W.E. Spicer)

Recent Developments in the Physics and Chemistry of Semiconductor Interfaces

- Surface Science and Catalysis Science Seminar, Lawrence Radiation Laboratory, Berkeley, California, Mar. 18, 1982
- Solid State Physics Seminar, University of California at Irvine, Apr. 5, 1982
- Solid State Physics Seminar, Institute of Physics, Univ. of Cagliari, Italy, Sept. 20, 1982

Electronic Structure and Schottky Barriers at Pd_2 Si-Si(111) Interfaces

- 16th International Conference on the Physics of Semiconductors, Montpellier, France, Sept. 8, 1982 (with F. Casula and R.V. Kasowski)
- American Physical Society, Los Angeles, California, Mar. 21, 1983

Electronic Structure Calculations for Complex Crystals

- 5th International Conference on Ternary and Multinary Compounds, Cagliari, Italy, Sept. 14, 1982 (with F. Casula)

Electronic States in Model Ge-Al Interfaces

- American Vacuum Society, Baltimore, Maryland, Nov. 17, 1982 (with I.P. Batra)

Impact of Large-Scale Scientific Computation on Solid State Physics and Quantum Chemistry

- Laboratory for Scientific Computation, Rio de Janeiro, Brazil, Feb. 2, 1983

Two Lectures on Semiconductor Interfaces

- Summer School on Semiconductor Physics, University of Campinas, Brazil, Feb. 8 and 9, 1983

Electronic Structure of Semiconductor Interfaces

- International Conference on the Dynamics of Interfaces, Lille, France, Sept. 15, 1983 (Invited Paper)
- Solid State Physics Seminar, Max Planck Institute for Solid State Research, Stuttgart, Germany, Sept. 21, 1983

Cooperative Magnetism in Metallic Jellium and in the Insulating Wigner Electron Crystal

- American Physical Society, Detroit, Mar. 26, 1984 (with N.H. March)

Electronic and Magnetic Structure of Idealized Ferromagnetic - Antiferromagnetic Multilayers

- American Physical Society, Detroit, Mar. 26, 1984 (with P. Lambin)

Electronic and Magnetic Structure of Idealized Cobalt-Chromium Multilayers

- American Physical Society, Detroit, Mar. 26, 1984 (with P. Lambin and O. Jepsen)

Electronic Structure of Interfaces between Crystalline and Amorphous Tetrahedrally Coordinated Semiconductors

- 17th International Conference on the Physics of Semiconductors, San Francisco, Aug. 7, 1984 (with P. Lambin)

11. ACKNOWLEDGMENTS

We are grateful to the Office of Naval Research, particularly Dr. George B. Wright, for continuing interest and partial financial support. Much of this research was done in collaboration with two IBM World Trade Fellows, Dr. Francesco Casula of the University of Cagliari, Italy, and Dr. Philippe Lambin of the Facultes Universitaires, Notre Dame de la Paix, Namur, Belgium. We are grateful to IBM Italy and IBM Belgium for their interest and partial financial support. Our other principal collaborators include Dr. Robert V. Kasowski, Dupont Experimental Station, Wilmington, Delaware; Prof. Norman H. March, Oxford University; Dr. Ove Jepsen, Max Planck Institute for Solid State Research, Stuttgart, West Germany; Prof. William E. Spicer and Dr. Peter M. Stefan, Stanford University; and Drs. Inder P. Batra and Douglas J. Henderson, IBM San Jose Research Laboratory. Finally, we wish to express our appreciation to various members of the IBM San Jose Research Laboratory management, particularly Drs. George Castro, Edward M. Engler, Eric Kay, Richard L. Greene, and Jerry B. Torrance, for their continuing interest and encouragement.

Invited Paper Presented at the International Conference on the Dynamics of Interfaces, Lille, France, September 12 to 16, 1983. Publication: Journal de Physique (Paris), Colloque 45 C5-375 (1984).

ELECTRONIC STRUCTURE OF SEMICONDUCTOR INTERFACES*

Frank Herman, IBM Research Laboratory
San Jose, California 95193 USA

Résumé. — Bien que nous ayons aujourd'hui une bonne compréhension de la structure électronique des interfaces idéaux entre semi-conducteurs, incluant la nature des états localisés d'interface, des études expérimentales récentes suggèrent que la structure atomique des interfaces réels est considérablement plus complexe que celle décrite par les modèles idéalisés utilisés en recherche théorique actuelle. Pour comprendre plus complètement les propriétés électroniques des interfaces, il est donc essentiel de développer une modèlisation plus réaliste de la structure atomique de ces interfaces. Nous illustrerons les points faibles et les points forts des théories d'aujourd'hui par une discussion de la structure électronique des interfaces Ge/GaAs, Si/SiO_2 et $Pd_2Si/Si(111)$. Nous discuterons également le développement de modèles atomiques améliorées d'interface entre semi-conducteurs cristallins et amorphes.

Abstract. — Although we now have a good understanding of the electronic structure of idealized semiconductor interfaces, including the nature of localized interface states, recent experimental studies suggest that the atomic structure of actual interfaces is considerably more complicated than that described by the idealized models used in current theoretical research. If we are to understand the electronic properties of interfaces more fully, it is essential that we develop more realistic structural models for interfaces. We will illustrate the strengths and weaknesses of present-day theories by discussing the electronic structure of Ge/GaAs, Si/SiO_2, and $Pd_2Si/Si(111)$ interfaces. We will also discuss the development of improved atomic-scale models for interfaces between crystalline and amorphous semiconductors.

I. INTRODUCTION

One of the most exciting and rapidly expanding subjects in solid state physics is the study of semiconductor heterostructures and superlattices.[1-4] Improved crystal growth techniques such as molecular beam epitaxy,[5] and the development of refined surface-sensitive spectroscopies, have stimulated wide-ranging scientific[1-3] and technological[4] research efforts on such systems as Ge/GaAs, $Al_xGa_{1-x}As/GaAs$, and InAs/GaSb. Recent improvements in sample preparation and measurement techniques have also inspired fundamental studies of technologically important interfaces such as oxide-passivated silicon surfaces[6-8] and rectifying metal-semiconductor contacts.[9,10]

In this paper we will sketch the present state of our understanding of the electronic structure of some important types of semiconductor interfaces. Most of our current ideas are based

on simple, highly idealized atomic interface models. For purposes of discussion, we will define the ideal semiconductor interface as the atomically abrupt boundary between two lattice-matched, crystallographically compatible constituents. It is assumed that each of the constituents has its bulk crystal structure right up to the interface, that there is exact lattice registry at the interface, and that there are no dangling bonds at or near the interface. If the two constituents are not exactly lattice-matched, it is assumed that the residual strain is relieved by well-separated misfit dislocations. By using crystals or alloys having different chemical compositions, crystal structures, and doping profiles, it is possible to synthesize heterostructures having a wide range of physical characteristics.

Recent experimental studies indicate that some semiconductor systems, such as $Al_xGa_{1-x}As/GaAs$[1] and strained-layer superlattices,[11] can be made smooth on the scale of a single atomic layer, and can be grown almost free of imperfections. The availability of nearly ideal interfaces and interfacial arrays (heterostructures and superlattices) is of course of the greatest scientific and technological importance. Most interfaces, however, contain a wide variety of structural and chemical imperfections; much current research is concerned with the identification, modification, or reduction of these imperfections.

II. SEMICONDUCTOR HETEROJUNCTIONS: Ge/GaAs INTERFACES

Because of its apparent simplicity, the Ge/GaAs system has been widely studied. Ge and GaAs have compatible crystal structures and nearly identical lattice constants (Ge: 5.65735 A; GaAs: 5.6537 A). Since the band gaps of GaAs and Ge differ by 0.9 eV, and the conduction band edges occur at different positions in the reduced zone, there must be a band structure discontinuity at the interface which can be represented by valence and conduction band offsets. In principle, these offsets can be different for interfaces having different crystallographic orientations.

It is important to know the band offsets because they determine the depth of quantum wells in heterostructures such as GaAs/Ge/GaAs and in superlattices. Theoretical estimates[12,13] of band offsets and experimental measurements[14] are only in rough agreement with one another. This is hardly surprising: some of the estimates are based on oversimplified models,[12] while the more detailed estimates[13] are usually based on idealized interface models which may differ in some important respects from real interfaces.

The discontinuity in crystal potential associated with the changes in crystal structure and chemical composition across the interface may give rise to localized electronic states. When the energies of such states lie within the thermal gap, they can serve as trapping and recombination centers, and hence are of considerable importance. (By thermal gap we mean the energy range between the highest occupied valence band level and the lowest unoccupied conduction band level.) Since the Ge/GaAs interface discontinuity is substantially weaker than the discontinuity at a free Ge or GaAs surface, interface states are pushed out of the valence and conduction bands to a much lesser extent than intrinsic surface states are.

Theoretical studies of ideal non-polar (110) Ge/GaAs interfaces[15-17] demonstrate that localized interface states do not extend into the thermal gap. But localized states associated with the Ge-Ga and Ge-As bonds at the interface do occur within the "stomachs" of the projected valence and conduction bands and in the forbidden band just outside thermal gap.

Localized interface states associated with Ge overlayers on GaAs have been detected by photoemission.[18]

In the case of ideal polar (100) Ge/GaAs interfaces, theoretical studies[19,20] indicate that localized interface states form a band that extends into the thermal gap. Since the Fermi level passes through this interface band, this ideal interface would exhibit metallic behavior, contrary to experimental results. It must be concluded, therefore, that ideal (100) interfaces are not actually formed. It is possible that the metallic interface band is eliminated by interfacial relaxation or reconstruction, or by local interdiffusion and reordering.[21] It is conceivable that some macroscopic polar interfaces are composed primarily of non-polar terraces and steps on an atomic scale.

Recent experimental studies[22,23] suggest that Ge/GaAs interfaces are considerably more complicated chemically and structurally than was originally believed. Because of the similarity in atomic size of Ge, Ga, and As, it is difficult to prevent interdiffusion, so that interfaces tend to be diffuse rather than atomically abrupt. Moreover, it is found that interfacial chemical reactions take place, and that the interface is rough on an atomic scale. When GaAs is grown on Ge, antiphase boundaries can be formed in the growing GaAs, further complicating the interfacial structure. Some attempts have already been made to incorporate various types of defects into interface calculations.[13] However, much remains to be done before we have an adequate understanding of the effects of chemical impurities, vacancies, interstitials, antisite defects, and stoichiometric mixing on interfacial electronic structure and properties. The same applies for misfit dislocations, stacking disorder, relaxation, and reconstruction.

III. PASSIVATING OXIDE LAYERS: Si/SiO_2 INTERFACES

It is well known that suitably oxidized silicon substrates are protected from environmental contaminants and have rather low densities of localized interface states in the thermal gap. Because of the important role that surface passivation plays in MOS technology,[24] there is strong motivation for understanding the physics and chemistry of the Si/SiO_2 interface.[6-8] In this section we will be concerned with the atomic-scale structure of the Si/SiO_2 interface, including the residual defects that occur near well-prepared Si/SiO_2 interfaces and give rise to residual trapping sites and fixed charge.

In contrast to the Ge/GaAs interfaces that we have been dealing with so far, the Si/SiO_2 interface connects a crystalline substrate (Si) to a non-crystalline overlayer (vitreous SiO_2, abbreviated v-SiO_2). Whatever the nature of this interface actually is on an atomic level, the observed low density of interface states is compelling evidence for the fact that nearly all of the silicon atoms on the substrate surface have their bonds saturated one way or another. How does this come about?

Before discussing the Si/SiO_2 interface itself, it is desirable to say a few words about bulk v-SiO_2. It is generally believed[25] that a non-crystalline material such as v-SiO_2 can be represented by a continuous random network (CRN) of SiO_4 tetrahedra joined to one another at their common oxygen positions, so that all Si and O bonds are saturated. Computer simulation studies[25,26] indicate that the distributions of Si-O bond lengths and O-Si-O angles are relatively narrow, so that the SiO_4 tetrahedra maintain their structural integrity

even when embedded in v-SiO_2. In contrast, the distribution of Si-O-Si bond angles involving adjacent tetrahedra is relatively broad. Undoubtedly, the random structure of the SiO_4 tetrahedra in v-SiO_2 is made possible by the softness of the Si-O-Si bond angle. The fact that the SiO_4 tetrahedra can accommodate themselves to different SiO_2 crystal structures must also reflect this bond angle softness. In the present context, this softness would be expected to play an important role in accommodating v-SiO_2 to a crystalline Si substrate.

What is the exact nature of this contact? Is the silicon substrate atomically smooth or rough? Does it have steps and terraces? Are the outermost silicon layers strained to accommodate the SiO_2 overlayer? Is there a transition region between the Si substrate and the "bulk" v-SiO_2 which extends over several atomic layers, or is the transition atomically abrupt? If there is a gradual change in average composition, described by the stoichimetric formula SiO_x, where x ranges from 0 (at Si) to 2 (at v-SiO_2), what are the bonding arrangements that contribute to this average composition? We do not have the space to summarize recent experimental evidence bearing on these questions,[24] so we will limit ourselves to discussing some of these issues in terms of two recently developed theoretical models which are highly idealized but nevertheless instructive.

The first of these is a ball-and-stick model developed by Pantelides and Long[27] to demonstrate that an atomically abrupt Si/SiO_2 interfaces can be formed between a CRN model of v-SiO_2 and the (100) face of Si. Using the same Si-O bond length everywhere, they were able to connect v-SiO_2 to Si on the scale of one atomic layer, but they had to distort many of the O-Si-O and Si-O-Si bond angles near the interface considerably to avoid introducing dangling bonds. The successful construction of this ball-and-stick model dramatically demonstrates the adaptability of v-SiO_2 to a silicon substrate, but does not prove that such an atomically abrupt Si/SiO_2 interface would actually form under experimental conditions.

Since the more distorted bond angles are energetically unfavorable, and hence unlikely to be realized in nature, it appears necessary to incorporate two additional ingredients into the Pantelides-Long model in order to make it more realistic. In constructing a more realistic version of this model, one can avoid excessively distorted bond angles by allowing dangling bonds to appear, and one can saturated these dangling bonds by O and H atoms and OH groups, as undoubtedly happens during actual growth conditions.[28,29] The extra energy needed to support dangling bonds would be largely offset by the saturation of these bonds by the entities just mentioned. (The construction of a model embodying these features is currently being investigated at our laboratory by P. Lambin and the author.)

The net effect would be an incomplete connection between a discontinuous random network of v-SiO_2 and the silicon substrate. There would be many voids of varying sizes present at or near the interface, but most of the dangling bonds defining these voids would be saturated by O and H atoms and OH groups. Thus, strain-relieving voids and (O,H,OH)-saturated dangling bonds are the two extra ingredients that should be added to the Pantelides-Long model to make it more realistic. The local stoichiometry described by the expression SiO_x would of course be determined in large measure by the O atoms and OH groups which saturate Si bonds and represent deviations from a continuous random network of v-SiO_2.

An analogous picture emerges from a totally different type of idealized Si/SiO_2 interface model that we developed recently.[30] In this other model, the non-crystalline SiO_2 overlayer is replaced by an idealized crystalline SiO_2 overlayer which can be brought into exact

registry with the Si substrate. If one begins with a silicon crystal, expands the lattice by a factor of $\sqrt{2}$, and places an oxygen atom at the midpoint of each dilated Si-Si bond, one obtains an idealized version of the cristobalite SiO_2 structure having very nearly the same Si-O bond length as the actual structure, but straight rather than crooked Si-O-Si bond angles. This is a reasonable approximation in view of the softness of the Si-O-Si bond angle. One can now obtain exact registry between the (100) face of Si and the (100) face of idealized cristobalite SiO_2 by rotating one of these 45 degrees with respect to the other and bringing them together.

The Si atoms on the (100) substrate form a square array which can be regarded as a checkerboard with half the Si atoms occupying "red" squares and the remaining half "black" squares. At the idealized Si/SiO_2 interface, the Si atoms occupying the "red" squares are shared by the Si substrate and the SiO_2 overlayer, while the Si atoms on the "black" squares are connected only to the Si substrate, having two dangling bonds each. One can improve the realism of this model slightly by retaining the lattice topology and allowing the atomic positions to relax, but this does not change the essential features of the model.

This construction leads to a concrete, easily visualized interface model which emphasizes that the connection between the Si substrate and the (idealized) SiO_2 overlayer involves only half the Si substrate atoms directly. The remaining half of the Si substrate atoms are not attached to the SiO_2 overlayer at all. For this model to describe an actual interface, it is again essential that virtually all the Si substrate dangling bonds are saturated by H or O atoms or OH groups introduced during interface formation. Since SiO_2 has a very open structure, it is reasonable to expect such entities if present to migrate to the growing interface and saturate the dangling bonds.

Since very few experiments provide direct and unambiguous information concerning the exact nature of the atomic structure of an Si/SiO_2 interface, it is essential for theoreticians to develop atomic-scale models that can be used as a guide to interpreting experimental measurements. The two models already discussed are clearly idealizations, but they are instructive. In order to make further progress, one should consider the atomic processes by which the interface actually forms, rather than straightforward attachments between crystalline SiO_2[30] or amorphous SiO_2[27,31] to a Si substrate.

There is a vast literature on defects in SiO_2[6-8] covering interface electronics and also radiation-damaged glass. It is encouraging that increasingly refined theoretical models have begun to appear in recent years,[32] as well as experimental studies based on surface-sensitive spectroscopies.[6-8,24] Nevertheless, the identification of the defects primarily responsible for trapping and recombination at Si/SiO_2 interfaces is still largely an open question. Since the thermal (Si) gap is only 1.1 eV and the top of this gap lies about 3.1 eV below the top of the 10 eV forbidden band of SiO_2, most of the defects in the SiO_2 structure would be expected to give rise to levels that lie outside the thermal gap. It is far more likely that defects such as dangling Si substrate bonds which are closely coupled to the Si band structure give rise to levels in the thermal gap. Support for this view comes from the fact that the deliberate introduction of hydrogen or deuterium during processing removes these defect levels, presumably by saturating these particular dangling bonds.[28,29]

Finally, we note that there is considerable tailing of the valence and conduction bands into the thermal gap. This tailing is supposedly associated with the disordered atomic structure at

the Si/SiO_2 interface, but the details are still not understood. Clearly, a great deal of additional experimental and theoretical work will have to be done before we have a more comprehensive picture of this interface.

IV. METAL-SEMICONDUCTOR CONTACTS: $Pd_2Si/Si(111)$ INTERFACES

The formation of ohmic or non-ohmic metal-semiconductor contacts is of immense technological importance. During the past few years, many attempts have been made to understand the physical, chemical, metallurgical, and structural factors determining Schottky barrier heights in rectifying contacts.[9,10] Although informative chemical trends have been established by correlating barrier heights with electrochemical data for many systems, the relationship between barrier height and local atomic structure at the interface remains elusive. Unfortunately, the atomic arrangements at most interfaces are too poorly characterized to provide a basis for serious theoretical analysis.

For most metal-semiconductor interfaces, lattice-matched constituents and atomically abrupt interfaces are the exception rather than the rule. The metal and semiconductor regions are usually separated by a disordered transition region which accommodates the discontinuity in lattice constant as well as the transition from metallic and covalent binding. Most of these interfaces are spatially diffuse because of interdiffusion. For some systems, chemical reactions may take place between the metal and semiconductor, leading to a transition region composed of ordered or disordered compounds. Such non-ideal systems are exceedingly difficult to treat theoretically, though some progress can be made by considering idealized lattice-matched metal-semiconductor interfaces.[33]

Most elementary models of ideal rectifying contacts are based on early ideas by Schottky and Bardeen, according to which chemical equilibrium is established by the flow of electrons between the metal and the semiconductor, leading to bending of the semiconductor bands and the creation of a rectifying potential barrier at the interface. The absence or presence of localized interface states plays a crucial role in these models: In the Schottky limit (negligible interface states), the barrier height is given by the difference between the metal work function and the semiconductor electron affinity. In the Bardeen limit, there are sufficiently many interface states present to pin the Fermi level, so that the barrier height is determined by the highest occupied interface state, and is largely independent of the metal work function.

If the Fermi level is indeed pinned by localized interface states whose energy levels lie in the forbidden band of the semiconductor, how do these interface states arise? The first possibility is that they are similar to intrinsic surface states on the semiconductor, as originally envisioned by Bardeen. However, in many semiconductors, relaxation and reconstruction at free surfaces push surface states out of the forbidden band;[13,34] the same could happen at metal-semiconductor interfaces.[35] Moreover, intrinsic semiconductor interface states can only partially resemble intrinsic surface states because of screening by the adjacent metallic region.

A second possibility is that electrons can be localized just inside the semiconductor by occupying the tails of the wave functions which spill over into the semiconductor from the metal. These are known as metal-induced gap states,[36] or MIGS. Such localized states are

expected to occur when the metal is at least several atomic layers thick, but they may not occur when the metal is only one atomic layer thick. Since the Schottky barrier height may already have its limiting ("bulk") value when the metal coverage is monoatomic or sub-monoatomic for some systems, there may be no direct connection between MIGS and Schottky barrier heights for such systems.[35]

A third possibility, particularly appropriate for "strong" (reactive) contacts, is that the frontier metal and semiconductor atoms form chemical bonds,[37] and that the energy levels associated with these chemical bonds or hybridized metal-semiconductor states extend into the forbidden band. A fourth possibility is that the localized interface states arise from structural or chemical imperfections in the semiconductor.[38] Such imperfections include vacancies, self-interstitials, substitutional and interstitial metal impurities, metallic clusters, antisite defects, and dislocations. In the case of contacts between metals and hydrogenated amorphous silicon,[39] states in the gap already present because of structural disorder in the silicon are expected to play a key role in pinning the Fermi level.

Many investigators are currently making a concerted effort to interpret a rapidly increasing body of detailed experimental information in terms of different defect models.[9,10,35,38] In view of the fact that most experimental probes do not have the spatial resolution necessary to identify structural imperfections unambiguously on an atomic scale, a general consensus has not yet been reached regarding the mechanisms responsible for Schottky barrier formation. There may well be many different mechanisms at play in different systems, or even in the same system, so sorting out the key mechanisms is an exceedingly difficult problem.

The demands of sub-micron electronics are focusing attention on rectifying contacts formed by reacting transition metals with silicon. There is considerable interest in such interfaces because the silicides form close-packed metallic structures which are impervious to bonding metals such as Al. Thus, diffuse Al-Si contacts can be replaced by relatively abrupt Al-silicide-Si contacts. Moreover, some of the silicides form epitaxial layers on Si, so there is a greater opportunity to synthesize interfaces which are more nearly ideal and hence easier to investigate experimentally and theoretically.[9,10,40]

There have already been a number of experimental and theoretical studies of the electronic structure of bulk silicides.[40] Some attempts are currently being made to study the electronic structure of silicide-silicon interfaces theoretically, taking advantage of their epitaxial character.[41,42] In the following, we will discuss the essential features of a model we have recently developed for understanding Schottky barriers at $Pd_2Si/Si(111)$ interfaces.[42] This model is of general interest because it goes beyond the idea of localized interface states being solely responsible for Schottky barrier heights.

According to our model, Pd impurities diffuse into the Si substrate in advance of the growing interface, forming triangular clusters between pairs of Si vacancies.[43] Since these clusters are more easily accommodated in hexagonal (2H) Si than in cubic (3C) Si, the presence of these clusters induces a hexagonal Si transition region between the cubic Si substrate and the Pd_2Si overlayer. The measured Schottky barrier height (0.71 to 0.73 eV) is readily accounted for by noting first that the forbidden band width of the hexagonal Si transition region is about 0.85 eV, and second that the Fermi level is pinned slightly above the Si valence band edge by hybridized Pd-Si states at the interface.[41,42] The same overall effect could be achieved by having stacking disorder in the Si near the interface, rather than a coherent

hexagonal crystal structure. We would again argue that the stacking disorder is induced by the presence of the triangular Pd impurities.

In short, our $Pd_2Si/Si(111)$ model suggests that Schottky barrier heights can be determined not only by interface states which pin the Fermi level, but also by the presence of a different crystal structure or stacking disorder near the interface. Such structural features -- coherent or random -- can affect the host band structure, modifying the effective semiconductor band gap at the interface, and hence the Schottky barrier height as well. Incidentally, stacking faults have also been invoked recently to account for certain reconstructions of free silicon surfaces.[44]

V. CONSTRUCTION OF ATOMIC-SCALE INTERFACE MODELS

One popular theoretical approach for determining the atomic structure of interfaces (and surfaces) involves calculating the electronic structure for a number of plausible models, and then determining which set of results agrees most closely with experiment.[13,34] Even assuming that the experimental data are reproducible and correctly interpreted, this approach may overlook physically significant atomic arrangements altogether, and in the end not provide insight as to why one particular model gives a better account of experiment than another.

Another popular theoretical approach involves calculating the total energy of the system, and then determining the equilibrium geometry by minimizing the total energy as a function of atomic positions. This is a very powerful approach, and has been applied with great success recently to a number of relatively simple systems.[13,34] Because of the extensive computational effort involved, it is unlikely that this approach will soon encompass the more complicated systems that are of primary experimental interest.

So it is essential to look for still other approaches, bearing in mind that further progress in determining the electronic structure of interfaces is severely limited by our ability to construct realistic atomic models of interfaces. Instead of assuming plausible atomic positions at the outset and then relaxing these positions so as to minimize the total energy, keeping the topology or connectivity the same, we believe theoreticians should focus directly on the atomic processes by which interfaces are formed by the progressive accumulation of atoms and molecules. We should attempt to simulate the growth of covalently bonded crystals at the atomic level using computers, perhaps interactively. The challenge is to establish algorithms that will guide this growth along physically and chemically reasonable paths, possibly taking advantage of concepts arising in the field of artificial intelligence.

Computer simulation studies[45] have already provided us with considerable insight into the nature of crystal growth, but such studies have been confined almost exclusively to systems such as metals and simple liquids which can be described by hard sphere interactions.[46] Current attempts at modeling covalently bonded systems are still rather primitive,[47,48] but this avenue of theoretical research is of the greatest importance, and deserves considerably more attention than it has received so far.

VI. FORMATION OF NOVEL INTERFACES AND SUPERLATTICES

During the next few years we anticipate increasing experimental, theoretical, and computational efforts directed at understanding the growth and stabilization of novel interfaces and superlattices, with particular emphasis on the underlying atomic processes:

• Amorphous overlayers on crystalline substrates. — We have already discussed the Si/SiO_2 interface as an important example of a crystalline-amorphous interface. A somewhat simpler example is the interface between crystalline Si and amorphous Si. Recent activity in laser processing and laser annealing[49] has focused attention on the fundamental processes associated with localized melting and subsequent solidification of Si into the amorphous phase, as well as with recrystallization of amorphous Si. Some attempts have already been made to model crystalline-amorphous Si transformations as well as the growth of SiO_2 on Si on an atomic scale,[50] but progress thus far has been minimal. We don't really know very much about the dynamical processes responsible for the interconversion between crystalline and amorphous phases of covalently bonded solids. If we could understand the atomic dynamics by which crystals transform into amorphous structures and vice versa, we would be able to determine the atomic arrangements at crystalline-amorphous interfaces. This is clearly a challenge for the future.

• Metastable overlayers on solid substrates.[51] — Perhaps the best-known examples are strained-layer interfaces and superlattices.[11] These metastable structures have many attractive physical properties, so they are being intensively studied. An important challenge is to find ways of stabilizing such structures so that they can perform electronic functions under widely varying conditions. Other examples are low-temperature phase α tin ("grey tin") and α-Sn:Ge alloys grown on InSb and CdTe substrates.[52] Still other examples are single-crystal $(GaAs)_{1-x}Ge_{2x}$ alloys, whose band gaps vary non-monotonically with composition in a most remarkable manner.[53] This behavior has been interpreted as evidence for an order-disorder transition.[54]

• Polytypism,[55] stacking disorder,[56] and random superstructures.[57] — The boundary between cubic ZnS (sphalerite) and hexagonal ZnS (wurtzite) is a classic example of a polymorphic interface.[58,59] Long-period polytypes of SiC and ZnS can be rightfully regarded as structurally modulated superlattices. The mechanisms leading to the growth of such superlattices are still not understood, in spite of decades of study. Admixed random and non-random stacking sequences of ZnS can be formed by evaporating thin films of ZnS on suitable substrates. These films are composed of random striations of cubic and hexagonal ZnS.[58,60] Such films are of interest because they can be used to generate photovoltages considerably larger than the band gap of ZnS. Another challenge for the future is learning to synthesize structurally modulated heterostructures as well as we have already learned to synthesize compositionally modulated heterostructures[1,2,5,11] and modulation doped heterostructures.[3] Hopefully, an improved theoretical understanding of interface formation will accelerate progress.

VII. CONCLUDING REMARKS

Recent experimental studies have provided a great deal of important information concerning the nature of semiconductor interfaces. Many experimental results can be readily interpreted in terms of electronic structure pictures based on idealized interface geometries. However, it has proved difficult to elucidate the atomic arrangements at interfaces unambiguously because even the most refined surface-sensitive spectroscopies lack the necessary resolution. Further theoretical progress on electronic structure and more incisive interpretation of experimental measurements both await a better understanding of the atomic structure of real interfaces. The development of realistic atomic structure models is a challenging theoretical problem which is ideally suited for imaginative computational analysis.

REFERENCES

* Supported in part by ONR Contract Number N00014-79-C-0814.

1. For recent reviews, see: ESAKI, L. (these proceedings); CHANG, L.L., J. Vac. Sci. Technol. B 1 (1983) 120; GOSSARD, A.C., Thin Solid Films 104 (1983) 279; MADHUKAR, A., J. Vac. Sci. Techn. 20 (1982) 149.
2. See, for example: DINGLE, R., STORMER, H.L., GOSSARD, A.C., and WIEGMANN, W., Appl. Phys. Lett. 33 (1978) 665; KROEMER, H., Proc. IEEE 79 (1982) 13; KROEMER, H., J. Vac. Sci. Technol. B 1 (1983) 126; EASTMAN, L.F., ibid, p. 131; CAPASSO, F., ibid, p. 457; HESS, K., Physica 117B and 118B (1983) 723; PRICE, P.J., in FERRY, D.K. (ed.), *Physics of Sub-Micron Semiconductor Devices* (Plenum Press, New York), 1984 (in press)
3. RUDEN, P. and DÖHLER, G.H., Phys. Rev. B 27 (1983) 3538, 3547; DÖHLER, J. Vac. Sci. Technol. B 1 (1983) 278; RUDEN, P., ibid, p. 285. (modulation-doped superlattices)
4. ANDO, T., FOWLER, A., and STERN, F., Revs. Mod. Phys. 54 (1982) 437. (physics of two-dimensional electronic systems confined to interfacial regions)
5. For recent reviews, see: CHANG, L.L. and ESAKI, L., Prog. Crystal Growth Charact. 2 (1979) 3; STRINGFELLOW, G.B., Repts. Prog. Phys. 45 (1982) 469; CHO, A.Y., J. Vac. Sci. Technol. B 1 (1983) 119.
6. PANTELIDES, S.T. (ed.), *The Physics and Chemistry of SiO_2 and its Interfaces* (Pergamon Press, New York) 1978.
7. LUCOVSKY, G., PANTELIDES, S.T., and GALEENER, F.L. (eds.), *The Physics of MOS Insulators* (Pergamon Press, New York) 1980.
8. SCHULZ, M. and PENSL, G. (eds.), *Insulating Films on Semiconductors* (Springer-Verlag, Berlin) 1981.
9. SZE, S.M., *Physics of Semiconductor Devices* (Wiley-Interscience, New York) 1981, Second Edition. For recent reviews, see: SCHLUTER, M., Thin Solid Films 93 (1982) 3; BRILLSON, L.J., Surf. Sci. Repts. 2 (1982) 123; WILLIAMS, R.H., Contemp. Phys., 23 (1982) 329; MARGARITONDO, G., Solid State Electron. 26 (1983) 499; HO, P.S., J. Vac. Sci. Technol. A 1 (1983) 745.
10. For forthcoming reviews, see: RUBLOFF, G.W., Adv. Solid State Phys. 23 (1983), in press; FREEOUF, J.L. in: RUBLOFF, G.W. and HO, P.S. (eds.), *Metal-Si and Silicide-Si Interfaces* (Elsevier, Amsterdam) 1983, in press; BACHRACH, R.Z., in SHARMA, B.L. (ed.), *Metal-Semiconductor Schottky Barrier Junctions* (Plenum Press, New York) 1984, in press.

11. OSBOURN, G.C., J. Vac. Sci. Technol. B 1 (1983) 379; GOURLEY, P.L. and BIEFELD, R.M., ibid, p. 383; for a popular account, see: Physics Today 36 (1983) June issue, p. 19.
12. See, for example: HARRISON, W.A., J. Vac. Sci. Technol. 14 (1977) 1016; FRENSLEY, W.R. and KROEMER, H., Phys. Rev. B 16 (1977) 1962; KATNANI, A.D. and MARGARITONDO, G., J. Appl. Phys. 54 (1983) 2522.
13. For recent reviews, see: HERMAN, F., J. Vac. Sci. Technol. 16 (1979) 1101; COHEN, M.L., Adv. Electron. Electron Phys. 51 (1980) 1; POLLMANN, J., Adv. Solid State Phys. 20 (1980) 117; POLLMANN, J. and MAZUR, A., Thin Solid Films 104 (1983) 257.
14. GRANT, R.W., KRAUT, E.A., KOWALCZYK, S.P., and WALDROP, J.R., J. Vac. Sci. Technol. B 1 (1983) 320; and references cited.
15. HERMAN, F. and KASOWSKI, R.V., Phys. Rev. B 17 (1978) 672.
16. PICKETT, W.E., LOUIE, S.G., and COHEN, M.L., Phys. Rev. B 117, (1978) 815.
17. MAZUR, A., POLLMANN, J., and SCHMEITS, M., Solid State Commun. 36 (1980) 961; J. Phys. Soc. Japan 49 (1980) Suppl. A 1121 (segregated interfaces).
18. DENLEY, D., MILLS, K.A., PERFETTI, P., and D.A. SHIRLEY, D.A., J. Vac. Sci. Technol. 16 (1979) 1501.
19. BARAFF, G.A., APPELBAUM, J.A., and HAMANN, D.R., Phys. Rev. Lett. 38 (1977) 237; J. Vac. Sci. Technol. 14 (1977) 999.
20. POLLMANN, J. and PANTELIDES, S.T., Solid State Commun. 30 (1979) 621; J. Vac. Sci. Technol. 16 (1979) 1498; Phys. Rev. B 21 (1980) 709.
21. HARRISON, W.A., KRAUT, E.A., WALDROP, J.R., and GRANT, R.W., Phys. Rev. B 115 (1978) 4402; see also KUNC, K. and MARTIN, R.M., J. Phys. Soc. Japan 49 (1980) Suppl. A. 1117; Phys. Rev. B 24 (1981) 3445.
22. BAUER, R.S. and MIKKELSEN, J.C. Jr., J. Vac. Sci. Technol. 21 (1982) 491; MÖNCH, W., BAUER, R.S., GANT, H., and MURSCHALL, R., ibid, p. 498; MÖNCH, W., Thin Solid Films 104 (1983) 285.
23. CHANG, C. and KUAN, T., J. Vac. Sci. Technol. B 1 (1983) 315.
24. HELMS, C.R., J. Vac. Sci. Technol. 16 (1979) 608; in BALK, P. (ed.), *The Si-SiO_2 System* (Elsevier, Amsterdam), 1984 (in press).
25. ZIMAN, J.M., *Models of Disorder* (Cambridge University Press) 1979; ZALLEN, R., *The Physics of Amorphous Solids* (Wiley, New York) 1983.
26. See, for example: GASKELL, P.H. and TARRANT, I.D., Phil. Mag. B 42 (1980) 265; MITRA, S.K., Phil. Mag. B 43 (1981) 365; Phil Mag. B 45 (1982) 529.
27 PANTELIDES, S.T. and LONG, M., in Ref. 6, p. 339.
28. REVESZ, A.G., in Ref. 6, p. 222; JOHNSON, N.M., BIEGELSEN, D.K., and MOYER, M.D., in Ref. 7, p. 311; in Ref. 8, p. 35; JOHNSON, N.M., J. Vac. Sci. Technol. 21 (1982) 303.
29. The idea of strain-relieving voids at the Si/SiO_2 interface is consistent with present-day models of hydrogenated amorphous silicon, according to which large numbers of dangling Si bonds at voids are saturated by H atoms: cf. STREET, R.A., Adv. Phys. 30 (1981) 593.
30. HERMAN, F., BATRA, I.P., and KASOWSKI, R.V., in Ref. 6, p. 333; HERMAN, F., HENDERSON, D.J., and KASOWSKI, R.V., in Ref. 7, p. 107; HERMAN, F., in Ref. 8, p. 2; HERMAN, F. and KASOWSKI, R.V., J. Vac. Sci. Technol. 19 (1981) 395.
31. See, for example: LAUGHLIN, R.B., JOANNOPOULOS, J.D., and CHADI, D.J., in Ref. 6, p. 321; CHING, W.Y., Phys. Rev. B 26 (1982) 6610, 6622, 6633.

32. See, for example: NAGI, K.L. and WHITE, C.T., J. Appl. Phys. 52 (1981) 320; EDWARDS, A.H. and FOWLER, W.B., Phys. Rev. B 26 (1982) 6649; O'REILLY, E.P. and ROBERTSON, J., Phys. Rev. B 27 (1983) 3780.
33. BATRA, I.P. and HERMAN, F., J. Vac. Sci. Technol. A 1 (1983) 1080; BATRA, I.P., J. Vac. Sci. Technol. B 1 (1983), in press.
34. See, for example: CHADI, D.J., J. Phys. Soc. Japan 49 (1980) Suppl. A 1035; HANEMAN, D., Adv. Phys. 31 (1982) 165; PANDEY, K.C., Physica 117B and 118B (1983) 761; NORTHRUP, J.E. and COHEN, M.L., Phys. Rev. B 27 (1983) 6553; and references cited.
35. ZUNGER, A., Thin Solid Films 104 (1983) 301.
36. HEINE, V., Phys. Rev. 138 (1965) A1689; LOUIE, S.G. and COHEN, M.L., Phys. Rev. B 13 (1976) 2461.
37. PHILLIPS, J.C., J. Vac. Sci. Technol. 11 (1974) 947.
38. SPICER, W.E., EGLASH, S., LINDAU, I., SU, C.Y., and SKEATH, P., Thin Solid Films 89 (1982) 447.
39. NEMANICH, R.J. and THOMPSON, M.J., in SHARMA, B.L. (ed.), *Metal-Semiconductor Schottky Barrier Junctions* (Plenum Press, New York) 1984, in press.
40. See, for example: FRANCIOSI, A. and WEAVER, J.H., Phys. Rev. B 27 (1983) 3554; ROSSI, G., JAEGER, R., STÖHR, J., KENDELEWICZ, T., and LINDAU, I., Phys. Rev. B. 27 (1983) 5154; TERSOFF, J. and HAMANN, D.R., Phys. Rev. B 28 (1983) 1168; and references cited (in all these papers).
41. IHM, J., COHEN, M.L., and CHELIKOWSKY, J.R., Phys. Rev. B 22 (1980) 4610.
42. HERMAN, F., CASULA, F., and KASOWSKI, R.V., Physica 117B and 118B (1983) 837.
43. These particular clusters were suggested by the Pd triangles belonging to the Si-rich planes of Pd_2Si. The centers of the Pd triangles are assumed to lie at points midway between adjacent Si divacancies oriented in the (111) direction. Preliminary estimates suggested that the energy levels associated with these Pd clusters do not lie in the Si band gap. We are presently carrying out more detailed molecular cluster calculations in collaboration with D.A. Case to obtain improved estimates of these energy level positions.
44. PETROFF, P.M. and WILSON, R.J., Phys. Rev. Lett. 51 (1983) 199; BENNETT, P.A., FELDMAN, L.C., YUK, Y., McRAE, E.G., and ROWE, J.E., Phys. Rev. Lett. 51 (1983), in press.
45. JAMES, Repts. Prog. Phys. 43 (1980) 1145; VAN DER EERDEN, J.P., BENNEMA, P., and CHEREPANOVA, T.A., Prog. Crystal Growth Charact. 1 (1978) 219.
46. See, for example: WEEKS, J.D. and GILMER, G.H., Adv. Chem. Phys. 40 (1979) 157; GILMER, G.H., Science 208 (1980) 355; GILMER, G.H. and BROUGHTON, J.Q., J. Vac. Sci. Technol. B 1 (1983) 298; ABRAHAM, F.F., Repts. Prog. Phys. 45 (1982) 1113.
47. SINGH, J. and MADHUKAR, A., J. Vac. Sci. Technol. B 1 (1983) 305; Phys. Rev. Lett. 51 (1983), in press.
48. GOODNICK, S.E., POROD, W., GRONDIN, R.O., GOODNICK, S.M., WILMSEN, C.W., and FERRY, D.K., J. Vac. Sci. Techn. B 1 (1983), in press.
49. APPLETON, B.R. and CELLER, G.K. (eds.), *Laser and Electron Beam Interactions in Solids* (North-Holland, New York) 1982, Vol. 4; KURZ, H., LIU, J.M., and BLOEMBERGEN, N., Physica 117B and 118B (1983) 1010.

50. See, for example: SPAEPEN, F., Acta Metall. 26 (1978) 1167; FRATELLO, V.J., HAYS, J.F., SPAEPEN, F., and TURNBULL, D., J. Appl. Phys. 51 (1981) 6160; SAITO, T. and OHDOMARI, I., Phil. Mag. B 43 (1981) 673.
51. For recent reviews, see: FARROW, R.F.C., J. Vac. Sci. Technol. B 1 (1983) 222; GREENE, J.E., ibid, p. 229; GRUNTHANER, F.J. and MADHUKAR, A., ibid, p. 462.
52. FARROW, R.F.C., ROBERTSON, D.S., WILLIAMS, G.M., CULLIS, A.G., JONES, G.R., YOUNG, I.M., and DENNIS, P.N.J., J. Cryst. Growth 54 (1981) 507.
53. BARNETT, S.A., RAY, M.A., LASTRAS, A., KRAMER, B., GREENE, J.E., RACCAH, P.M., and ABELS, L.A., Electron. Lett. 18 (1982) 891.
54. NEWMAN, K.E. and DOW, J.D., Phys. Rev. B 27 (1983) 7495.
55. VERMA, A.R. and KRISHNA, P., *Polymorphism and Polytypism in Crystals* (Wiley, New York) 1966); WELLS, A.F., *Structural Inorganic Chemistry* (Clarendon Press, Oxford) 1967, Third Edition, p. 186.
56. For recent reviews, see: BARONNET, A., Prog. Crystal Growth Charact. 1 (1978) 151; TRIGUNAYAT, G.C. and VERMA, A.R., in *Crystallography and Crystal Chemistry of Materials with Layered Structures* (Reidel, Dordrecht, Holland) 1976, p. 269.
57. DOW, J.D., REN, S.Y., and HESS, K., Phys. Rev. B 25 (1983) 6218; DOW, J.D. (these proceedings).
58. NORTHRUP, J.E., IHM, J., and COHEN, M.L., Phys. Rev. B 22 (1980) 2060.
59. HERMAN, F., J. Vac. Sci. Techn. 21 (1982) 643.
60. ELLIS, S.G., HERMAN, F., LOEBNER, E.E., MERZ, W.J., STRUCK, and C.W., WHITE, J.G., Phys. Rev. 109 (1958) 1860.

Published in "Insulating Films on Semiconductors"
M. Schulz and G. Pensl, editors (Springer-Verlag, Berlin, 1981), p. 2.
(Proceedings of INFOS81 Conference, Erlangen, Germany, May, 1981).

ELECTRONIC STRUCTURE OF THE Si/SiO_2 INTERFACE

Frank Herman
IBM Research Laboratory
San Jose, CA 95193 USA[1]

ABSTRACT. After sketching various theoretical models that have been proposed for describing the Si/SiO_2 interface on an atomic scale, we will discuss an idealized model which is designed to simulate the average contact between a silicon crystal and its oxide overlayer. According to this model, the Si/SiO_2 interface is represented by the boundary between two crystalline domains, the first being the silicon substrate, and the second an idealized crystalline form of SiO_2, diamond-like beta cristobalite. Nearly perfect registry between Si and SiO_2 is obtained by placing the (100) face of the former next to the 45° rotated (100) face of the latter. Half the Si atoms at the interface are four-fold coordinated, connecting the Si and SiO_2 regions to one another. The remaining half are connected only to the silicon substrate and are thus two-fold coordinated. Localized electronic states in the thermal gap at the interface are associated with the dangling bonds at the two-fold coordinated Si atoms. If H, O, or OH groups are attached to these Si atoms, eliminating the dangling bonds, the thermal gap interface states are also eliminated. Even though this model ignores structural disorder, it does provide considerable insight into the nature of the Si/SiO_2 interface. We will discuss some of the implications of this model, as well as the results of model-based theoretical calculations. In particular, we will consider the electronic structure of the interface including the effects produced by the introduction of Si and O vacancies and interstitials and other types of localized defects.

1. INTRODUCTION

Because of the important role played by the Si/SiO_2 interface in modern semiconductor technology, considerable experimental and theoretical effort has been devoted to the study of this interface.[2-8] Oxidation of a silicon surface produces an amorphous oxide layer whose atomic arrangement is not well understood. Many authors have suggested that there is a non-stoichiometric transition layer, often described as SiOx, separating the silicon substrate from the stoichiometric SiO_2 layer. (Here x lies between 1 and 2.) The detailed atomic structure of the transition layer, including its uniformity and width, its structural disorder, its affinity for impurity atoms, etc., continues to be a subject of debate. Of course, the nature of the transition layer is expected to depend on the manner in which the oxide layer is formed. By the same token, a better understanding of the transition layer could lead to further improvements in the preparation of Si/SiO_2 interfaces.

The technological importance of the Si/SiO_2 interface arises from the fortunate circumstance that suitably oxidized silicon substrates are protected from environmental contaminants and have rather low densities of localized interface states in the thermal gap. There

continues to be considerable interest in the nature and identity of the residual defects that occur near well-prepared interfaces, giving rise to residual trapping sites and fixed charge. Many imaginative models of defects at the Si/SiO_2 interface and in SiO_2 have been proposed,[2-11] but relatively few of these defects have been unambiguously identified, even by such precise measurements as ESR.[11] In view of the difficulties encountered in practice in attempting to interpret most experimental measurements in terms of specific defects, we thought it would be useful to develop a simple model for the Si/SiO_2 interface which could provide a conceptual framework for thinking about interface defects as well as a theoretical framework for carrying out numerical calculations.

In the first paper on this subject,[12] we described the construction of idealized Si/SiO_2 interfaces and superlattices and demonstrated by first principles band structure calculations that there are no localized interface states in the thermal gap if all the Si atoms at the interface are saturated. In a second paper,[13] we showed how localized defects in SiO_2 could be investigated theoretically by introducing periodic arrays of non-interacting defects in a SiO_2 supercell normally containing 24 atoms. In a third paper,[14] we introduced periodic arrays of non-interacting defects in idealized Si/SiO_2 superlattices, thereby simulating the presence of localized defects at or near the Si/SiO_2 interface. In the present paper we will first mention some recent attempts by others to develop a theoretical model of SiO_2 and the Si/SiO_2 interface, and then we will discuss our own model briefly and summarize some of our principal conclusions.

2. THEORETICAL MODELS OF THE Si/SiO_2 INTERFACE

The extensive literature on crystalline and non-crystalline SiO_2 and on Si/SiO_2 interfaces[2-11] contains a variety of models of the oxide layer and the Si/SiO_2 interface. In this paper, we will focus on atomic scale rather than on phenomenological models. Nearly all the models that have been proposed for describing the atomic arrangements at the interface are speculative. Some of the proposals are quite specific. They assume particular types of linkages between Si and SiO_2, well-defined structural imperfections arising from modifications in the normal linkages, as well as chemical imperfections due to the presence of specific foreign species. The remaining proposals tend to be descriptive or impressionistic, invoking dislocations, disjunctions, varying degrees of stoichiometry and crystallinity, etc. The first set of proposals can be distinguished from the second by the ease with which ball-and-stick models can be constructed to illustrate the proposed arrangements.

There has also been considerable debate regarding the initial formation of the oxide layer, and how this layer might change as it grows.[2-8] Some authors believe that a better understanding of the initial stages of oxidation could provide valuable clues concerning the nature of the ultimate oxide layer; other authors disagree. In any event, it is very important to have heuristic atomic models of the formation and ultimate structure of the Si/SiO_2 interface, because such ideas could lead to improved processing techniques, new device concepts, and better understanding of still more complex semiconductor/insulator interfaces.

Up to now, most Si/SiO_2 interface modeling studies have been qualitative, being based on simple physical and chemical reasoning. Many of the arguments put forward in favor of specific atomic models seem quite plausible, but it is usually difficult to verify these interface models experimentally. Therefore, a constructive step would be to study some of these

models theoretically and obtain quantitative estimates of crucial electronic properties. If one wishes to carry out detailed electronic structure calculations for model systems, it is obviously necessary to have specific atomic arrangements in mind. The essential difficulty is that we do not know the actual structure of the Si/SiO_2 interface on an atomic scale.

The overall problem can be dealt with in three parts: In the first and easiest part, one makes certain assumptions about the silicon substrate. For example, one chooses a specific crystalline orientation, and then assumes that the silicon is structurally perfect up to the interface. Relaxation and reconstruction effects can be deferred to a later stage or expressly ignored. The second part concerns the description of the oxide film proper, allowing if possible for its non-crystalline nature. In dealing with non-crystalline SiO_2, one can build on our improved knowledge of amorphous and glassy semiconductors.[9,15-19] The third part, the most difficult of all, involves connecting the silicon substrate to the non-crystalline oxide layer in a physically and chemically plausible manner.

One popular model for non-crystalline SiO_2 and the Si/SiO_2 interface is the cluster Bethe lattice model,[20,21] which takes topological aspects of structural disorder into account in an elegant manner. Because this model is rather simple in form and can be easily parameterized, it can be used to study electronic and lattice vibrational spectral properties associated with ideal and defective interfaces. But because these models are based on adjustable parameters that are assigned ad hoc values, they are not particularly trustworthy from a quantitative point of view.[22] Nevertheless, they do have considerable pedagogical value.

Another popular model of non-crystalline SiO_2 is the continuous random network model,[15-19] according to which SiO_2 is composed of a randomly oriented collection of SiO_4 tetrahedra which are linked to one another to form a continuous network of Si-O-Si bonds. It is assumed that the SiO_4 tetrahedra tend to maintain their structural integrity (bond lengths and bond angles) in different environments, and that the necessary structural versatility is provided by the Si-O-Si bond, whose angle may assume a wide range of values at little cost in energy.[4] Models of this type have recently been used to study bulk SiO_2[23] as well as the Si/SiO_2 interface.[24] In the study of bulk SiO_2, cyclic boundary conditions were imposed on a large disordered molecular SiO_2 cluster, producing a computationally tractable model of non-crystalline SiO_2. The object here was to investigate electron and hole localization induced by the structural disorder.

In the study of the Si/SiO_2 interface, it was demonstrated that a rather abrupt interface could be constructed within the framework of a continuous random network model, a rather important result. Unfortunately, the resulting atomic model is much too complex for detailed electronic structure studies. In both Refs. 23 and 24, the construction of continuous random network models is based on ideas regarding the nature of non-crystallinity which are highly subjective and which may not necessarily describe the experimental situation. It is possible that non-crystalline SiO_2 near a Si/SiO_2 interface does not actually form a completely continuous random network. That is to say, the network may contain discontinuous elements such as non-bridging O atoms or three-fold coordinated Si atoms connected to H or OH groups, or voids composed of aggregates of such discontinuous elements.[19]

There are many theoretical efforts currently underway[18,19,25] whose aim is to formulate general guiding principles for constructing atomic models of non-crystalline materials. Combined with intuitive notions[26] and computer modeling,[27,28] these theoretical studies may

eventually lead us to objective atomic models which we can use with confidence for electronic structure studies of non-crystalline SiO_2. In the meanwhile, the atomic architecture of the Si/SiO_2 interface remains an open question.

We already know from extensive experimental and theoretical studies[2,3,29] that the gross features of the electronic structure of non- crystalline and various crystalline forms of SiO_2 are essentially the same, reflecting the common SiO_4 building block. Only the finer details of electronic structure are affected by the special manner in which the SiO_4 tetrahedra are linked together in a particular structural modification. In view of the overwhelming importance of the short range order (linked SiO_4 tetrahedra) in determining the essential features of the electronic structure of SiO_2, and the likelihood that the long range disorder affects only the finer details, we will explicitly ignore the structural disorder of SiO_2 and concentrate on models of the interface which represent the average contact between Si and SiO_2.

3. IDEALIZED Si/SiO_2 SUPERLATTICES AND INTERFACES

Our overall program is as follows. First, we will disregard structural disorder in SiO_2, and represent SiO_2 by a suitably chosen periodic structure. We will then form ordered Si/SiO_2 interfaces by attaching crystalline SiO_2 to crystalline Si. Next, we will construct a Si/SiO_2 superlattice by stacking Si and SiO_2 slabs on top of one another. The slabs will be made sufficiently thick so that successive interfaces will not interact with one another. Because the Si/SiO_2 superlattice is a periodic structure in three dimensions, we can use the highly developed methods of band theory[30] to calculate the electronic structure. The results of such calculations include a description of localized interface states, including their energy levels and charge distributions. Finally, we can introduce structural and chemical imperfections, and study their effects on the electronic structure.

To carry out the above program, we begin by representing the oxide layer by an idealized crystalline form of SiO_2 having as simple a unit cell as possible. For this purpose we will use beta cristobalite,[31] except that we will straighten out the Si-O-Si bonds in the actual structure, making them all linear rather than crooked (all bond angles 180° rather than about 140°). Assuming an Si-O bond length of 1.633 Å,[32] the linear Si-O-Si bond length becomes twice this, and the unit cube edge of idealized diamond-like SiO_2 becomes 7.543 Å, which is 5 percent larger than the unit cube edge of actual beta cristobalite, 7.16 Å. This 5 percent difference reflects the contraction produced by the bent bonds in the actual structure. Except as otherwise noted, we will henceforth regard SiO_2 as having the idealized diamond-like beta cristobalite structure with linear Si-O-Si bonds.

It is an interesting exercise to find ways of attaching crystalline SiO_2 to crystalline Si so that as many bonds as possible are formed. The simplest arrangement of all is to place the (100) face of Si next to the 45°-rotated face of (100) SiO_2. This produces almost perfect registry because the ratio of the lattice constants of SiO_2 and Si is very nearly equal to the square root of 2 (7.543/5.431 = 1.39). To put it more directly, we obtain nearly perfect registry in this fashion because the ratio of the straight Si-O-Si bond length in SiO_2 to the Si-Si bond length in silicon is very nearly equal to the square root of 2. (For actual calculations, we will increase the Si-O-Si bond length slightly so that the registry is exact.)

We thus obtain an extremely simple model of the Si/SiO_2 interface, namely, a fully coherent, ideally abrupt interface between silicon and crystalline SiO_2.[12-14] This construction leads to an interface at which half the Si substrate atoms are four-fold coordinated, the remaining half being two-fold coordinated, with two dangling bonds each. We can describe the interface as a checkerboard with Si atoms common to Si and SiO_2 occupying the red squares, and unsaturated Si atoms (two dangling bonds each) occupying the black squares. It is possible to use other Si and SiO_2 crystal faces and join them together in a similar manner, but these alternate constructions lead to more complex interface matching patterns, stretched Si-O-Si bonds, and larger repeat periods, making them less suitable for modeling. It is interesting, nevertheless, that even these more complex models exhibit the property that roughly half the Si substrate atoms are attached to the SiO_2, while the remaining half are unattached. If we are to adopt an idealized model, we might as well adopt the simplest one possible, and this is unquestionably the (100) 45°-rotated geometry already described.

Because of the 45° rotation at the interface, the four bonds emanating from the common Si atoms deviate from ideal tetrahedral geometry. Earlier studies[13] suggest that the silicon lattice is considerably more rigid than the SiO_2 lattice, so that most of the strain would be relieved by lattice relaxation in the SiO_2 region. We have made some progress in taking lattice relaxation effects into account, but on the basis of our work to date[13] we view the distortion from ideal tetrahedral geometry at the common Si atoms as a relatively minor shortcoming of our model. The thermal (Si) band gap is determined in part by the common Si atoms and the fact that they are saturated. The deviation from local tetrahedral geometry appears to be only of secondary importance.

It is possible to avoid the lattice strain associated with the 45° rotation altogether by considering a more exotic interface model. Here each common Si atom is replaced by a Si=Si molecule, one end of which terminates the silicon substrate, and the other end the SiO_2 region. The 45° rotation is then absorbed by the Si=Si double bonds. The net result is that all bond angles at the interface and elsewhere are tetrahedral. In this model the Si-Si bond length is 2.352 Å in the silicon crystal and slightly less (2.252 Å) in Si=Si[32]. We have not adopted this more exotic model for two reasons. First, the Si=Si bond is a weak one,[33] so there is some question as to whether it would be stable in the environment just described. Secondly, we have carried out comparison calculations using the more exotic as well as the original model, and we find that the Si double bonds lead to a significant reduction in the Si/SiO_2 thermal gap, which is contrary to experiment. So we will stick with the original model.

We do not regard the use of straight rather than crooked Si-O-Si bonds in SiO_2 as a serious defect in our model. We have already said that there is very little energy required to change the Si-O-Si bond angle from 140 to 180°.[4] Some bond distortion is inevitable at the Si/SiO_2 interface anyway. Moreover, the Si-O-Si bond angles are not expected to play a major role in determining the electronic structure.[29]

By using a periodic model and introducing an idealized interface, we have focused attention on the average contact between Si and SiO_2, highlighting the fact that this average contact requires approximately half the Si substrate atoms to be attached to the SiO_2, and the remaining half to be unattached. The unattached (two-fold coordinated) Si atoms face onto cavities in the adjoining SiO_2 region, presumably making it easy for species such as O, H, or OH to find their way to the beckoning dangling bonds. Because of the periodicity, and the

simple manner in which we have been able to attach SiO_2 to the silicon substrate, we can describe various forms of the transition layer, so-called non-stoichiometric SiOx, on an atomic scale. According to our model, this transition layer does not actually exist if each two-fold coordinated Si atom at the interface is saturated by two H atoms. That is to say, the passage from Si to SiO_2 is essentially abrupt. By saturating some or all of these two-fold coordinated Si atoms with O or OH groups, we can introduce varying O concentrations in one atomic layer just beyond the silicon substrate, this now becoming the transition layer. Perhaps simple geometrical pictures such as these will prove more helpful in interpreting experimental measurements than complex models of a non-stoichiometric transition layer.

4. ELECTRONIC STRUCTURE CALCULATIONS FOR INTRINSIC INTERFACES

Having constructed an idealized interface model, we proceed to study its electronic structure by considering an Si/SiO_2 superlattice composed of alternating Si and SiO_2 slabs which are sufficiently thick to isolate adjacent interfaces from one another. Most of our studies are based on a 21 atom per unit cell superlattice consisting of 5 Si layers (2 atoms per layer) alternating with 3 tiers of SiO_4 tetrahedra (11 atoms). This superlattice with two additional O atoms forming Si=O double bonds with the two-fold coordinated Si atoms is shown in.[12]

Our studies are based on the first-principles extended muffin tin orbital (EMTO) method.[34] All of the calculations reported in Refs. 12 to 14 and summarized below are based on superlattice charge distributions constructed from neutral free atom self-consistent charge densities.[35] Although the superlattice charge distributions themselves are not exactly self-consistent, such calculations give a good account of Si, SiO_2, and many other types of semiconductors and insulators. A fully self-consistent EMTO computer program has recently been developed,[36] and this program will be used in subsequent studies of Si/SiO_2 interfaces. We believe that the EMTO calculations done to date on Si/SiO_2 provide reasonable estimates of the electronic structure of ideal and defective Si/SiO_2. Refinements based on fully self-consistent EMTO calculations will be reported in due course.

The essential results for an intrinsic Si/SiO_2 superlattice can be summarized as follows: (a) Localized interface states occur in the thermal gap of Si if the dangling bonds are left unsaturated. (b) These localized states are removed from the thermal gap if the dangling bonds are saturated by pairs of H atoms, single O atoms, OH groups, etc. These conclusions apply to unrelaxed lattice geometries. We have made some attempts to relieve the lattice strain using Monte Carlo methods.[13]. Because of the limited width of the SiO_2 region and the severe constraints imposed by the rigid intervening Si regions, the SiO_2 regions relax only slightly, leading to negligible changes in the energy level structure and to no change in conclusions (a) and (b) above.

5. Si AND O VACANCIES AND INTERSTITIALS

Within the framework of a band structure approach it is natural to introduce periodic arrays of non-interacting defects in the SiO_2 region near the interface. Before embarking on such calculations, we first performed exploratory studies of this type using a 24-atom SiO_2 supercell to simulate bulk SiO_2, as reported in an earlier paper.[13] Similar studies were carried out some time ago using the extended Huckel method.[37] The essential idea is to

introduce one defect such as a Si or O vacancy or interstitial per supercell, and then calculate the energy band structure at two or more well-separated points in the reduced zone. In this way one obtains not only the valence and conduction bands of the host SiO_2, but also impurity bands corresponding to the defects introduced. If the supercell is sufficiently large, and the defects sufficiently localized, the impurity bands will have negligible dispersion, and the centers of gravity of these impurity bands will describe the energy levels of isolated defects.

An important advantage of the periodic defect array approach over molecular cluster methods is that the energy levels of the defects are located relative to the valence and conduction band edges of the host crystal. We will now briefly recapitulate our earlier SiO_2 defect investigations.[13]

By trial and error we find that a unit cube of SiO_2 containing 24 atoms places adjacent defects sufficiently far apart (7.68 A) to produce impurity bands with dispersions of the order of 0.1 eV, which is small enough for our purposes. For some defects it is even possible to use a smaller unit cell (SiO_2 with 6 atoms per unit cell) and still end up with acceptably small impurity band dispersions. To illustrate our approach, we consider the 24 atom supercell, which is constructed by placing Si atoms at (0,0,0), (1/4,1/4,1/4), etc., and O atoms at (1/8,1/8,1/8), etc., where distances are measured in units of the cube edge. The intrinsic SiO_2 supercell contains 128 valence electrons, so there are normally 64 filled bands. We test the dispersion properties of defect-related bands by determining the band structure of the supercell at the zone center and also at the zone corner. The essential results are as follows:

5.1 Interstitial Silicon Atoms

Let us introduce a neutral silicon atom at the interstitial position located at the center of the SiO_2 cage in the SiO_2 supercell, (1/2,1/2, 1/2). The 64 filled valence bands are perturbed only slightly. There is a filled interstitial band roughly midway in the SiO_2 band gap arising from the Si 3s level, containing 2 of the 4 valence electrons contributed to the SiO_2 supercell by the Si interstitial. There are also empty interstitial bands located well above the SiO_2 conduction band minimum (CBM). The lowest (perturbed) conduction band is also filled, accounting for the remaining 2 electrons associated with the Si interstitial.

Taking into account the nature of a band-theoretic description of a periodic array of non-interacting defects in an otherwise perfect crystal, the above results can be interpreted as follows: If we introduce a Si+4 interstitial ion core into SiO_2, plus the 4 electrons required to establish charge neutrality, 2 of these electrons will occupy a level in the mid-range of the forbidden band, while the other 2 will be ionized, occupying low-lying conduction band states. This view is somewhat naive, reflecting the limitations of a model in which the defects are separated just far enough so that they don't interact to any appreciable degree. In practice, the final 2 electrons required for local charge neutrality would not be uniformly distributed throughout the crystal, but would be concentrated on the atoms defining the cage surrounding the Si interstitial atom.

It is interesting to find that a Si interstitial produces a level roughly midway in the SiO_2 forbidden band. This suggests that Si interstitials, if they actually exist in SiO_2, could create levels within striking distance of the thermal gap of the Si/SiO_2 interface. Our calculations

are too crude at this stage and the possible positions of the Si interstitial too numerous in actual SiO_2 for us to make predictions more precise than this just now.

In a subsequent study,[14] we investigated the effect of putting a neutral interstitial Si atom at the center of a SiO_2 cage lying next to a Si/SiO_2 interface. In this particular study we added the interstitial Si atom to a 17 atom Si/SiO_2 superlattice (cf. Fig. 1 in Ref. 12) composed of 5 Si layers (2 atoms each), one tier of SiO_4 tetrahedra (5 atoms), and 2 O atoms doubly bonded to the two-fold coordinated Si atoms at the interfaces. For this particular geometry, the interstitial Si atom is close enough to the doubly bonded O atoms to interact with them, leading to a lowering of the Si 3s and 3p atomic levels, relative to their positions in the SiO_2 supercell. The net result is that the Si 3s band lies well below the Si/SiO_2 thermal gap, while the Si 3p bands lie within this gap.

These studies represent the first stage of an investigation of interstitial Si atoms at an interface interacting with O atoms originally doubly bonded to the silicon substrate. The object is to study the formation of Si-O-Si-O-Si bridges in which the O atoms are singly bonded to the Si substrate atoms as well as to the bridging Si atom (originally the interstitial). The bridging Si atom could be doubly charged, representing one form of fixed positive charge at the interface.

5.2 Interstitial Oxygen Atoms

We have also introduced neutral O interstitial atoms at the center of one of the cages in the 24-atom SiO_2 supercell, position (1/2,1/2,1/2). This leads to an occupied interstitial O 2s band about 11 eV below the SiO_2 valence band maximum (VBM), two occupied O 2p bands about 2 eV above the VBM, and an empty O 2p band about 3 eV above the VBM. In practice, such interstitial O atoms would be expected to complete their valency by attaching themselves to a pair of H atoms, for example, to form water.

If we place the neutral O interstitial atom at the center of the SiO_2 cage in the 17-atom Si/SiO_2 superlattice described above, we find that the O 2s and 2p impurity bands lie about 7 to 8 eV below their corresponding values in the SiO_2 supercell. The reason again is the proximity of the interstitial O to the nearby O atoms attached to the silicon substrate. This situation represents a step in the direction of creating a Si-O-O-O-Si bridge, where the interstitial O lies at the middle of the span. Because the O interstitial has acquired its full valency of 8 electrons, the highest valence band is empty, simulating a shallow acceptor level.

These studies suggest that the O interstitial is not likely to produce localized levels within the range of the thermal (Si) gap, in contrast to the Si interstitial. Roughly speaking, the highest occupied interstitial O levels will tend to line up with the highest occupied O levels in SiO_2 (within a few eV), this energy range being well below the thermal gap.

5.3 Neutral Si Vacancies

Returning to the normal 24-atom SiO_2 supercell, let us now introduce a neutral Si vacancy by removing a Si atom, say from position (0,0,0). This removes 4 electrons from the supercell, so the lowest 62 rather than the lowest 64 valence bands are occupied. Because the uppermost valence bands in the normal supercell are built up from O 2p non-bonding orbitals, the removal of a Si atom has negligible influence on the energies of these bands. As

a consequence, the 2 vacant acceptor levels (bands 63 and 64) remain essentially degenerate with the topmost valence band (band 62). If these acceptor levels become occupied, a negatively charged Si vacancy would be created. The situation remains essentially the same if we remove a Si atom from the center of the SiO_4 tetrahedron in the 17-atom Si/SiO_2 superlattice.

However, if in this superlattice we remove the four-fold coordinated Si atom at the interface, i.e., the atom common to the Si and SiO_2 regions, the dominant effect is the creation of two dangling Si bonds and the concomitant formation of localized electronic states at the interface. The levels associated with the non-bridging O atoms are similar to those generated by the removal of a Si atom from the center of a SiO_4 tetrahedron far away from the interface (as in the 24-atom SiO_2 supercell).

5.4 Neutral Oxygen Vacancies

Returning once more to the SiO_2 supercell and removing a neutral O atom, we are left with 128 - 6 = 122 electrons in the unit cell. These electrons fill the lowest 60 valence bands as well as one O vacancy band located about 2 eV below the CBM. On the other hand, if we remove an O atom from the Si-O-Si bond which connects directly to the Si/SiO_2 interface, we create dangling Si bonds and localized interface states in the thermal gap. In all the studies reported here, we have not attempted to relax the lattice after the introduction of a vacancy or interstitial. Some of the most interesting defects of all involve vacancies and interstitials associated with relaxed lattices[9-11] and vacancies leading to broken bonds which are subsequently saturated by the attachment of H or OH groups.[9-11]

6. INTERSTITIAL O_2, SiO, AND H_2O MOLECULES

We have also placed neutral O_2, SiO, and H_2O molecules inside the SiO_2 cages in the 17-atom Si/SiO_2 superlattice.[14] Each molecule was inserted so that its center of gravity coincides with the cage center, and its longest dimension is perpendicular to the interface. For O_2, which normally has 12 valence electrons, we find that there are 7 occupied O_2-related bands (2 electrons of opposite spin per band). Our calculations thus indicate that the O_2 molecule has acquired 2 additional electrons, becoming doubly negatively charged. The highest valence band is now empty, corresponding to a shallow acceptor level. We are presently investigating the possibility that O_2 molecules close to an interface can form bridges between adjacent pairs of two-fold coordinated Si substrate atoms. To form Si-O=O-Si bridges, the terminal Si atoms would have to contribute one dangling bond each to the spanning O=O molecule.

For SiO, which normally has 10 valence electrons, we find that there are six occupied SiO-related bands, so the SiO molecule acquires 2 additional electrons, emptying the highest valence band and producing a shallow acceptor level. For H_2O, which normally has 8 valence electrons, there are 4 occupied H_2O-related bands, so the molecule remains neutral. Of course, these results apply to the particular interstitial position chosen, but the conclusions are instructive nevertheless.

7. SUBSTITUTIONAL Al AND SUBSTITUTIONAL Al + INTERSTITIAL H

Finally, let us consider the substitution of a neutral Al atom for a neutral Si atom in the SiO_2 supercell. The valence and conduction bands of SiO_2 are not affected significantly by this replacement. The removal of one electron from the supercell leads to a half-empty highest valence band (the 64 highest band). Within the present framework, this represents a partially filled acceptor level located slightly above the VBM of SiO_2. We can fill this acceptor level by supplying an additional electron to the supercell. For purposes of illustration, let us introduce a neutral interstitial H atom close to the substitutional Al atom in the SiO_2 supercell, at position (-1/8,-1/8,-1/8). The H atom donates its electron to the Al defect, completing the occupation of all the valence bands, and producing an empty H level roughly midway within the SiO_2 forbidden band. The exact position of the empty level depends on the relative positions of the Al and H atoms, but the midrange of the SiO_2 band gap is the indicated range. Thus we see that such a complex could produce localized states within the thermal gap of Si/SiO_2, which also lies in the midrange of the SiO_2 band gap. Similar effects would be expected if we introduced an interstitial monovalent atom such as Na instead of H.

8. SPECULATIONS ON THE U-SHAPED CONTINUUM OF INTERFACE STATES

Various authors[38] have called attention to the fact that there is often a sharp peak in the density of Si/SiO_2 interface states at about 0.3 eV above the Si VBM, and that this peak can be removed by exposing the interface to hydrogen. Once this peak is removed, the distribution of interface states in the thermal gap of Si appears to be U-shaped, rising toward the valence and conduction band edges and falling to minimal values in between. A plausible explanation[38] for the disappearance of the sharp peak is that the dangling Si bonds at the interface responsible for this peak are removed by the formation of Si-H bonds.

The origin of the U-shaped continuum is not understood. There are obviously many possible explanations. Using our own studies as a guide, and in particular the fact that substitutional Al + interstitial M can lead to interface states in or near the thermal gap (M = monovalent metal atom or H), we will go one step further and ask: Are there different Si positions at or near the interface at which substitutional Al + interstitial M could produce different interface state distributions, for example, one peaked below the Si VBM and another above the Si CBM, so that the superposition of the tails from these two peaks would resemble a U-shaped curve in the thermal gap?

The explanation we propose is that there are Al impurities near the interface, some occupying the centers of AlO_4 tetrahedra, and others the four-fold coordinated positions at the interface where the Si and SiO_2 regions are joined. The latter Al impurities occupy the centers of distorted $Si2\text{-}Al\text{-}O_2$ tetrahedra. Allowing for the different positions that neighboring interstitial M atoms would occupy at an actual interface, we would get two distinct distributions of interface levels, one offset in energy from the other. The distribution corresponding to AlO_4 + M would lie above the one corresponding to $Si2\text{-}Al\text{-}O_2$ + M, so the tail from the former would account for the upper part of the U, and the tail from the latter for the lower part. The individual pieces of this explanation are consistent with our calculations. Finally, we note that the exposure of the interface to H can be regarded not only as a means for saturating the dangling Si bonds, but also as a means for forming the

AlO_4 + H and Si2-Al-O_2 + H complexes that could be responsible (in whole or in part) for the U-shaped continuum.

9. CONCLUDING REMARKS

We have shown how idealized Si/SiO_2 superlattices can be used to describe the Si/SiO_2 interface and to construct simple models of defects such as Si and O vacancies and interstitials. The calculations we have discussed represent early attempts at dealing with complex geometrical situations. The results to date have been sufficiently encouraging to suggest that a more detailed understanding of these and other defects can be achieved by carrying out first principles calculations self-consistently, taking lattice relaxation effects into account.

The author is grateful to many individuals for stimulating discussions and correspondence, particularly R. S. Bauer, B. E. Deal, D. J. Henderson, B. E. Hobbs, N. M. Johnson, R. V. Kasowski, A. G. Revesz, and W. E. Rudge.

REFERENCES

1. Supported in part by ONR Contract Number N00014-79-C-0814
2. S. T. Pantelides (ed.): *The Physics and Chemistry of SiO_2 and its Interfaces* (Pergamon Press, New York, 1978)
3. G. Lucovsky, S. T. Pantelides, F. L. Galeener (eds.): *The Physics of MOS Insulators* (Pergamon Press, New York, 1980)
4. A. G. Revesz: J. Non-Cryst. Solids 11, 309 (1973); Phys. Status Solidi (a) 57, 235,657 (1980); ibid (a) 58, 107 (1980); A. G. Revesz, G. V. Gibbs: In Ref. 3, p. 92
5. B. E. Deal: J. Electrochem. Soc. 121, 198C (1974)
6. Y. C. Cheng: Prog. Surf. Sci. 8, 181 (1977)
7. M. Pepper: Contemp. Phys. 18, 423 (1977)
8. C. R. Helms: J. Vac. Sci. Technol. 16, 608 (1979)
9. N. F. Mott: Adv. Phys. 26, 363 (1977); In Ref. 2, p. 1; J. Non-Cryst. Solids 40, 1 (1980)
10. G. N. Greaves: Phil. Mag. B 37, 447 (1977); In Ref. 2, p. 268; C. M. Svensson: In Ref. 2, p. 328; G. Lucovsky, D. J. Chadi: In Ref. 3, p. 301; R. H. D. Nuttall: J. A. Weil: Solid State Commun. 33, 99 (1980)
11. D. L. Griscom: J. Non-Cryst. Solids 40, 211 (1980); In Ref. 2, p. 232; Phys. Rev. B 20, 1823 (1979)
12. F. Herman, I. P. Batra, R. V. Kasowski: In Ref. 2, p. 333
13. F. Herman, D. J. Henderson, R. V. Kasowski: In Ref. 3, p. 107
14. F. Herman, R. V. Kasowski: J. Vac. Sci. Technol., in press
15. N. F. Mott, E. A. Davis: *Electronic Processes in Non-Crystalline Materials* (Clarendon Press, Oxford, 1979), Second Edition; N. F. Mott: J. Phys. C: Solid State Phys. 13, 5433 (1980)
16. J. M. Ziman: *Models of Disorder* (Cambridge Univerity Press, 1979)
17. M. H. Brodsky (ed.): *Amorphous Semiconductors* (Springer-Verlag, Berlin, 1979)
18. D. R. Uhlmann: J. Non-Cryst. Solids 42, 119 (1980); D. Adler: ibid 42, 315 (1980); A. C. Wright, G. A. N. Connell, J. W. Allen: ibid 42, 509 (1980)

19. J. C. Phillips: Phys. Stat. Sol. (b) 101, 473 (1980); Comments Solid State Phys. 9, 191 (1980)
20. R. B. Laughlin, J. D. Joannopoulos, D. J. Chadi: In Ref. 2, p. 321; Phys. Rev. B 20, 5228 (1979); Phys. Rev. B 21 5733 (1980)
21. T. Sakurai, T. Sugano: In Ref. 3, p. 241
22. F. L. Galeener: J. Non-Cryst. Solids 40, 527 (1980)
23. W. Y. Ching: Phys. Rev. Lett. 46, 607 (1980)
24. S. T. Pantelides, M. Long: In Ref. 2, p. 339
26. G. H. Dohler, R. T. Dandoloff, H. Bilz: J. Non-Cryst. Solids 40, 87 (1980)
26. J. D. Bernal, Proc. Roy. Inst. (London) 37, 355 (1959); Scientific American, Aug., 1960
27. R. J. Bell, P. Dean: Phil. Mag. 25, 1381 (1972); P. H. Gaskell, I. D. Tarrant: Phil. Mag. 42, 265 (1980)
28. G. S. Cargill III, P. Chaudhari (eds.): *Atomic Scale Structure of Amorphous Solids* (North-Holland, Amsterdam, 1979); also published in J. Non-Cryst. Solids 31, pp. 1-286 (1978)
29. S. T. Pantelides, W. A. Harrison: Phys. Rev. B 13, 2667 (1976); S. T. Pantelides, Comments Solid State Phys. 8, 55 (1977)
30. F. Herman: J. Vac. Sci. Technol. 16, 1101 (1979)
31. R. W. G. Wyckoff: *Crystal Structures* (Interscience, New York, 1963), Second Ed., Vol. 1
32. L. E. Sutton (ed.): *Interatomic Distances Supplement* (The Chemical Society, London, 1965), p. S 12S
33. K. F. Purcell and J. C. Kotz: *Inorganic Chemistry* (W. B. Saunders Co., Philadelphia, 1977), p. 318 ff
34. R. V. Kasowski, E. Caruthers: Phys. Rev. B 21, 3200 (1980)
35. F. Herman: *Atomic Structure Calculations* (Prentice-Hall, Englewood Cliffs, N. J., 1963)
36. R. V. Kasowski, to be published
37. A. J. Bennett, L. M. Roth: J. Phys. Chem. Solids 32, 1251 (1971); T. Iizuka, T. Sugano: Japan. J. Appl. Phys. 12, 73 (1973)
38. A. Goetzberger, E. Klausmann, M. Schulz: CRC Crit. Rev. Solid State Sci. 6, 1 (1976); E. H. Nicollian: J. Vac. Sci. Technol. 14, 1112 (1977); N. M. Johnson, D. K. Biegelsen, M. D. Moyer: In Ref. 3, p. 311

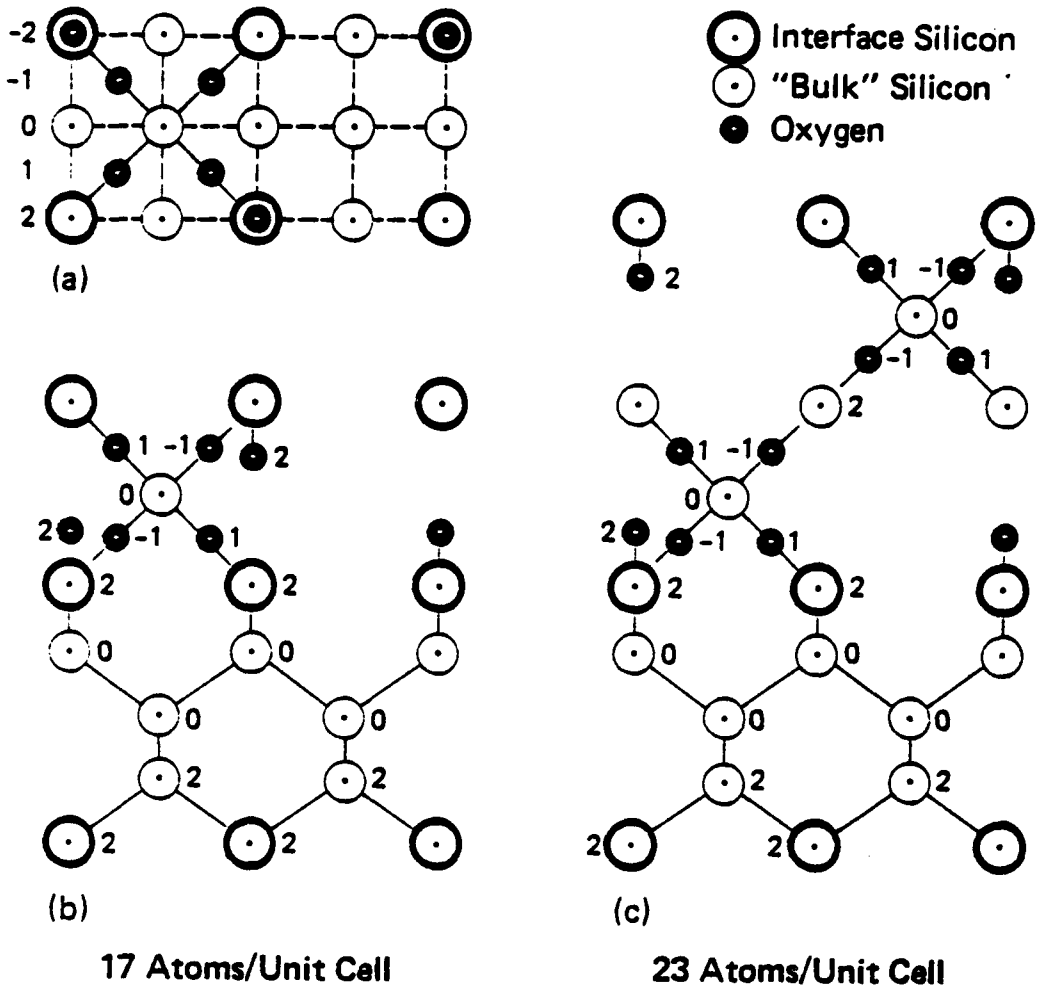

FIGURE 1. Si/SiO_2 superlattices and interfaces. Panel (a) shows a view of the upper interface and the SiO_2 region as seen from just below the SiO_2 region in panel (b). Panels (b) and (c) represent front views of superlattices having 17 and 23 atoms per unit cell, respectively. Both superlattices have five silicon layers (2 atoms each). All the two-fold coordinated Si interface atoms are doubly bonded to O atoms. In panel (b) there is one tier of SiO_4 tetrahedra (5 atoms), while in panel (c) there are three such tiers (11 atoms). The numbers denote the planes in which the various atoms lie, the 2 representing the front-most plane, etc. For clarity, the O atoms in the backmost (-2) plane are not shown. As best seen in panel (a), the interface Si atoms (heavier outer circles) form a checkerboard, with the Si atoms attached to the SiO_4 tetrahedra corresponding to "red" squares, and the Si atoms doubly bonded to O atoms corresponding to "black" squares. The "bulls-eyes" in panel (a) represent the Si=O groups as seen from the O end. For another view of these superlattices, see C. R. Helms, J. Vac. Sci. Technol. 16, 608 (1979).

Proceedings of 5th International Conference on Ternary and
Multinary Compounds, Cagliari, Italy, Sept. 14-16, 1982
Il Nuovo Cimento *2D*, 1636 (1983)

ELECTRONIC STRUCTURE CALCULATIONS FOR COMPLEX CRYSTALS

Frank Herman
IBM Research Laboratory, San Jose, California 95193 USA*
and
Francesco Casula
GNSM-CNR and Institute of Physics, University of Cagliari
I09100 Cagliari, Italy

ABSTRACT: We discuss some new ideas for improving first-principles muffin-tin-orbital-type electronic structure calculations for complex crystals such as ternary and multinary compounds. The new ideas include: construction of generalized muffin-tin orbitals and energy-dependent double MTO basis sets; cellular decomposition based on strongly overlapping atomic spheres; and evaluation of matrix elements in the residual interstitial region by extrapolation.

In the mid-1970s, Andersen and his coworkers[1] developed a simplified version of the linear combination of muffin-tin orbitals (LCMTO) method based on the atomic sphere approximation (ASA). This simplified approach has been used successfully to study the electronic structure of many types of close-packed solids, particularly transition metals.[2] The original LCMTO method[3] has by now been superseded by the more sophisticated extended muffin-tin orbital (EMTO) method.[4] In a recent paper,[5] we discussed extensions of the LCMTO/EMTO method aimed at increased accuracy and reduced running times. Our own work focuses on loosely packed structures containing many atoms per unit cell, including surfaces and interfaces represented by repeating slab geometries.[5,6] In the present paper we will indicate the essential ideas underlying these extensions. These ideas are well suited to first-principles studies of ternary and multinary compounds such as chalcopyrites and their derivatives.

It is possible to apply the ASA to some types of loosely packed solids after first transforming them into quasi-close-packed solids by replacing part of the interstitial region with "empty" spheres. In this way, most of the physically relevant space is spanned by weakly overlapping atomic and "empty" spheres. However, this transformation is practical only for certain geometries,[7] and even for these geometries the adequacy of this approach can be obscured by the arbitrary choice of "empty" sphere radii.

For more general types of open structures, it becomes necessary to use more rigorous treatments such as LCMTO/EMTO methods, which unfortunately require significantly longer running times. In these methods, the wave functions are represented by exponentially-damped MTOs (expMTOs) with tails having the form $\exp(-\kappa r)/r$, as well as by oscillatory-damped MTOs (oscMTOs) with tails having the form $\cos(\kappa r)/r$. Evaluation of matrix elements in the interstitial region by three-dimensional integration accounts for the

greatly increased computational effort.

Although first-principles LCMTO/EMTO calculations have been carried out successfully for many different types of surfaces, interfaces, and loosely packed solids, some having as many as 44 atoms per unit cell,[5,6] the usefulness of these calculations could be greatly enhanced if their accuracy could be increased without substantially increasing the running time. The same would be true if the running time could be decreased by one or two orders of magnitude, even at the cost of a slight decrease in accuracy.

In order to improve the accuracy of LCMTO/EMTO calculations, it is necessary to increase the variational flexibility of the MTO basis sets. This flexibility is presently limited by the use of single-term tail functions, such as $\exp(-\kappa r)/r$, outside the MT-spheres; and by the use of energy- independent radial functions inside the MT-spheres. The need for increased accuracy is particularly acute for inhomogeneous systems such as surfaces and interfaces, where localized surface and interface states must be represented by compact, highly adaptable basis functions. The single expMTOs presently in use often prove inadequate for certain systems. If one represents these states by a linear combination of two expMTOs having different values of κ, as suggested by Harris and Painter,[8] the variational flexibility can be increased, but the computational effort is roughly doubled. The reason is that modified spherical Bessel functions must now be evaluated for two values of κ rather than just one.

The computational effort is also roughly doubled if a double MTO basis set composed of oscMTOs as well as expMTOs is introduced in an attempt to improve the variational adaptability of the basis set. This approach usually works well for homogeneous systems but often fails for inhomogeneous ones. The most serious difficulty, at least for some types of inhomogeneous systems, is that the oscMTOs are of longer-range than the expMTOs, leading to undesirable coupling between adjacent surfaces or interfaces.

We have enhanced the variational flexibility of localized MTO basis functions by constructing generalized MTOs composed of linear combinations of single expMTOs and their first and second derivatives with respect to κ. Since these derivatives can be expressed in terms of the leading expMTO by recursion relations, and since the generalized MTOs satisfy expansion theorems analogous to those of ordinary expMTOs, the standard LCMTO/EMTO formalism is readily generalized.[5] Although the generalized formalism is more complicated as a result of the additional variational flexibility built into the basis functions, the computational effort is expected to increase only slightly over that required for state-of-the-art LCMTO/EMTO calculations. The reason is that all the modified spherical Bessel functions appearing depend only on a single value of κ, and all these functions can be generated efficiently with the aid of recursion relations.

Moreover, energy-dependent double-MTO basis sets can be constructed by suitably rearranging and manipulating the matrix element information. Since this procedure will normally lead to large and small MTO components, it is possible to achieve further computational economies by solving the double-dimension secular equations by the Lowdin partitioning scheme.[9] In addition to improving the variational adaptability still further, the use of energy-dependent basis sets enables us to solve the secular equations over a wider energy range than would otherwise be possible.

In order to make the study of extremely large, loosely packed systems practical, it is essential to reduce the computational effort drastically. This can be accomplished only by drastically simplifying the most time-consuming step in LCMTO/EMTO calculations, namely, the evaluation of the interstitial matrix elements. Instead of dealing with the interstitial region as a whole, or partitioning this region into space-filling Wigner-Seitz atomic polyhedra, as in the original LCMTO method,[3] we surround each (non-overlapping) MT-sphere with a larger, concentric outer sphere, and then replace this set of overlapping outer atomic spheres by an equivalent set of truncated atomic spheres Limiting the radii of the outer spheres so that no two of these spheres overlap inside a third, and representing each of the truncated atomic spheres by a three-dimensional Heaviside operator,[5,10] the matrix elements of this operator can be determined analytically, which is considerably easier to do than integrating over a three-dimensional mesh as would be necessary for polyhedral atomic cells. Moreover, the matrix elements themselves can be determined inside the truncated atomic spheres by angular and radial integrations, which is again considerably easier than three-dimensional integration.

In earlier scattered wave calculations for large planar organic molecules,[11] we studied the convergence of solutions based on sequences of overlapping atomic sphere models having progressively larger radii. Based on this earlier experience with open structures, we developed an extrapolation procedure for obtaining accurate estimates of the matrix elements in the residual interstitial region, i.e., in the region outside the overlapping atomic spheres.[5] The essential idea is to use overlapping atomic spheres which are not unreasonably large for the angular and radial integrations, and then to simulate the use of still larger overlapping atomic spheres by extrapolation. Of course, there will be a slight loss in accuracy due to the extrapolation, but this should be insignificant compared with the gain in accuracy arising from the use of improved MTO basis sets. Although there is some arbitrariness in the choice of the overlapping sphere radii, the consequences of this arbitrariness can be virtually eliminated by employing carefully designed extrapolation procedures.[5]

A complete description of the mathematical formalism appears in Ref. 5, and a detailed discussion of three-dimensional Heaviside operators is given in Ref. 10. Detailed calculations based on these ideas are currently in progress, and will be reported elsewhere.

* Supported in part by the Office of Naval Research, Contract Number N00014-79-C-0814.

1. O.K. Andersen, Phys. Rev. B *12*, 3060 (1975); O. Jepsen, O.K. Andersen, and A.R. Mackintosh, Phys. Rev. B *12*, 3084 (1975).
2. A.R. Mackintosh and O.K. Andersen in *Electrons at the Fermi Surface*, edited by M. Springford (Cambridge, 1980), p. 149.
3. O.K. Andersen and R.V. Kasowski, Phys. Rev. B *4*, 1064, (1971); R.V. Kasowski and O.K. Andersen, Solid State Commun. *11*, 799 (1972); O.K. Andersen and R.G. Wooley, Mol. Phys. *26*, 905 (1973); R.V. Kasowski, Phys. Rev. B *14*, 3398 (1976).
4. R.V. Kasowski and E.B. Caruthers, Phys. Rev. B *21*, 3200 (1980); R.V. Kasowski, W.Y. Hsu, and E.B. Caruthers, J. Chem. Phys. *72*, 4896 (1980); R.V. Kasowski, Phys. Rev. B *25*, 4189 (1982).
5. F. Casula and F. Herman, J. Chem. Phys. *78*, 858 (1983).

6. For a recent EMTO study of $Pd_2Si/Si(111)$ superlattices, see F. Herman, F. Casula, and R.V. Kasowski, Physica B, in press. For extensive references to earlier LCMTO/EMTO calculations, see Ref. 5.
7. F. Herman and R.V. Kasowski, IBM Internal Report RJ 2658 (Oct. 3, 1979) unpublished; T. Jarlborg and A.J. Freeman, Phys. Lett. *47A*, 349 (1979); D. Glotzel, B. Segall, and O.K. Andersen, Solid State Commun. *36*, 403 (1980).
8. J. Harris and G.S. Painter, Phys. Rev. B *22*, 2614 (1980).
9. P.O. Lowdin, J. Chem. Phys. *19*, 1396 (1951).
10. F. Casula and F. Herman, IBM Research Report RJ 3558 (July 28, 1982) unpublished.
11. F. Herman, A.R. Williams, and K.H. Johnson, J. Chem. Phys. *61*, 3508 (1974); F. Herman in *Electrons in Finite and Infinite Structures*, edited by P. Phariseau and L. Scheire, (Plenum, New York, 1977), p. 382.

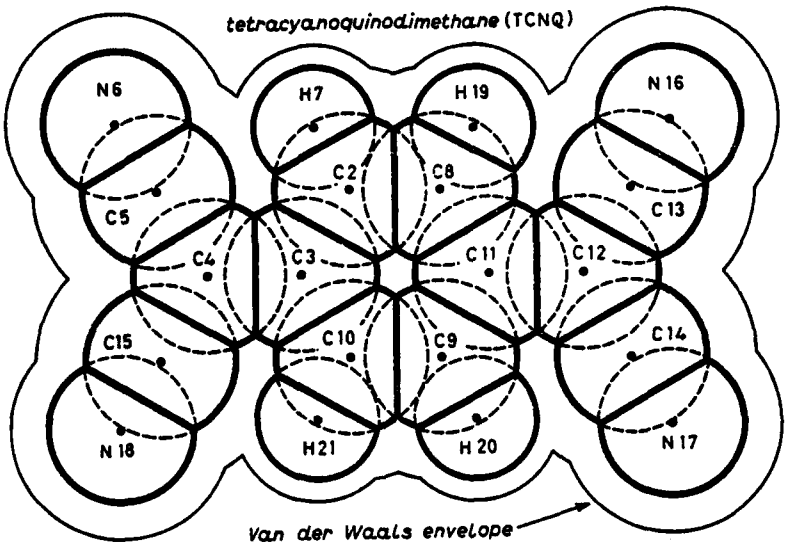

FIGURE 1. Truncated atomic sphere model for TCNQ molecule based on strongly overlapping atomic spheres. The centers of the C, N, and H spheres are indicated by symbols such as C5. The overlapping spheres are represented by the dashed lines, and the truncated spheres by the heavy lines. This model satisfies the multiple overlap restriction; that is to say, different overlap regions do not overlap one another. The function of the extrapolation procedure described in the text is to include more and more of the residual interstitial region inside a sequence of overlapping atomic sphere models having progressively larger radii. In the limit, these spheres become the Van der Waals spheres, whose envelope describes the physically relevant portion of the interstitial region. For further details, see Refs. 5, 10, and 11.

Note. The published paper includes a mathematical appendix which has not been included here.

Physica 117B & 118B (1983) 837-839
North-Holland Publishing Company

ELECTRONIC STATES AND SCHOTTKY BARRIERS AT Pd_2Si/Si(111) INTERFACES

Frank Herman,* IBM Research Laboratory, San Jose, California 95193 USA
Francesco Casula,† Institute of Physics, University of Cagliari, Italy
Robert V. Kasowski, Experimental Station, Dupont, Wilmington, Delaware 19898 USA

It is possible to account for measured Pd/Si Schottky barrier heights (0.71-0.73 eV) by assuming that the interface between Si and Pd_2Si includes a hexagonal Si transition region induced by the presence of Pd impurities. With the Fermi level pinned slightly above the Si valence band edge by hydridized Pd-Si states at the interface, as calculations indicate, the Schottky barrier height is determined primarily by the band gap of hexagonal Si, which is about 0.85 eV. Since Pd atoms are larger than Si atoms, isolated substitutional and interstitial Pd atoms are not readily incorporated into the Si lattice. We believe that the Pd impurities form triangular clusters at Si vacancies. Since these clusters are more easily accommodated in hexagonal than in cubic Si, the Si stacking sequence changes from cubic to hexagonal, giving rise to the transition region.

1. INTRODUCTION

In spite of extensive research on rectifying metal-semiconductor contacts, our understanding of the factors determining Fermi level pinning and Schottky barrier heights is still rudimentary.[1-3] In order to gain further insight into the nature of transition metal - semiconductor interfaces, we decided to study the Pd/Si system, for which a wealth of experimental information is available.[4,5] In contrast to earlier theoretical calculations of idealized Pd/Si compounds[6] and Pd monolayers chemisorbed on the Si(111) surface,[7] our studies are concerned explicitly with Pd_2Si/Si interfaces. Using a repeating slab geometry and the first-principles extended muffin-tin orbital method, we investigated the electronic structure of various Pd_2Si/Si superlattices as well as the effects of introducing Pd impurities into the Si substrate. Because of space limitations, we will confine our attention here to one particular set of ideas that have emerged from our work. The details of our calculations will be reported elsewhere.[8]

2. Pd_2Si/Si INTERFACES AND SUPERLATTICES

One of the major obstacles to understanding metal-semiconductor interfaces is our limited knowledge of the atomic structure of such interfaces. In order to avoid many of the problems associated with compositionally graded interfaces and other manifestations of structural disorder, we decided to study epitaxial systems. Our interest in the Pd_2Si/Si system was reinforced by the fact that Pd_2Si can be grown epitaxially on a Si substrate.[9,10] To a first approximation, the Pd_2Si/Si interface can be regarded as a Pd_2Si crystal in perfect registry with a Si crystal. For computational reasons, it is convenient to study Pd_2Si/Si(111) superlattices whose interfaces are sufficiently far apart to be noninteracting.[11] As can be seen from Figure 1, each Si(111) layer contributes 3 Si atoms to a superlattice unit cell, while the Si-rich and Pd-rich Pd_2Si layers contribute 3 Pd + 2 Si, and 3 Pd + 1 Si, respectively.

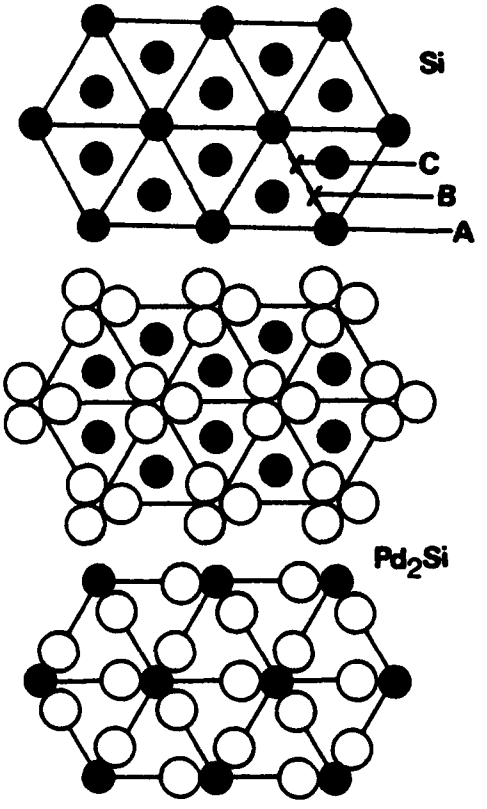

Figure 1. The Si(111) plane is shown at the top, the Si-rich layer of Pd_2Si in the middle, and the Pd-rich layer of Pd_2Si at the bottom. In the top panel, the symbols C, B, and A denote the positions of Si atoms in different Si(111) layers. We also use these symbols to denote individual Si layers (not double Si layers) in superlattices.

We investigated the electronic structure of various Pd_2Si/Si(111) superlattices. The repeat unit of one of the simplest (8 atomic layers) contains 6 layers of cubic Si (stacking sequence A-C-C-B-B-A) followed by the Si-rich and Pd-rich layers of Pd_2Si. Altogether, the unit cell contains 6 Pd + 21 Si atoms. We also investigated an even simpler 6-layer Pd_2Si/Si(111) superlattice composed of 4 layers of hexagonal Si (stacking sequence (A-B-B-A) and the Si-rich and Pd-rich layers of Pd_2Si. The unit cell here contains 6 Pd + 15 Si atoms.

For all such superlattices, there are clearly two different types of Pd_2Si/Si interfaces, corresponding to Si-rich or Pd-rich frontier layers of Pd_2Si. For both types, the relative positions of substrate Si atoms and adjacent Pd atoms are different from the on-top and triangular sites used in Ref. 7 to describe a Pd monolayer chemisorbed on the Si(111) surface. Nevertheless, using reasonable estimates of Pd-Si distances across the interface and more realistic interface geometries, our own preliminary results are consistent with those of Ref. 7 in suggesting that the Fermi level is pinned by hybridized Pd-Si states just above the Si valence band edge. The pinning is slightly different at the Si-rich and Pd-rich Pd_2Si interfaces, so that different samples having a preponderance of one interface type or the other would have slightly different Schottky barrier heights.[8]

3. HEXAGONAL SILICON INDUCED BY Pd CLUSTERS

In order to account for the fact that measured Pd_2Si/Si Schottky barrier heights (0.71-0.73 eV)[5] are considerably lower than theoretical estimates (1.0-1.1 eV),[7] it is necessary to consider deviations from ideally abrupt interface models separating perfect Pd_2Si and Si crystals. High resolution electron microscope studies[10] suggest that actual Pd_2Si/Si interfaces may be rough on the scale of a several atomic layers, may consist of both interface types, and may contain rotationally twinned domains as well. Instead of exploring such complicated situations, which is clearly beyond our scope, we decided to explore the effects of introducing simpler types of defects, including Pd impurities and stacking disorder, into our Si substrates. Using half the nearest neighbor distances in Pd metal (2.75 A) and Si (2.35 A) as measures of atomic size, the Pd atom is 17 percent larger than the Si atom, and so would not be readily accommodated at either substitutional or interstitial Si sites. This would be true regardless of the local Si stacking sequence.

In trying to imagine how Pd atoms would arrange themselves in the Si substrate if they diffused into this substrate in advance of a growing interface, we realized that triangular Pd clusters such as those belonging to the Si-rich Pd_2Si layer could be accommodated quite well at Si vacancies in a hexagonal Si environment, and less well at Si vacancies in a cubic Si environment. The hexagonal sequence A-B-B-A leads to prismatic hexagonal cavities, while the cubic sequence A-B-B-C leads to adamantine-like cavities. Using ball-and-stick models, it is easily seen that three adjacent interstitial cavities surrounding a Si vacancy provide more room for triangular Pd clusters in hexagonal than in cubic Si.

We were originally led to the idea of introducing hexagonal Si regions into our Pd_2Si/Si superlattices in order to simplify our calculations by dealing with unit cells containing as few as 21 rather than 27 atoms. However, once we realized that triangular Pd clusters could be accommodated more easily in hexagonal Si than in cubic Si, we decided to pursue this idea on its own merits and to report this aspect of our work here. Accordingly, let us set aside the model of an ideal Pd_2Si/Si interface, and consider instead a more realistic interface where individual Pd atoms or small Pd clusters diffuse into the Si region somewhat in advance of the growing Pd_2Si/Si interface.

We believe that individual Pd atoms are unlikely to enter the Si lattice substitutionally or interstitially because of their large size, but instead would form triangular clusters which would replace individual Si atoms. During interface formation, we would expect the Si stacking sequence in the neighborhood of the interface to fluctuate. In order to accommodate the triangular Pd clusters, the hexagonal Si structure would eventually form. Even though the total energy of a hexagonal Si lattice is higher than that of a cubic Si lattice, the energy difference is quite small, and is easily compensated by the reduction in elastic energy associated with the improved accommodation of the triangular Pd clusters at Si vacancies. It would probably take only a small number of such clusters to influence the stacking sequence over an extended region.

In short, we believe that a hexagonal Si transition region would be generated just in front of the growing Pd_2Si/Si interface. Bearing in mind that the Si-rich Pd_2Si layer is an ordered triangular array of triangular Pd clusters and Si atoms (cf. Figure 1), a Si layer containing triangular Pd clusters at random isolated Si vacancy sites can be regarded as an incipient Si-rich Pd_2Si layer. It is difficult to estimate the width of this transition region, but this width would probably be comparable to the scale of the interface roughness, that is to say, several atomic layers. Even if the hexagonal Si transition region consists of only several atomic layers, its electronic structure would be characteristic of hexagonal Si, and the Schottky barrier at the Pd_2Si/Si interface would be determined in large measure by the bandgap of hexagonal Si, rather than by that of the cubic Si substrate.

4. BAND STRUCTURE OF HEXAGONAL SILICON

It is well known that direct band gap semiconductors such as ZnS have nearly the same band gap in the cubic and hexagonal structures. It is perhaps less well known that the polytypes of indirect band gap materials such as SiC have different band gaps because the conduction band minima are shifted to different positions in reduced

zones having different symmetries.[12] For example, in going from cubic (3C) SiC to hexagonal (2H) SiC, the conduction band edge shifts from the X point to the K point in the corresponding reduced zones, and the indirect band gap changes from 2.3 to 3.3 eV.[12] Clearly, these effects can be quite large.

The electronic structure of various polytypes of Si and Ge including hexagonal (2H) Si and Ge was studied some time ago.[13,14] When the stacking sequence is changed from cubic to hexagonal, the indirect conduction band edge of Si shifts from a point on the (100) axis of the cubic reduced zone to the M point of the hexagonal reduced zone, and the indirect band gap is reduced about 0.3 eV from 1.12 to 0.85 eV. The Ge conduction band edge at L is folded back to the zone center, so that hexagonal Ge has a direct band gap of about 0.55 eV, roughly 0.2 eV less than the 0.76 eV indirect band gap of cubic Ge (relative to the center of gravity of the spin-orbit split valence band edge.) In view of the possible importance of hexagonal Si (and Ge) in the present context, it would be desirable to recalculate hexagonal Si and Ge bandgaps using improved potentials and calculational techniques. For our immediate purposes, however, it is sufficient to use the earlier values just quoted.

5. SCHOTTKY BARRIER HEIGHTS

If a hexagonal Si region lies between Pd_2Si and the (cubic) Si substrate, and if this transition region is at least several atomic layers thick so that it can be characterized by a local forbidden band width, the contact between metallic Pd_2Si and semiconducting Si would involve the hexagonal Si band gap of 0.85 eV rather than the 1.12 eV band gap characteristic of cubic Si. This would place an upper limit of about 0.85 eV on the Pd_2Si/Si Schottky barrier height. The other factor determining the Schottky barrier height is the position of the Fermi level, which appears to lie just above the Si valence band edge.[7,8]

6. CONCLUDING REMARKS

By postulating the existence of a hexagonal Si transition region, the maximum Schottky barrier height is reduced from a value equal to the band gap of cubic Si (1.12 eV) to the corresponding quantity for hexagonal Si (0.85 eV). Our model of a reduced effective band gap at the semiconductor-metal interface is reminiscent of Inkson's model,[15] except that we invoke the hexagonal phase of Si rather than many-electron effects to account for the reduced band gap at the interface. Having offered a specific atomic model to account for Schottky barrier heights at $Pd_2Si/Si(111)$ interfaces, we encourage experimentalists to search for evidence of triangular Pd clusters and a hexagonal Si transition region at such interfaces. High energy ion channeling and Rutherford backscattering measurements would appear particularly promising for this purpose. These ideas can also be extended to other silicide-Si interfaces, and possibly also to transition metal-Ge interfaces.

ACKNOWLEDGMENTS

We are grateful to J.L. Freeouf, W. Krakow, and G.W. Rubloff for fruitful discussions.

REFERENCES

* Supported in part by Office of Naval Research Contract Number N00014-79C-0814.

† IBM World Trade Fellow, 1980-1981.

[1] Rhoderick, E.H., Metal-Semiconductor Contacts (Clarendon Press, Oxford, 1978).

[2] Sze, S.M., Physics of Semiconductor Devices (Wiley-Interscience, N.Y., 1981), 2nd Ed.

[3] Schluter, M., Thin Solid Films, (Proc. 1981 M.R.S. Meeting), in press.

[4] Freeouf, J.L., in Rubloff, G.W. and Ho, P.S. (eds.), Metal/Si and Silicide/Si Interfaces (Elsevier, Amsterdam, 1983), in press.

[5] Ho, P.S. and Rubloff, G.W., Thin Solid Films 89 (1982) 433-446.

[6] Ho, P.S., Rubloff, G.W., Lewis, J.E., Moruzzi, V.L., and Williams, A.R., Phys. Rev. B22 (1980) 4784-4790.

[7] hm, J., Cohen, M.L., and Chelikowsky, J.R., Phys. Rev. B22 (1980) 4610-4619.

[8] Herman, F., Casula, F., and Kasowski, R.V., to be published.

[9] Buckley, W.D. and Moss, S.C., Solid-State Electronics 15 (1972) 1331-1337.

[10] Krakow, W., Thin Solid Films, (Proc. 1981 M.R.S. Meeting), in press.

[11] Herman, F., J. Vac. Sci. Technol. 16 (1979) 1101-1107; Herman, F. and Kasowski, R.V., ibid 19 (1981) 395-401.

[12] Herman, F., Van Dyke, J.P., and Kortum, R.L., Mat. Res. Bull. 4 (1969) S167-S178.

[13] Ortenberger, I.B., Rudge, W.E., and Herman, F., J. Noncrystal. Solids 8-10 (1972) 653-657.

[14] Joannopoulos, J.D. and Cohen, M.L., Phys. Rev. B7 (1973) 2644-2657.

[15] Inkson, J.C., J. Vac. Sci. Technol. 11 (1974) 943-946.

Presented at 17th International Conference on the Physics of Semiconductors, San Francisco, August 6 to 10, 1984. To be Published in the Proceedings of ICPS-17 (Springer-Verlag, Berlin) 1984.

ELECTRONIC STRUCTURE OF INTERFACES BETWEEN CRYSTALLINE AND AMORPHOUS TETRAHEDRALLY-COORDINATED SEMICONDUCTORS*

Ph. Lambin** and F. Herman
IBM Research Laboratory, San Jose, California 95193

ABSTRACT. We have generated an atomic-scale model of the (001) interface between amorphous and crystalline tetrahedrally-coordinated semiconductors. The construction is based on original computer algorithms which transform random and ordered close-packed lattices into corresponding covalent networks. Calculations of the electronic density of states indicate the presence of gap states in the amorphous region and near the interface. These gap states arise from structural imperfections, primarily dangling bonds, which occur naturally in this fully computer-generated model, as do voids and lattice distortions. The spatial extent of the interface is a few atomic layers.

I. INTRODUCTION

Although a great deal of theoretical effort has been devoted to the study of idealized interfaces connecting lattice-matched crystalline semiconductors,[1] interfaces between crystalline (c) and amorphous (a) semiconductors have received only scant attention.[2] To our knowledge, the only existing atomic-scale models of such interfaces are small (about 100 atom) hand-built clusters.[3-5] In order to avoid subjective influences in the construction of such models, we have developed a fully automatic technique and applied this to the study of the c-Si/a-Si interface. (We will use Si for purposes of discussion, even though our structural results apply in principle equally well to C, Si, Ge, and grey Sn.) As a first step, we generate Lennard-Jones crystal/melt interfaces by Monte Carlo simulation. This leads to dense configurations which are then transformed into adjoining ordered and disordered covalent networks, thereby creating an atomic model of the interface between c-Si and a-Si. The geometrical transformation between close-packed and covalent structures[6] is similar to those used earlier in generating bulk amorphous Si clusters from random hard-sphere configurations.[7,8] Finally, the local electronic density of states near the interface is determined by tight-binding/recursion methods.

II. AMORPHOUS/CRYSTAL SEMICONDUCTOR INTERFACES

We have applied the transformation from close-packed to covalent networks to the crystal/melt interface of the Lennard-Jones system[9] governed by the interatomic potential $V(r) = 4\varepsilon[(\sigma/r)^{12} - (\sigma/r)^{6}]$, where ε and σ are the units of energy and length, respectively. Our starting configuration is a fcc lattice composed of 27 (001)-planes, each containing 50 atoms. Our choice of parameters is based on coexistence data[10] for the Lennard-Jones system at the temperature $kT=1.35\varepsilon$: In the ordered regions (planes 1 to 5 and 23 to 27),

the density was set equal to $\rho_s = 1.053\sigma^{-3}$, and in the disordered region to $\rho_{liq} = 0.964\sigma^{-3}$, the density of the liquid phase. The corresponding interplanar spacings are 0.780σ and 0.852σ. The 400 atoms in planes 1 to 4 and 24 to 27 are then held fixed at their fcc positions, while the positions of the 950 atoms in the remaining planes are rearranged according to Monte Carlo techniques, with periodic boundary conditions imposed in the x and y directions.

Once the crystal/melt/crystal Lennard-Jones system has been created, we suppress the periodic boundary conditions and construct the Delauney or simplicial graph. This graph subdivides space into distinct non-overlapping tetrahedra whose vertices are the atomic positions.[11] The simplicial graph for our system contains about 6700 tetrahedra. After eliminating ill-shaped tetrahedra,[12] specially designed algorithms are used to select a simplicial subgraph which only includes tetrahedra not sharing any common edge with one another. This subgraph is not unique because the order in which tetrahedra are considered for inclusion or rejection may influence the selection process. The simplicial subgraph is then decorated by placing Si atoms at all the vertices, as well as at the centroids of all the tetrahedra. Keeping all the vertex atoms fixed, the positions of the centroid atoms are then relaxed. The final position of each interior atom is determined by minimizing the Keating elastic energy[13] of the five-atom cluster composed of the interior atom and the four surrounding vertex atoms. Finally, bonds are established between the vertex atoms of the residual tetrahedra and their respective interior atoms.[7-8] Since the vertex atoms of the residual subgraph can be shared by fewer than four tetrahedra, dangling bonds and voids are normally present in the structure. This process leads to residual subgraphs containing about 800 tetrahedra and to covalent networks containing about 2,100 atoms. Since the method transforms the fcc lattice into the diamond structure, atoms located in planes 1 to 4 and 24 to 27 of the initial fcc configuration are automatically arranged in the diamond structure. The choice of geometry clearly insures the creation of the (001) c-Si/a-Si interface.

The entire process just described was repeated five times in order to generate five independent final configurations. The mean interatomic distance in the amorphous phase was found to be 0.701σ, with a r.m.s. deviation of 0.068σ. The corresponding values for the bond-angle distribution were 110° and 12°. The Si-Si distance in the crystalline phase is 0.676σ, so the crystalline phase is slightly more dense than the amorphous phase. This result is due partly to the presence of voids and dangling bonds in the amorphous region, and partly to the initial choice of the interplanar spacings in the ordered and disordered regions. (We used slightly different interplanar spacings initially in order to insure melting of the disordered region.) In Fig. 1 we show some key results obtained by averaging the results for the five final configurations. The connectivity (average number of bonds per atom) is less than four in the amorphous region because of the presence of dangling bonds. The dangling bond density remains roughly constant throughout this region, except near the interfaces, where the average coordination number increases.

III. ELECTRONIC DENSITY OF STATES OF THE c-Si/a-Si INTERFACE

In Fig. 2 we show local densities of states (LDOS) that were calculated using a first-neighbor tight-binding Hamiltonian whose two-center integrals were obtained by fitting a recent LCAO band structure of c-Si.[14] The moments of the LDOS were computed using the recursion method. Averages over the five configurations were then taken. Since only a small number of moments was included, the energy resolution of the LDOS is relatively low.

Nevertheless, the existence of states in the gap is clearly seen in Fig. 2. The states in the gap are due primarily to dangling bonds, and to a lesser degree to lattice distortion. The gap state density increases as one moves away from the crystalline region across the interface into the amorphous region, the range of variation being a few atomic spacings.

IV. CONCLUDING REMARKS

In summary, we have succeeded in constructing atomic-scale models of c-Si/a-Si interfaces fully automatically. These computer-generated interfaces are a few atomic spacings wide and are undoubtedly more realistic in this respect than atomically abrupt c-Si/a-Si (and c-Si/a-SiO_2) interfaces that have been constructed by hand in the past.[3-5] The atomic models could be improved by refining the construction so as to reduce the number of voids and dangling bonds. Further (but probably only slight) improvements could also be realized by relaxing all the atoms in the system, and by retaining periodic boundary conditions at all stages of the work. The present approach can be readily extended to describe interfaces between c-Si and hydrogenated a-Si or a-SiO_2, as well as to other types of covalently bonded networks.

REFERENCES

* Supported in part by Office of Naval Research Contract N 00014-79-C -0814.

** IBM World Trade Fellow. On leave from Facultes Universitaires Notre Dame de la Paix, 5000 Namur, Belgium.

1. F. Herman, J. Vac. Sci. Technol. 16, 1101 (1979).
2. F. Herman, J. Vac. Sci. Technol. 21, 643 (1982); J. Phys (Paris) Colloque 1984.
3. F. Spaepen, Acta Metall. 26, 1167 (1978).
4. S.T. Pantelides and M. Long, in The Physics of SiO_2 and its Interfaces, ed. S.T. Pantelides (Pergamon, New York, 1978), p. 339.
5. T. Saito and I. Ohdomari, Phil. Mag. B 43, 673 (1981).
6. A.C. Wright, G.A.N. Connell, and J.W. Allen, J. Non-Cryst. Solids 42, 69 (1980).
7. P. Chaudhari, J.F. Graczyk, D. Henderson and P. Steinhardt, Phil. Mag. 31, 727 (1975).
8. Ph. Lemaire and J.P. Gaspard, unpublished. The present authors are grateful to Ph.L. and J.P.G. for helpful conversations.
9. F.F Abraham, Rep. Prog. Phys. 45, 1113 (1982).
10. J.P. Hansen and L. Verlet, Phys. Rev 184, 151 (1969).
11. F.W. Smith, Can. J. Phys. 42, 304 (1964).
12. Ill-shaped tetrahedra are eliminated by calculating the Keating elastic energy of five-atom clusters, as described later in this paragraph. If this energy exceeds a certain threshold, we conclude that the cluster has a physically unreasonable shape (radical departure from tetrahedral symmetry), and it is eliminated. We plan to describe our algorithms in detail in a subsequent publication.
13. P.N. Keating, Phys. Rev. 145, 637 (1966).
14. Yuan Li and P.J. Lin-Chung, Phys. Rev. B 27, 3465 (1983).

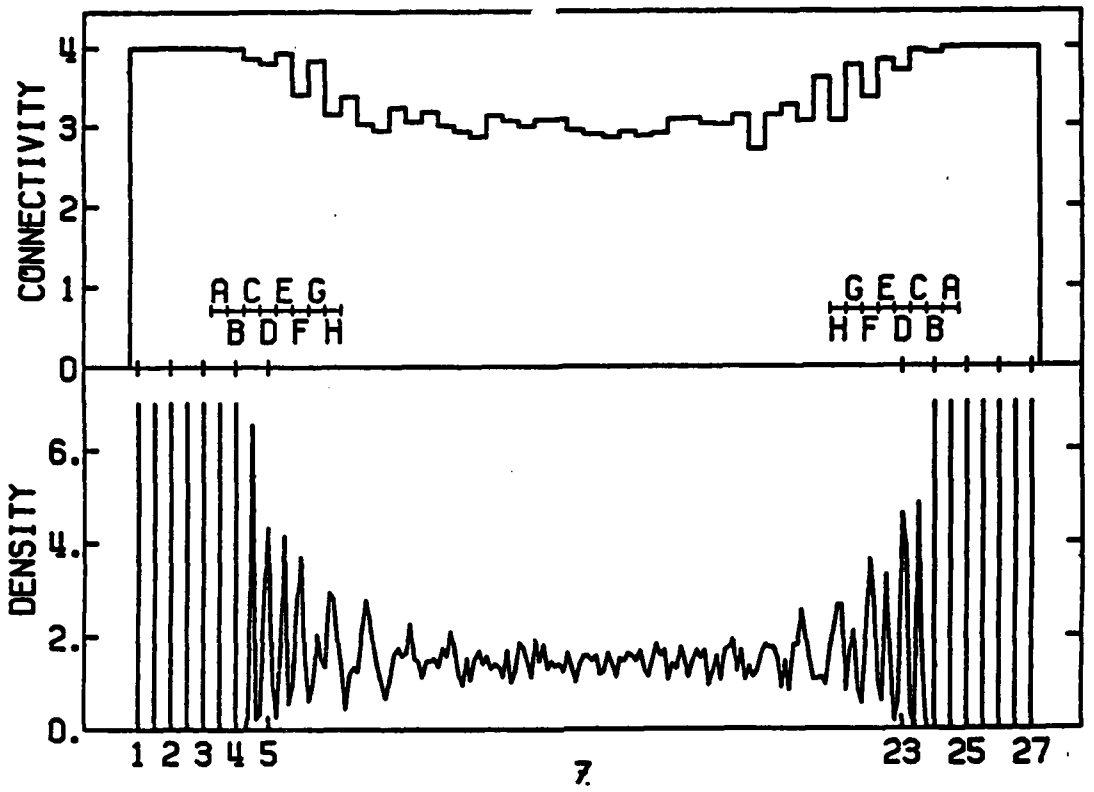

Fig. 1. Profiles of coordination number and atomic density (in units of atoms per σ^3) averaged over five configurations. Lateral boundary effects are avoided by ignoring atoms lying near the surface. Fcc planes in the initial configuration are labeled 1 through 27.

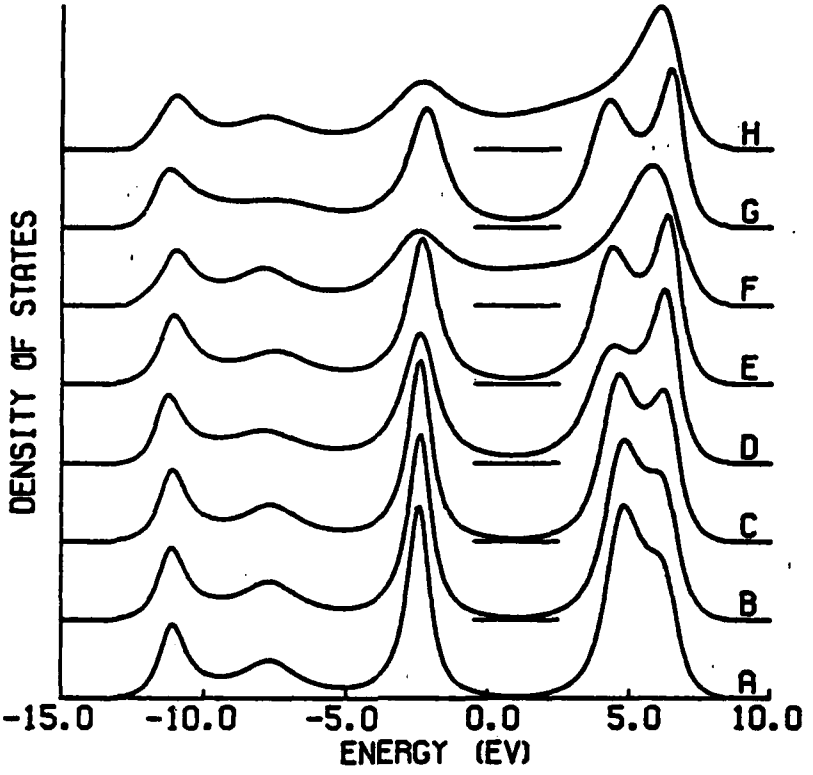

Fig. 2. Local electronic density of states averaged over five configurations. Panels A through H correspond to the intervals identified in Fig. 1. Periodic boundary conditions were applied only in the z direction. Only atoms lying far away from the lateral surfaces were considered so as to avoid boundary effects. The zero of energy corresponds to the top of the valence band of c-Si ($\Gamma_{25'}$).

Submitted to 30th Annual Conference on Magnetism and Magnetic Materials
San Diego, California, November 27 - 30, 1984

ELECTRONIC AND MAGNETIC STRUCTURE OF ULTRATHIN COBALT-CHROMIUM MULTILAYERS*

F. Herman and P. Lambin,** IBM Research Laboratory, San Jose, California 95193
O. Jepsen, Max Planck Institute for Solid State Research, Stuttgart, W. Germany

ABSTRACT: In order to study exchange coupling and spin distributions at atomically abrupt ferromagnetic/antiferromagnetic interfaces, we construct lattice-matched Co/Cr multilayer models. Here we consider strained-layer superlattices composed of alternating regions of ferromagnetic bcc Co and antiferromagnetic bcc Cr with repeat periods ranging from 4 to 8 atomic layers. For computational simplicity, Cr is represented by a theoretically-stabilized commensurate antiferromagnetic spin arrangement. The multilayer spin distributions are determined by carrying out first-principles self-consistent spin-polarized LMTO/ASA electronic structure calculations. We find that the magnetic properties of the Co/Cr superlattices are dominated by the ferromagnetic Co layers, though the antiferromagnetic character of bcc Cr is still evident. For multilayers containing 1 Co layer and 3 to 7 Cr layers per repeat period, there is only one stable spin arrangement corresponding to ferromagnetic coupling across the Co/Cr interfaces. For superlattices containing thicker Co regions, e.g., 3 Co layers and 5 Cr layers, there are two distinct spin arrangements corresponding to ferromagnetic as well as antiferromagnetic coupling across the Co/Cr interfaces. The implications of these results for more complicated Co/Cr multilayers are discussed.

PACS numbers: 75.10.Lp, 75.70. - i, 75.50.Cc, 75.30.Cr

INTRODUCTION

In this paper we study exchange coupling and spin distributions in crystallographically coherent ferromagnetic/antiferromagnetic multilayers (superlattices) composed of alternating ultrathin slabs of Co and Cr. Since these elements have nearly the same atomic volumes (within about 2 percent), it is reasonable to use a strained-layer superlattice as the theoretical model. In such a model all atoms lie on a common lattice having suitably averaged dimensions. We will focus on Cr-rich superlattices having repeat periods ranging from 4 to 8 atomic layers, with [001]-oriented interfaces. Since the crystal structure of strained-layer superlattices should be dictated by the majority constituent, we will assume that all Co and Cr atoms in our Cr-rich structures lie on a common bcc lattice. Although we regard these hypothetical multilayers primarily as theoretical models, we note that bcc Co overlayers have recently been grown on bcc Cr substrates,[1] suggesting that the laboratory synthesis of Co/Cr superlattices also bears looking into.

We will determine the spin distributions in bcc Co/Cr superlattices by carrying out self-consistent spin-polarized electronic structure calculations using frozen cores, the first-principles LMTO/ASA method,[2,3] and the spin-density functional approximation of von Barth and Hedin.[4] We recently carried out similar studies for ordered fcc superlattices containing ferromagnetic Ni_3Fe (Permalloy) and antiferromagnetic MnFe.[5] In a forthcom-

ing publication,[6] we will discuss the present work more fully, as well as lattice-matched superlattices composed of ferromagnetic hcp Co and antiferromagnetic bcc Cr.

THEORETICAL AND COMPUTATIONAL CONSIDERATIONS

It is not expedient to carry out first-principles calculations for spin-density wave (SDW) antiferromagnetic Cr because of the long wavelength (21 lattice spacings).[7] Moreover, it is likely that SDW-antiferromagnetism would be suppressed in ultrathin Cr slabs. We turn instead to the commensurate antiferromagnetic (C-AF) model,[8] according to which bcc Cr consists of two interpenetrating simple cubic lattices, with the atoms on the two lattices having opposite spins. Although C-AF-Cr provides only a rough approximation of SDW-AF-Cr, we can justify using the C-AF model for three reasons:

First and foremost, the calculations are simplified considerably. Even with the C-AF model, 8-layer superlattice studies require substantial computational effort. Second, the C-AF state of bulk Cr can be stabilized experimentally by the addition of certain transition metal impurities,[9] suggesting that ultrathin antiferromagnetic Cr slabs could be similarly stabilized. Third, the impurity-stabilized C-AF-state of Cr is not likely to be suppressed by the 1 percent or so reduction in lattice dimensions that Cr would suffer during the formation of Co/Cr strained-layer superlattices. In contrast, the SDW-AF-state of bulk Cr is destroyed by even smaller reductions in lattice dimensions.[10]

In order to gain some experience with Co/Cr superlattices, we first carried out some preliminary calculations for bulk Co and Cr, and then examined several composite systems, always using the C-AF model for Cr. Contrary to earlier studies,[8] we found that sustained self-consistent iteration of C-AF-Cr leads to a paramagnetic rather than an antiferromagnetic state. Because of the extremely slow convergence of antiferromagnetic calculations, some earlier workers had concluded, incorrectly, that their solutions had converged to the C-AF state. We are presently developing improved LMTO/ASA computer programs which we intend to use to re-examine the question of the C-AF state of bulk Cr.

As an outgrowth of these studies, we developed a heuristic method for theoretically stabilizing the C-AF model of Cr. Since this treatment[6] appears to work quite well for composite systems such as Co/Cr multilayers, as well as for bulk Cr, we decided to base the present study entirely on this stabilized C-AF model, which we regard as the theoretical equivalent of experimental impurity-stabilization.[9]

Having thus set our course, we proceeded to study the convergence properties of the spin distributions as a function of the number of mesh points used in the three-dimensional integrations over the reduced zone in k-space. For materials having high symmetry and few atoms per unit cell, such as (bulk) hcp Co, bcc Co, and bcc Cr, it is necessary to use many hundreds of mesh points in order to obtain say 1 percent accuracy.[8] Because of the lower (tetragonal) symmetry of our superlattices, and the larger number of atoms per unit cell, achieving such accuracy would require enormous computational effort. Accordingly, we had to reach a compromise between accuracy and computer time. We found that a 72-point mesh was adequate for our purposes. In order to be able to compare the magnitudes of Co and Cr spin moments in the superlattices with their corresponding bulk values — at the same

level of convergence — we also studied all-Co and all-Cr 4-, 6-, and 8-layer bcc superlattices.

STRAINED-LAYER COBALT/CHROMIUM SUPERLATTICES

We investigated the following structures:

- 4-layer superlattices — Co(I)Cr(III), Co(IV), and Cr(IV)
- 6-layer superlattices — Co(I)Cr(V), Co(VI), and Cr(VI)
- 8-layer superlattices — Co(I)Cr(VII), Co(III)Cr(V), Co(VIII), and Cr(VIII),

where roman numerals denote the number of successive Co or Cr atoms in the repeat period. For example, the repeat period of Co(I)Cr(III) is Co(1)Cr(2)Cr(3)Cr(4), where the arabic numerals identify the atomic site or layer. We started off our calculations for these Co/Cr superlattices using a variety of assumed spin distributions, and then iterated to self-consistency. We also tried different starting distributions to see whether we could generate alternate self-consistent solutions. The only restraint we imposed was that all atoms in the same atomic layer have the same spin moment and orientation, as would be expected for [001]-oriented interfaces and the C-AF model for Cr. The magnetic properties of all the composite superlattices were dominated by the ferromagnetic Co layers.

For the Co/Cr superlattices containing only one Co layer, namely, Co(I)Cr(III), Co(I)Cr(V), and Co(I)Cr(VII), there is only one self-consistent spin distribution, and this has the following key features:

- The spin moments of the interfacial Cr atoms are aligned parallel to the spin moments of the Co atoms (ferromagnetic coupling across the interfaces).
- The spin moments of the Cr atoms alternate from layer to layer (antiferromagnetic arrangement).
- The spin moments of the Co atoms are reduced and the spin moments of the interfacial Cr atoms are enhanced relative to their bulk values.

Generalizing these results, we anticipate that the interfacial coupling will always be ferromagnetic for Co/Cr superlattices having single Co layers separated by multiple Cr layers. In the simplest cases, successive Co layers will have parallel or antiparallel spins according as the number of intervening Cr layers is odd or even. More complicated spatially modulated spin distributions can also be visualized.

For Co(III)Cr(V), which contains 3 adjacent Co layers separated by 5 adjacent Cr layers, the essential results are as follows:

- There are two distinct spin distributions, corresponding to parallel and antiparallel alignments of the interfacial Co and Cr spins (ferromagnetic as well as antiferromagnetic interfacial coupling).
- For both cases, the Cr regions are antiferromagnetic (C-AF model).
- For both cases, all Co and Cr spin moments are reduced relative to their respective bulk values; moreover, the Co moments for the interfacial layers are smaller than the moments of the central Co layer.

Since there was only one spin distribution for Co(I)Cr(V), which also contains 5 adjacent Cr layers, we attribute the added degree of freedom in Co(III)Cr(V) to the presence of more than 1 adjacent Co layer. The added flexibility arises from the possibility of moment redistribution in the interfacial and central Co layers. We would expect analogous results for still thicker Co slabs.

The general features just found for [001] Co/Cr superlattices should also apply to [111] Co/Cr superlattices, because all atoms in interfacial Cr layers have the same spin for both of these orientations (C-AF model). On the other hand, for [110] Co/Cr superlattices, the interfacial Cr layers would be compensation planes (equal numbers of up and down spins). Since our calculations indicate that only ferromagnetic coupling is supported across single-layer Co interfaces, we would expect the C-AF state of Cr to be suppressed near [110] single-layer Co interfaces. By the same token, we would expect the C-AF state as well as more complicated antiferromagnetic spin orderings of Cr to be sustained near [110] multiple-layer Co interfaces.

CONCLUDING REMARKS

To recapitulate, we have calculated the exchange coupling and spin distributions in ferromagnetic/antiferromagnetic strained-layer superlattices composed of ultrathin bcc Co and bcc Cr slabs. By calling attention to these hypothetical superlattices, which are used here as convenient theoretical models, we hope to stimulate interest in the laboratory synthesis of such artificially layered structures, as well as the experimental study of their electronic and magnetic properties. We are currently exploring the possibility of incorporating magnetocrystalline anisotropy into the present theoretical model,[6] with a view to carrying out first-principles investigations of exchange anisotropy.[11] For further details concerning the present study, see Ref. 6.

ACKNOWLEDGMENTS

We are particularly grateful to H.L. Skriver for sending us a copy of his LMTO computer programs in advance of publication, and for fruitful discussions. We have also benefitted from stimulating discussions with our colleagues, O.K. Andersen, J. Kent Howard, and Roy Geiss. One of us (P.L.) wishes to thank IBM Belgium for making it possible for him to spend a year at IBM San Jose Research Laboratory as an IBM World Trade Fellow. We are also grateful to the Office of Naval Research for partial support.

REFERENCES

* Supported in part by the Office of Naval Research.

** On leave from Facultes Universitaires, Notre Dame de la Paix, Namur, Belgium

1. R. Walmsley, J. Thomson, D. Friedman, R.M. White, and T.H. Geballe, IEEE Trans. MAG-19, 1992 (1983).

2. O.K. Andersen, Phys. Rev. B 12, 3060 (1975); O. Jepsen, O.K. Andersen, and A.R. Mackintosh, ibid, p. 3084.

3. H.L. Skriver, "The LMTO Method," (Springer-Verlag, Berlin, 1984).

4. U. von Barth and L. Hedin, J. Phys. C: Solid State Phys. 5, 1629 (1972).

5. P. Lambin and F. Herman, Phys. Rev. B (in press).

6. F. Herman, P. Lambin, O. Jepsen, submitted to Phys. Rev. B.

7. W.M. Lomer, Proc. Phys. Soc. 80, 489 (1962); G. Shirane and W. Takei, J. Phys. Soc. Japan Suppl. 17 BIII, 35 (1962); T. Ukai and N. Mori, J. Appl. Phys. 53, 2038 (1982).

8. H.L. Skriver, J. Phys. F: Metal Physics 11, 97 (1981), and references cited.

9. W.C. Koehler, R.M. Moon, A.L. Trago, and A.R. Mackintosh, Phys. Rev. 151, 405 (1966); Y. Endoh, Y. Ishikawa, and H. Ohno, J. Phys. Soc. Japan 24, 263 (1968)

10. D.B. McWhan and T.M. Rice, Phys. Rev. Lett. 19, 846 (1967); P.C. Pattnaik, P.H. Dickinson, and J.L. Fry, Phys. Rev. B 28, 5281 (1983).

11. A. Yelon, Phys. Thin Films 6 205 (1971); B.D. Cullity, "Introduction to Magnetic Materials," (Addison-Wesley, Reading, Mass., 1972); N.H. March, P. Lambin, and F. Herman, J. Magn. Magn. Mater. (in press)

TABLE I. Spin magnetic moments for 4-layer bcc superlattices Co(IV), Cr(IV), and Co(I)Cr(III) = Co(1)Cr(2)Cr(3)Cr(4), for various meshes. For Co(I)Cr(III), atomic sites Cr(2) and Cr(4) are equivalent. Here and in the following tables, Cr is represented by theoretically stabilized commensurate antiferromagnetic model discussed in Ref. 6.

Mesh for tetragonal reduced zone	Co(IV) (all-Co)	Cr(IV) (all-Cr)	<---------- Co(I)Cr(III) ----------> Co(1)	Cr(2)	Cr(3)	Cr(4)
IK=20 (72)[a]	1.56	± 0.43	+ 1.37	+ 0.88	− 0.44	+ 0.88

(a) IK is number of inequivalent mesh points in irreducible sector of reduced zone. Total number of mesh points in reduced zone is shown in parentheses. See Ref. 6 for a discussion of the convergence of the spin moments as a function of the number of points in the mesh.

TABLE II. Spin magnetic moments for bcc superlattices Co(VI), Cr(VI), and Co(I)Cr(V) = Co(1)Cr(2)Cr(3)Cr(4)Cr(5)Cr(6). Atomic sites in same column are equivalent.

Mesh for tetragonal reduced zone	Co(VI) (all sites cobalt)	Cr(VI) (all sites chromium)	<---------- Co(I)Cr(V) ----------> Co(1)	Cr(2) Cr(6)	Cr(3) Cr(5)	Cr(4)
IK=20 (72)	1.65	± 0.38	+ 1.46	+ 0.94	− 0.42	+0.36

TABLE III. Spin magnetic moments for 8-layer bcc superlattices Cr(VIII) and Co(I)Cr(VII) = Co(1)Cr(2) ... Cr(8). Atomic sites in same column are equivalent.

Mesh for tetragonal reduced zone	Cr(VIII) (all sites chromium)	<---------- Co(I)Cr(VII) ----------> Co(1)	Cr(2) Cr(8)	Cr(3) Cr(7)	Cr(4) Cr(6)	Cr(5)
IK=20 (72)	± 0.53	+ 1.35	+ 0.97	− 0.41	+ 0.36	− 0.33

TABLE IV. Spin magnetic moments for 8-layer bcc superlattices Co(VIII) and Co(III)Cr(V) = Co(1)Co(2)Co(3)Cr(4) ... Cr(8). Atomic sites in same column are equivalent. Note two distinct solutions.

Mesh for tetragonal reduced zone	Co(VIII) (all sites cobalt)	<---------- Co(III)Cr(V) ----------> Co(1)	Co(2) Co(8)	Cr(3) Cr(7)	Cr(4) Cr(6)	Cr(5)
IK=20 (72)	+ 1.72	+ 1.52	+ 1.28	− 0.29	+ 0.22	− 0.11
IK=20 (72)	+ 1.72	+ 1.53	+ 1.38	+ 0.16	− 0.22	+ 0.47

END

FILMED

12-84

DTIC